B. Model equations and finite discretization form

B-1. Governing equations

2-dimensional equations are considered for simplicity in sections B-1 $\sim$ B-4.

B-1-1. Fundamental equations in Cartesian coordinates

a) State equation of moist air with hydrometeors

$$\begin{aligned}\rho &= \rho_{\rm dry} + \rho_v + \rho_c + \rho_r + \rho_i + \rho_s + \rho_g \\ &= \rho_{\rm dry}(1 + Qv + Qc + Qr + Qi + Qs + Qg),\end{aligned} \tag{1-1}$$

$$p = (\rho_{\rm dry} + \rho_v)R(1 + 0.61Qv)T, \tag{1-2}$$

where $\rho_{\rm dry}$, ρ_v, ρ_c, ρ_r, ρ_i, ρ_s and ρ_g are the densities of dry air, water vapor, cloud water, rain, cloud ice, snow and graupel, respectively; Qv, Qc, Qr, Qi, Qs and Qg are mixing ratios of water vapor, cloud water, rain, cloud ice, snow and graupel, respectively; R is the gas constant for dry air; T is temperature (K). By approximation of $\rho_{\rm dry} + \rho_v = \rho(1 - Qc - Qr - Qi - Qs - Qg)$, Eq. (1-2) is rewritten as

$$\begin{aligned}p &= \rho R T_m \\ &= \rho R(1 - Qc - Qr - Qi - Qs - Qg)T_v \\ &= \rho R(1 - Qc - Qr - Qi - Qs - Qg)(1 + 0.61Qv)T,\end{aligned} \tag{1-3a}$$

or alternatively

$$\rho \equiv \frac{p_0}{R\Theta_m}\left(\frac{p}{p_0}\right)^{C_v/C_p}, \tag{1-3b}$$

where

$$\left.\begin{aligned}&T_m \equiv (1 - Qc - Qr - Qi - Qs - Qg)T_v; \\ &T_v \equiv (1 + 0.61Qv)T; \\ &\Theta \equiv \Pi^{-1}T; \quad \Theta_v \equiv \Pi^{-1}T_v; \quad \Theta_m \equiv \Pi^{-1}T_m; \quad \Pi = \left(\frac{p}{p_0}\right)^{R/C_p};\end{aligned}\right\} \tag{1-4}$$

p is pressure; Θ is potential temperature; C_p is the specific heat of dry air at constant pressure; C_v is the specific heat at constant volume; p_0 equals 1000 hPa.

b) Mass conservation

By neglecting the fall-out of Qr, Qs and Qg, ρ is governed by

$$\sigma\frac{d\rho}{\rho dt}+\frac{\partial u}{\partial x}+\frac{\partial w}{\partial z}=0, \tag{1-5a}$$

or

$$\sigma\frac{\partial \rho}{\partial t}+\frac{\partial \rho u}{\partial x}+\frac{\partial \rho w}{\partial z}=0. \tag{1-5b}$$

Here, σ is a switching parameter; $\sigma=1$ represents the exact equation, while $\sigma=0$ represents an approximate equation from which sound waves are excluded.

c) Momentum equations

$$\rho\frac{du}{dt}+\frac{\partial p}{\partial x}=\mathrm{DIF}.u, \tag{1-6}$$

$$\rho\frac{dw}{dt}+\frac{\partial p}{\partial z}+\rho g=\mathrm{DIF}.w, \tag{1-7}$$

where DIF.f denotes the diffusion term for a field variable f.

d) Thermal equations

$$Qdt+C_v\mathrm{DIF}.Tdt=C_vdT+pd\alpha=(C_v+R)dT-\alpha dp=C_p\Pi d\Theta, \tag{1-8}$$

$$\frac{d\Theta}{dt}=\frac{Q}{C_p\Pi}+\mathrm{DIF}.\Theta, \tag{1-9a}$$

$$C_v\frac{dT}{dt}-\frac{p}{\rho^2}\frac{d\rho}{dt}=C_v\frac{dT}{dt}+\frac{p}{\rho}\left(\frac{\partial u}{\partial x}+\frac{\partial w}{\partial z}\right)=Q+C_v\mathrm{DIF}.T, \tag{1-9b}$$

where Q is the diabatic heating rate, $C_p\Pi\mathrm{DIF}.\Theta=C_v\mathrm{DIF}.T$ and $\alpha=1/\rho$.

From (1-3b),

$$\frac{1}{Cs^2}\frac{\partial p}{\partial t}=\frac{\partial \rho}{\partial t}+\frac{\rho}{\Theta_m}\frac{\partial \Theta_m}{\partial t}, \tag{1-10a}$$

or

$$\frac{1}{Cs^2}\frac{dp}{dt}=\frac{d\rho}{dt}+\frac{\rho}{\Theta_m}\frac{d\Theta_m}{dt}, \tag{1-10b}$$

where Cs is the sound wave speed $Cs^2=(C_p/C_v)RT$.

From Eqs. (1-10) and (1-5b),

$$\frac{\sigma}{Cs^2}\frac{\partial p}{\partial t}+\frac{\partial \rho u}{\partial x}+\frac{\partial \rho w}{\partial z}=\sigma\frac{\rho}{\Theta_m}\frac{\partial \Theta_m}{\partial t}, \tag{1-11a}$$

or

$$\frac{\sigma}{Cs^2}\frac{dp}{dt}+\rho\left(\frac{\partial u}{\partial x}+\frac{\partial w}{\partial z}\right)=\sigma\frac{\rho}{\Theta_m}\frac{d\Theta_m}{dt}. \tag{1-11b}$$

By use of Eq. (1-5) and $\sigma=1$, momentum equations (1-6) and (1-7) are written in flux form as follows:

$$\frac{\partial\rho u}{\partial t}+\frac{\partial p}{\partial x}=-\frac{\partial\rho uu}{\partial x}-\frac{\partial\rho wu}{\partial z}+\mathrm{DIF}.u, \tag{1-12}$$

$$\frac{\partial\rho w}{\partial t}+\frac{\partial p}{\partial z}+\rho g=-\frac{\partial\rho uw}{\partial x}-\frac{\partial\rho ww}{\partial z}+\mathrm{DIF}.w. \tag{1-13}$$

The equation for the scalar variable f (Θ, Qv, Qc, $\ldots$, Qg)

$$\rho\frac{df}{dt}=\rho\mathrm{SRC}.f+\rho\mathrm{DIF}.f \tag{1-14a}$$

is also written in flux form as

$$\frac{\partial\rho f}{\partial t}=-\frac{\partial\rho uf}{\partial x}-\frac{\partial\rho wf}{\partial z}+\rho\mathrm{SRC}.f+\rho\mathrm{DIF}.f, \tag{1-14b}$$

where SRC.f is the source term of f.

It is noted that the above equations include sound waves, and no approximation is made for a dry case. The thermal equation (1-9b) in combination with Eqs. (1-5), (1-6) and (1-7) yields the equation of the total energy conservation such as

$$\frac{\partial(\rho E)}{\partial t}+\frac{\partial(\rho Eu)}{\partial x}+\frac{\partial(\rho Ew)}{\partial z}+\frac{\partial pu}{\partial x}+\frac{\partial pw}{\partial z}=(u\mathrm{DIF}.u+w\mathrm{DIF}.w)+\rho(Q+C_v\mathrm{DIF}.T), \tag{1-15}$$

where

$$E=\frac{1}{2}(u^2+w^2)+gz+C_vT.$$

The above beautiful equation cannot be obtained from Eq. (1-9a). Aihara and Okamura (1985) adopted Eq. (1-9b) instead of Eq. (1-9a), and obtained the scheme of the flux form which conserves the total energy E exactly.

B-1-2. Reference atmosphere and approximate equations

The reference basic state is assumed to be horizontally uniform and dependent only on z and in hydrostatic balance. All field variables are expressed as the sum of the values of the basic state ($^-$) and perturbations ($'$) from them as below:

$$p=\overline{p}+p';\ \rho=\overline{\rho}+\rho';\ \Theta=\overline{\Theta}+\Theta';\ T=\overline{T}+T', \tag{1-16}$$

$$\overline{p} = \overline{\rho} R \overline{T}_m, \tag{1-17}$$

$$\overline{\Theta}_m \equiv \overline{\Pi}^{-1} \overline{T}_m;\ \overline{\Pi} = \left(\frac{\overline{p}}{p_0}\right)^{R/C_p}, \tag{1-18}$$

$$\overline{\rho} \equiv \frac{p_0}{R\overline{\Theta}_m} \left(\frac{\overline{p}}{p_0}\right)^{C_v/C_p}, \tag{1-19}$$

$$\frac{\partial \overline{p}}{\partial z} = -\overline{\rho} g. \tag{1-20}$$

Note that the suffix "–" is different from the averaging operator in the horizontal, and hereafter the subscript 'ref' is also used in the same meaning as the suffix "–".

From Eqs. (1-3b) and (1-16) and (1-19), an approximate relation is obtained as

$$\rho' = \frac{p'}{Cs^2} - \frac{\overline{\rho}\Theta'_m}{\overline{\Theta}_m}. \tag{1-21}$$

By use of Eqs. (1-20) and (1-21), Eq. (1-13) is rewritten as

$$\frac{\partial \rho w}{\partial t} + \frac{\partial p'}{\partial z} + \frac{g p'}{Cs^2} = -\frac{\partial \rho u w}{\partial x} - \frac{\partial \rho w w}{\partial z} + \frac{g \overline{\rho} \Theta'_m}{\overline{\Theta}_m} + \mathrm{DIF}.w, \tag{1-22}$$

Eq. (1-11a) is rewritten as

$$\frac{\sigma}{Cs^2}\frac{\partial p'}{\partial t} + \left(\frac{\partial \rho u}{\partial x} + \frac{\partial \rho w}{\partial z}\right) = \sigma \frac{\rho \partial \Theta'_m}{\Theta_m \partial t} \tag{1-23}$$

The reference atmosphere is required to be not only as close as possible to the model atmosphere but also as smooth as possible.

It is noted that Clark's anelastic equations (1977) are obtained by formally setting $\sigma = 0$ and $\rho = \overline{\rho}$ in Eqs. (1-12), (1-14b), (1-22) and (1-23). $\sigma = 1$ includes acoustic modes, while $\sigma = 0$ filters out them. Hereafter, the governing equations which are formally obtained by setting $\rho = \overline{\rho}$ in Eqs. (1-12), (1-14b), (1-22) and (1-23) and replacing p by p' in Eq. (1-12) are used.

However, $\sigma = 1$ and $\rho = \overline{\rho}$ yield errors in the advection term of flux form for a variable f as shown below;

$$\begin{aligned} \overline{\rho}\frac{\partial f}{\partial t} &= -\frac{\partial \overline{\rho} u f}{\partial x} - \frac{\partial \overline{\rho} w f}{\partial z} + \overline{\rho}\mathrm{SRC}.f + \overline{\rho}\mathrm{DIF}.f \\ &= -\overline{\rho} u \frac{\partial f}{\partial x} - \overline{\rho} w \frac{\partial f}{\partial z} - f\left(\frac{\partial \overline{\rho} u}{\partial x} + \frac{\partial \overline{\rho} w}{\partial z}\right) \\ &\qquad\qquad\qquad\qquad -- \text{error} ---- \\ &\quad + \overline{\rho}\mathrm{SRC}.f + \overline{\rho}\mathrm{DIF}.f. \end{aligned} \tag{1-24}$$

This error can be reduced so as to be practically free from numerical trouble for some cases by damping sound wave modes as shown by Ikawa (1988). There are several other choices to avoid the error. One is the use of the advection term in advective form. However, this has some problems in making budget analysis. Another choice is the adjustment on the velocity in order to satisfy the non-divergence of the wind proposed by Yoshizaki (1988). Another choice is to predict time change of ρ by Eq. (1-5) exactly as Aihara and Okamura (1985) did. But this is currently not yet implemented in E-HI-VI and E-HE-VI schemes (see B-3 and B-4).

The anelastic equations of Ogura and Phillips (1962) conserve the total energy (the degenerated version of E). They are obtained by selecting the isentropic atmosphere as the reference atmosphere in addition to setting $\sigma = 0$ and $\rho = \overline{\rho}$. However, the isentropic atmosphere differs from the standard atmosphere, and this might result in large error.

B-1-3. Governing equations in terrain following coordinates

Formulation of the schemes without any special description is the same as that of Clark (1977). The pressure gradient force is expressed, not in terms of an Exner function but in terms of pressure. The terrain following coordinate system is introduced such as

$$\xi = \frac{H(z - Z_s)}{(H - Z_s)}, \tag{1-25}$$

where Z_s is the surface height, and H is the constant height of the top of the model domain.

Applying the chain rule for the coordinate transform from (x, z) to (x, ξ), the following relations are obtained for an arbitrary function ϕ:

$$G^{1/2}\frac{\partial \phi}{\partial x} = \frac{\partial}{\partial x}(G^{1/2}\phi) + \frac{\partial}{\partial \xi}(G^{1/2}G^{13}\phi) \tag{1-26a}$$

and

$$G^{1/2}\frac{\partial \phi}{\partial z} = \frac{\partial \phi}{\partial \xi}, \tag{1-26b}$$

where

$$G^{1/2} \equiv \frac{1}{(\partial\xi/\partial z)_{x=\mathrm{const}}} = 1 - Z_s/H;\ G^{13} \equiv \left(\frac{\partial \xi}{\partial x}\right)_{z=\mathrm{const}} = \frac{1}{G^{1/2}}\left(\frac{\xi}{H} - 1\right)\frac{\partial Z_s}{\partial x}. \tag{1-27}$$

The governing equations (Eqs. (1-5b), (1-12), (1-14b), (1-22) and (1-23)) are written in the (x, ξ) coordinate system as follows:

$$\frac{\partial U}{\partial t} + \frac{\partial}{\partial x}P + \frac{\partial}{\partial \xi}(G^{13}P) = -\mathrm{ADVU}, \tag{1-28}$$

$$\frac{\partial W}{\partial t} + \frac{1}{G^{1/2}}\frac{\partial P}{\partial \xi} + \frac{gP}{Cs^2} = \mathrm{BUOY} - \mathrm{ADVW}, \tag{1-29}$$

$$\sigma\frac{\partial(G^{1/2}\rho')}{\partial t} + \frac{\partial}{\partial x}U + \frac{1}{G^{1/2}}\frac{\partial W}{\partial \xi} + \frac{\partial}{\partial \xi}(G^{13}U) = 0, \tag{1-30a}$$

or alternatively

$$\sigma\frac{\partial(G^{1/2}\rho')}{\partial t} + \frac{\partial}{\partial x}U + \frac{\partial W^*}{\partial \xi} = 0, \tag{1-30b}$$

where

$$U \equiv \overline{\rho}G^{1/2}u, \quad W \equiv \overline{\rho}G^{1/2}w, \quad P \equiv G^{1/2}p', \tag{1-31}$$

$$\mathrm{ADVU} \equiv \frac{\partial Uu}{\partial x} + \frac{\partial W^*u}{\partial \xi}, \tag{1-32}$$

$$\mathrm{ADVW} \equiv \frac{\partial Uw}{\partial x} + \frac{\partial W^*w}{\partial \xi}, \tag{1-33}$$

$$W^* \equiv \frac{1}{G^{1/2}}\overline{\rho}G^{1/2}w + \overline{\rho}G^{1/2}G^{13}u \equiv \overline{\rho}G^{1/2}\omega \equiv \overline{\rho}G^{1/2}\frac{d\xi}{dt}, \tag{1-34}$$

$$\mathrm{BUOY} \equiv g\frac{G^{1/2}\overline{\rho}\Theta'_m}{\overline{\Theta}_m}. \tag{1-35}$$

Here σ is the switching parameter; $\sigma = 0$ for anelastic equations, and $\sigma = 1$ for elastic equations.

The thermal equation is given as

$$\frac{\partial \theta}{\partial t} = -\mathrm{ADV}\theta + \frac{Q}{C_p\Pi} + \mathrm{DIF}.\theta, \tag{1-36}$$

$$\mathrm{ADV}\theta \equiv \frac{1}{\overline{\rho}G^{1/2}}\left(\frac{\partial U\theta}{\partial x} + \frac{\partial W^*\theta}{\partial \xi}\right), \tag{1-37a}$$

$$\theta \equiv \Theta - \Theta_{\mathrm{bias}} = \overline{\Theta}(z) + \Theta' - \Theta_{\mathrm{bias}}. \tag{1-37b}$$

Here, Θ_{bias} is a constant prescribed value which is independent of z and close to the vertically averaged value of $\overline{\Theta}(z)$.

Eq. (1-23) is rewritten as

$$\frac{\sigma}{Cs^2}\frac{\partial P}{\partial t} + \frac{\partial}{\partial x}U + \frac{1}{G^{1/2}}\frac{\partial W}{\partial \xi} + \frac{\partial}{\partial \xi}(G^{13}U) = \sigma\mathrm{PFT}, \tag{1-38}$$

where

$$\mathrm{PFT} = \frac{\overline{\rho}G^{1/2}}{\Theta_m}\frac{\partial \Theta'_m}{\partial t} = \frac{1}{g}\frac{\partial \mathrm{BUOY}}{\partial t}. \tag{1-39}$$

Terms related to sound waves are isolated on the left side of Eqs. (1-28), (1-30) and (1-38).

It is noted that the state variables of the reference atmosphere such as $\overline{\Theta} = \Theta_{\mathrm{ref}}$ and $\overline{\rho} = \rho_{\mathrm{ref}}$ is dependent only on z in the Cartesian coordinate system, but dependent not only on

ξ but also on x in the terrain following coordinate system. However, $Cs^2_{\text{ref}} = (C_p/C_v)RT_{\text{ref}}$ is assumed to be dependent only on ξ for simplicity in the program.

The governing equations in the terrain following coordinate system have been derived in two different ways by tensor analysis (Gal-Chen and Somerville, 1975; Pielke and Martin, 1981; Pielke, 1984) and chain rule (Clark, 1977; Carpenter, 1979; Durran and Klemp, 1983; Aihara and Okamura, 1985). The equations between the two differ slightly and are believed to bring about little differences. A concise review is given by Yoshizaki (1988). The equations derived by chain rule predict the velocity components in the Cartesian coordinate system, while those derived by tensor analysis predict the components of the contravariant vector of the velocity in the terrain following coordinate system. Momentum equations by the two methods are the same in appearance (Wong and Hage, 1983; Pielke and Martin, 1981). However, the directions of the unit vector for the u-velocity component are different, although the equations for the magnitude of u-velocity component are the same. The diffusion terms are also different; but, usually, subgrid scale turbulence is parameterized with large uncertainty. This difference is also considered to be insignificant.

B-1-4. Summary

In summary, Eqs. (1-28), (1-29) (1-30) (1-36) and (1-38) are adopted as governing equations. The anelastic scheme implemented in the model (see B-2) uses $\sigma = 0$ and $\rho = \overline{\rho}$. Elastic schemes (both E-HI-VI and E-HE-VI) currently implemented in the model (see B-3 and 4) uses $\sigma = 1$ and $\rho = \overline{\rho}$ instead of explicit calculation of the prognostic equation (1-30) for density ρ (Eq. (1-30) is treated just as a dummy equation, currently). This is accompanied by errors in advection term as shown by Eq. (1-24). However, no serious problems have occurred as far as sound waves are damped enough ($|\text{div}(\rho V)|/\overline{\rho} < 10^{-6}\text{s}^{-1}$ seems to be sufficient) (Ikawa, 1988). In the next sections, these schemes are described, with emphasis on their pressure equations and solving methods. For elastic schemes, special attention is paid to the time integration methods which effectively damp sound waves.

Which scheme is the best among AE, E-HI-VI and E-HE-VI, still remains unclear. From limited numbers of simulations of large amplitude hydrostatic mountain waves in a homogeneous atmosphere (horizontal velocity, U, and Brunt-Väisälä frequency, N, are constant), it was found by Ikawa (1988) that the numerical results by those schemes are almost the same and that the CPU time consumed by E-HE-VI is almost twice that by AE or E-HI-VI. However, in the simulation of large-amplitude mountain waves of 2 or 4-layered atmosphers conducted by Ikawa and Nagasawa (1989), the E-HI-VI was found to succeed in longer computation without computational breakdown than AE for some cases. One purpose of the model in which the three schemes are available in the same computational environment is to compare the performance and efficiency of these three schemes, and to provide some information for deciding the best scheme among the three.

B-2. AE (anelastic) scheme

B-2-1. Pressure equation for AE scheme

An AE scheme is obtained by setting $\sigma = 0$ and $\rho = \overline{\rho}$ in equations in section B-1-3. In this scheme, sound waves are filtered out.

For convenience, operators are introduced as

$$\mathrm{DIVR}(A,B) = \frac{\partial(G^{13}A)}{\partial\xi} + \left(\frac{1}{G^{1/2}} - \frac{\widetilde{1}}{G^{1/2}}\right)\frac{\partial B}{\partial\xi}, \tag{2-1}$$

$$\mathrm{DIVS}(A,B) = \frac{\partial A}{\partial x} + \frac{\widetilde{1}}{G^{1/2}}\frac{\partial B}{\partial\xi}, \tag{2-2}$$

and

$$\begin{aligned}\mathrm{DIVT}(A,B) &= \frac{\partial A}{\partial x} + \frac{\partial(G^{13}A)}{\partial\xi} + \frac{1}{G^{1/2}}\frac{\partial B}{\partial\xi}\\ &= \mathrm{DIVS}(A,B) + \mathrm{DIVR}(A,B),\end{aligned} \tag{2-3}$$

where the symbol $\tilde{}$ indicates a constant value independent of x and ξ.

The pressure equation for the AE scheme is obtained from Eqs. (1-28), (1-29) and (1-30) by eliminating U^{it+1} and W^{it+1} in DIVT$(\partial U/\partial t,\ \partial W/\partial t) = 0$ as

$$\begin{aligned}&pt\frac{\partial^2 P}{\partial x^2} + \frac{1}{(G^{1/2})^2}\frac{\partial^2 P}{\partial\xi^2} + \frac{1}{G^{1/2}}\frac{\partial}{\partial\xi}\left(\frac{g}{Cs^2}P\right) + \frac{\partial^2}{\partial x\partial\xi}(G^{13}P)\\ &\quad + \frac{\partial}{\partial\xi}\left[G^{13}\left\{\frac{\partial P}{\partial x} + \frac{\partial}{\partial\xi}(G^{13}P)\right\}\right]\\ &= -\mathrm{DIVT}(\mathrm{ADVU},\ \mathrm{ADVW} - \mathrm{BUOY}) + \frac{\mathrm{DIVT}(U^{it-1}, W^{it-1})}{2\Delta t}\\ &= \mathrm{FP.AE.INV}.\end{aligned} \tag{2-4}$$

Here, superscript 'it' denotes the value at the time step 'it'. Theoretically, the term DIVT (U^{it-1}, W^{it-1}) would be zero, and the above equation would guarantee DIVT(U^{it+1}, W^{it+1}) $= 0$. However, in numerical simulation, the term becomes non-zero due to round-off errors, and this term may be considered as "sound wave"-like noises originated from numerical round-off errors. The purpose of adding this term to the forcing term, FP.AE.INV, of the pressure equation is to suppress the growth of these "sound wave"-like noises and make the continuity equation of AE be more completely fullfilled.

In the case where orography is included, $G^{1/2}$ is dependent on x, and G^{13} is dependent on x and ξ. It is difficult to solve Eq. (2-4) by the direct method (e.g., dimension reduction method: Ogura (1969), Ikawa (1981)) efficiently because of its non-separability. Eq. (2-4) can be solved by an iterative application of the direct method as follows:

$$\begin{aligned}&\frac{\partial^2 P_i}{\partial x^2}+\frac{\widetilde{1}}{(G^{1/2})^2}\frac{\partial^2 P_i}{\partial \xi^2}+\frac{\widetilde{1}}{G^{1/2}}\frac{\partial}{\partial \xi}\left(\frac{\widetilde{g}}{Cs^2}P_i\right)\\&=\mathrm{FP.AE.INV}+\mathrm{FP.AE.VAR}(P_{i-1}),\end{aligned}\tag{2-5}$$

where

$$\begin{aligned}\mathrm{FP.AE.VAR}(P_i)=&-\mathrm{DIVR}\left(\frac{\partial P_i}{\partial x},\ \left(\frac{\widetilde{1}}{G^{1/2}}\frac{\partial}{\partial \xi}+\frac{\widetilde{g}}{Cs^2}\right)P_i\right)\\&-\mathrm{DIVT}\left(\frac{\partial}{\partial \xi}G^{13}P_i,\ \left(\left[\frac{1}{G^{1/2}}\frac{\partial}{\partial \xi}+\frac{g}{Cs^2}\right]-\left[\frac{\widetilde{1}}{G^{1/2}}\frac{\partial}{\partial \xi}+\frac{\widetilde{g}}{Cs^2}\right]\right)P_i\right).\end{aligned}\tag{2-6}$$

The suffix i denotes the i-th solution obtained from the i-th iterative procedure.

At the lower and upper boundaries, the following condition must be satisfied (see Eq. (1-34)):

$$\frac{W}{G^{1/2}}+G^{13}U=\overline{\rho}G^{1/2}\frac{d\xi}{dt}=W^*=0.\tag{2-7}$$

From Eqs. (2-7), (1-28) and (1-29), the upper and lower boundary conditions for pressure are as follows:

$$\frac{1}{G^{1/2}}\frac{\partial P}{\partial \xi}+\frac{g}{Cs^2}P=-G^{1/2}G^{13}\left(\frac{\partial P}{\partial x}+\frac{\partial}{\partial \xi}(G^{13}P)+\mathrm{ADVU}\right)+\mathrm{BUOY}-\mathrm{ADVW}.\tag{2-8}$$

For these boundary conditions, an iterative procedure is also needed.

$$\frac{\widetilde{1}}{G^{1/2}}\frac{\partial P_i}{\partial \xi}+\frac{\widetilde{g}}{Cs^2}P_i=\mathrm{FPB.AE.VAR}(P_{i-1})+\mathrm{FPB.AE.INV},\tag{2-9}$$

$$\begin{aligned}\mathrm{FPB.AE.VAR}(P_i)=&\left(\frac{\widetilde{1}}{G^{1/2}}\frac{\partial P_i}{\partial \xi}-\frac{1}{G^{1/2}}\frac{\partial P_i}{\partial \xi}\right)+\left(\frac{\widetilde{g}}{Cs^2}-\frac{g}{Cs^2}\right)P_i\\&-G^{1/2}G^{13}\left(\frac{\partial P_i}{\partial x}+\frac{\partial}{\partial \xi}G^{13}P_i\right),\end{aligned}\tag{2-10}$$

and

$$\mathrm{FPB.AE.INV}=\mathrm{BUOY}-\mathrm{ADVW}-G^{1/2}G^{13}\mathrm{ADVU}.\tag{2-11}$$

The iterative application of the direct method to Eqs. (2-5) and (2-9) is found to work well. The method is described in detail in section B-6 (pressure equation solver). 3 or 4 iterations

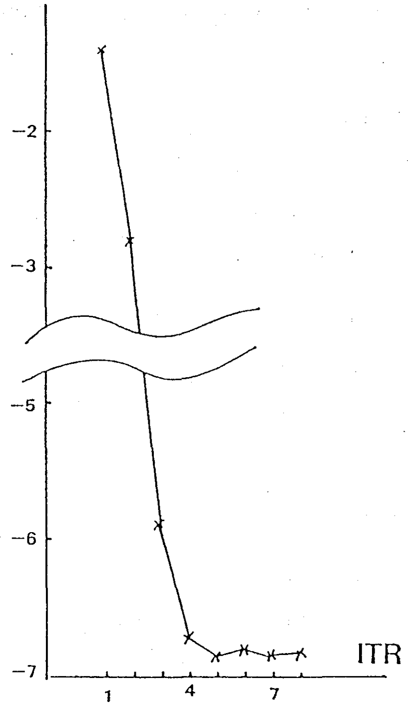

Fig. B-2-1 An example of a convergence of the iterative application of the direct method to Eqs. (2-5) and (2-9) at a certain grid point for the example case in section 3 of Ikawa (1988). The mountan height is set to 2000m and $\Delta G \fallingdotseq \max(\partial Z_s/\partial x) = 0.2$, $\Delta H \fallingdotseq \max(Z_s/H) = 0.14$ (for the definition of ΔG and ΔH, see B-3-2), where $Z_s(x)$ is a mountain shape function and H is the height of the model domain. The vertial axis denotes $\log_{10}|Pi - P_9|/|P_9|$. The horizontal axis represents i, the number of iterative applications of the direct method. The first guess P_0 is set to zero and P_9 denotes the solution obtained at the 9-th iteration. (adapted from Ikawa, 1988)

are sufficient to give the well converged solution up to 6 significant digits as shown in Fig. B-2-1.

B-2-2. Hydrostatic approximation of the anelastic nonhydrostatic model

This is given by Clark and Hall (1988). This hydrostatic version has not been implemented in the model yet. In hydrostatic approximation, the momentum equation for w is changed as

$$\frac{1}{G^{1/2}}\frac{\partial P}{\partial \xi} + \frac{gP}{Cs^2} = \mathrm{BUOY} \tag{2-12}$$

for $k = 1 + 1/2,\ 2 + 1/2 \ldots nz - 1/2$,

(for nz and the index k used in finite discretization form, see B-5).

The vertical velocity is diagnostically determined by use of Eq. (1-30b) with $\sigma = 0$. Eq. (2-12) alone is not sufficient for the diagnostic equation for pressure. The horizontal equations of motion are combined with the anelastic continuity equation (1-30b) with $\sigma = 0$ to form

$$\frac{\partial^2 P}{\partial x^2} + \frac{\partial^2}{\partial x \partial \xi}(G^{13}P) = -\mathrm{DIVS}(\mathrm{ADVU},\ 0) + \frac{1}{2\Delta t}\frac{\partial (W^{*it+1} - W^{*it-1})}{\partial \xi} \tag{2-13}$$

for $k = 2,\ 3, \ldots, nz - 1$.

Summing Eq. (2-13) over the vertical column results in the following diagnostic column pressure equation:

$$\frac{\partial^2(\sum^k \Delta z_k P_k)}{\partial x^2} + \frac{\partial}{\partial x}[(G^{13}\overline{P}^{xz})_{k=nz} - (G^{13}\overline{P}^{xz})_{k=1}]$$
$$= -\sum^k \mathrm{DIVS(ADVU,\ 0)}_k \Delta z_k + \frac{(W^{*it+1} - W^{*it-1})_{nz} - (W^{*it+1} - W^{*it-1})_1}{2\Delta t}. \quad (2\text{-}14)$$

For the definition of the space averaging operator $-xz$, see B-5-3. W^* at the lower and upper boundaries must be specified from outside.

The diagnostic pressure equations, (2-12) and (2-14) can be solved as follows: From Eq. (2-12), P_k $(k > 1)$ can be expressed as

$$P_k = a_k P_1 + b_k. \quad \text{for} \quad 1 < k \leqq nz.$$

Substitution of them into Eq. (2-14) results in the horizontal elliptic equation for P_1.

In this system, no external gravity waves are allowed, if the upper boundary condition is the rigid wall condition as is often used. On the other hand, the primitive (hydrostatic) equations currently used in many operational forecasting centers have the prognostic equation for the surface pressure and allow the external gravity waves, because the free upper surface is used instead of the rigid wall. The nesting of the hydrostatic version of the anelastic model into the primitive model may have difficulty in this point.

B-3. E-HI-VI (elastic-horizontally implicit-vertically implicit) scheme

In this scheme, sound waves are included, and the equations in B-1-3 with substitution of $\sigma = 1$ and $\rho = \overline{\rho}$ are used. In the time integration, terms related to sound waves are treated implicitly in both the horizontal and the vertical directions.

B-3-1. Formulation with $\overline{P}^t$ as unknown variables

Carpenter (1979) extended the non-orographic E-HI-VI of Tapp and White (1976) to that with orography, having slightly different governing equations from the present E-HI-VI. In this section, three kinds of E-HI-VI are formulated, *i.e.*, E-HI-VI-FI (full iteration, fully implicit), E-HI-VI-PI (partial iteration, partially implicit) and E-HI-VI-NI (no iteration, partially implicit).

a) E-HI-VI-FI

First, the E-HI-VI-FI is considered by handling all terms associated with sound waves implicitly as follows:

$$\delta_t U + \frac{\partial}{\partial x}\overline{P}^t + \frac{\partial}{\partial \xi}(G^{13}\overline{P}^t) = -\mathrm{ADVU}, \tag{3-1}$$

$$\delta_t W + \frac{1}{G^{1/2}}\frac{\partial \overline{P}^t}{\partial \xi} + \frac{g\overline{P}^t}{Cs^2} = \mathrm{BUOY} - \mathrm{ADVW}, \tag{3-2}$$

$$\delta_t P + Cs^2 \mathrm{DIVT}(\overline{U}^t, \overline{W}^t) = Cs^2 \mathrm{PFT} \tag{3-3a}$$

$$\frac{1}{Cs^2}\delta_t P + \frac{\partial}{\partial x}\overline{U}^t + \frac{1}{G^{1/2}}\frac{\partial \overline{W}^t}{\partial \xi} + \frac{\partial}{\partial \xi}(G^{13}\overline{U}^t) = \mathrm{PFT}, \tag{3-3b}$$

$$\overline{f}^t = \frac{1+\alpha}{2} f^{it+1} + \frac{1-\alpha}{2} f^{it-1}, \tag{3-4}$$

and

$$\delta_t f = \frac{f^{it+1} - f^{it-1}}{2\Delta t}, \tag{3-5}$$

where f^{it} indicates the value of f at the '*it*' time step, α is a constant parameter for time averaging and an operator DIVT is defined by Eq. (2-3).

The upper and lower conditions are the same as Eq. (2-7). In these equations, $\overline{P}^t$, $\overline{U}^t$ and $\overline{W}^t$ are regarded as unknown variables. After some manipulation, the equation of $\overline{P}^t$ is obtained, which is similar to the pressure equation of AE. To solve the equation, an iterative method must be needed. Then, E-HI-VI-FI (see section B-3-3) has no advantage in simplicity of solving the elliptic equation over the AE scheme.

b) E-HI-VI-PI

Next, formulation of E-HI-VI-PI is made by handling the part of terms associated with sound waves implicitly as follows:

$$\delta_t U + \frac{\partial}{\partial x}\overline{P}^t = -\mathrm{ADVU} - \frac{\partial}{\partial \xi}(G^{13}P), \tag{3-6}$$

$$\begin{aligned}\delta_t W + \frac{\widetilde{1}}{G^{1/2}}\frac{\partial \overline{P}^t}{\partial \xi} + \frac{\widetilde{g}}{Cs^2}\overline{P}^t = \mathrm{BUOY} - \mathrm{ADVW} + \left(\frac{\widetilde{1}}{G^{1/2}}\frac{\partial}{\partial \xi} - \frac{1}{G^{1/2}}\frac{\partial}{\partial \xi}\right)P \\ + \left(\frac{\widetilde{g}}{Cs^2} - \frac{g}{Cs^2}\right)P,\end{aligned} \tag{3-7}$$

and

$$\delta_t P + Cs^2\mathrm{DIVS}(\overline{U}^t, \overline{W}^t) = Cs^2(\mathrm{PFT} - \mathrm{DIVR}(U, W)) \tag{3-8a}$$

$$\frac{1}{Cs^2}\delta_t P + \frac{\partial}{\partial x}\overline{U}^t + \frac{\widetilde{1}}{G^{1/2}}\frac{\partial \overline{W}^t}{\partial \xi} = \mathrm{PFT} + \left(\frac{\widetilde{1}}{G^{1/2}} - \frac{1}{G^{1/2}}\right)\frac{\partial W}{\partial \xi} - \frac{\partial}{\partial \xi}(G^{13}U). \tag{3-8b}$$

Here, operators DIVR and DIVS are defined by Eqs. (2-1) and (2-2). From Eqs. (2-7), (3-6) and (3-7), boundary conditions are obtained as follows:

$$\frac{\widetilde{1}}{G^{1/2}}\frac{\partial \overline{P}^t}{\partial \xi} + \frac{\widetilde{g}}{Cs^2}\overline{P}^t + G^{1/2}G^{13}\frac{\partial}{\partial x}\overline{P}^t = \mathrm{FPBE}. \tag{3-9}$$

All terms on the righthand sides of Eqs. (3-6), (3-7), (3-8) and (3-9) are known. $\overline{P}^t$, $\overline{U}^t$ and $\overline{W}^t$ are regarded as unknown variables, and the equation for $\overline{P}^t$ is obtained, which is similar to that of AE for the case of no-orography, except for the boundary conditions. However, the boundary condition Eq. (3-9) requires iteration since $G^{1/2}G^{13}$ is dependent on both x and ξ.

c) E-HI-VI-NI

To avoid iteration completely, a slight change in the boundary condition Eq. (3-9) is made as follows:

$$\frac{\widetilde{1}}{G^{1/2}}\frac{\partial \overline{P}^t}{\partial \xi}+\frac{\widetilde{g}}{Cs^2}\overline{P}^t=-G^{1/2}G^{13}\frac{\partial}{\partial x}P+\mathrm{FPBE}. \tag{3-10}$$

The elliptic equation for $\overline{P}^t$ obtained from Eqs. (3-6), (3-7), (3-8) and (3-10) needs no iteration. However, this boundary condition is not consistent with Eqs. (2-7), (3-6), (3-7) and (3-8) unless U at the lower boundary is always zero due to the non-slip condition at the lower boundary, and imposes erroneous forcing at the boundary which is large for a steep slope. This method will be called E-HI-VI-NI hereafter.

d). Discussion on the stability of E-HI-VI scheme

If the mountain is very high or steep, the terms associated with sound waves, which are transferred to the righthand sides for convenience, become large in both E-HI-VI-PI and E-HI-VI-NI. For E-HI-VI-NI, the boundary condition, Eq. (3-8), is not exact for the free-slip lower boundary condition. Kurihara (1965) examined the instability of a partially implicit method for a simple hyperbolic equation. The partially semi-implicit method for the primitive equations has experienced instability for the case in which the deviation from the basic reference state is large (Simmons *et al.*, 1978). The conjecture that E-HI-VI-PI and E-HI-VI-NI are subject to instability should be checked in a linear stability analysis and numerical experiments.

The linear stability analysis for sound waves in a nonorographic E-HI-VI for the case of $\alpha=0$ was given by Tapp and White (1976). That of E-HI-VI-PI for $0<\alpha<1$ with orography will be given in the next subsection B-3-2, where both acoustic and gravity wave modes are taken into account simultaneously. The analysis for only the sound waves shows that, in the case of orography incorporated, $\alpha=0$ causes an instability, and $\alpha>0$ becomes necessary. However, for a very steep mountain, E-HI-VI-PI is found unstable, no matter what value of α is chosen in the range $0 \leqq \alpha \leqq 1$. The analysis for both fast and slow modes shows that a weak destabilization occurs even for the case which is shown to be stable by a linear analysis taking into account only sound waves. However, Asselin's (1972) time filter works effectively to suppress this weak destabilization.

B-3-2. A linear stability analysis of E-HI-VI-PI with orography

In order to conduct a linear analysis, we simplify the governing equations ((3-6)–(3-9)) of E-HI-VI-PI as follows:

$$\frac{1}{Cs^2}\delta_t P + \frac{\partial}{\partial x}\overline{U}^t + \frac{\partial \overline{W}^t}{\partial \xi} = -\Delta H \frac{\partial W}{\partial \xi} - \Delta G \frac{\partial \overline{U}^{x\xi}}{\partial \xi}, \tag{3-11}^\dagger$$

$$\delta_t U + \frac{\partial}{\partial x}\overline{P}^t = -U_m \frac{\partial U}{\partial x} - \Delta G \frac{\partial}{\partial \xi}\overline{P}^{x\xi}, \tag{3-12}$$

$$\delta_t W + \frac{\partial \overline{P}^t}{\partial \xi} = N\Theta'' - \Delta H \frac{\partial P}{\partial \xi} - U_m \frac{\partial W}{\partial x}, \tag{3-13}$$

$$\delta_t \Theta'' = -NW - U_m \frac{\partial \Theta''}{\partial x}, \tag{3-14}$$

$$\Theta'' = (\Theta'/N)(g\overline{\rho}/\overline{\Theta}), \tag{3-15}$$

where U_m is the constant of the basic state wind velocity, N the Brunt-Väisälä frequency defined as $N^2 \equiv g(\partial\Theta/\partial z)/\Theta$, $\Delta H \equiv [1/(1 - Z_s/H) - 1]$ a measure of mountain height, $\Delta G \equiv G^{13}$ a measure of mountain steepness.

The grid structure is a staggered one, as in Clark (1977) (see section B-5). We substitute the finite difference operators as follows:

$$\left.\begin{aligned}
\frac{\partial}{\partial x} &\longrightarrow ik_x{}^* = i\frac{2\sin(k_x \Delta x/2)}{\Delta x},\\
\frac{\partial}{\partial \xi} &\longrightarrow ik_z{}^* = i\frac{2\sin(k_z \Delta \xi/2)}{\Delta \xi},\\
\frac{\partial^{-x\xi}}{\partial \xi} &\longrightarrow ik_z{}^{**} = i\frac{\sin(k_z \Delta\xi)\cos(k_x \Delta\chi)}{\Delta \xi},
\end{aligned}\right\} \tag{3-16}$$

where k_x and k_z are horizontal and vertical wave numbers respectively, and $\Delta\chi$ and $\Delta\xi$ are horizontal and vertical grid distances respectively, and $i^2 = -1$.

† Eq. (3-11) should be replaced by

$$\frac{1}{Cs^2}\delta_t P + \frac{\partial}{\partial x}\overline{U}^t + \frac{\partial \overline{W}^t}{\partial \xi} = -\frac{N^2}{g}\left[W + \frac{U_m}{N}\frac{\partial \Theta''}{\partial x}\right] - \Delta H \frac{\partial W}{\partial \xi} - \Delta G \frac{\partial \overline{U}^{x\xi}}{\partial \xi}.$$

Ikawa (1988) used Eq. (3-11) by mistake. The additional term is assumed to be related to slow modes in the program, and this term is expected to bring about little difference in the qualitative conclusion of the linear analysis made by Ikawa (1988). This expectation is supported by the recent linear analysis made by Gohda and Kurihara (1991).

The equations (3-11)–(3-14) are rewritten in matrix form as follows:

$$S^{it+1} = (\boldsymbol{A} + 2\Delta t\boldsymbol{C})^{-1}\boldsymbol{B}S^{it} + (\boldsymbol{A} + 2\Delta t\boldsymbol{C})^{-1}(\boldsymbol{A} - 2\Delta t\boldsymbol{D})S^{it-1} \tag{3-17}$$

where

$$\left.\begin{aligned}
&(S^{it})^{tr} = (P^{it},\ U^{it},\ W^{it},\ \Theta''^{it}) \\
&\boldsymbol{A} \equiv \begin{bmatrix} 1/Cs^2 & 0 & 0 & 0 \\ 0 & 1 & 0 & 0 \\ 0 & 0 & 1 & 0 \\ 0 & 0 & 0 & 1 \end{bmatrix}, \\
&\boldsymbol{B} \equiv 2\Delta t \begin{bmatrix} 0 & -\Delta G i k_z{}^{**} & -\Delta H i k_z{}^{*} & 0 \\ -\Delta G i k_z{}^{**} & -U_m i k_x{}^{*} & 0 & 0 \\ -\Delta H i k_z{}^{*} & 0 & -U_m i k_x{}^{*} & N \\ 0 & 0 & -N & -U_m i k_x{}^{*} \end{bmatrix}, \\
&\boldsymbol{C} \equiv \frac{(1+\alpha)}{2} \begin{bmatrix} 0 & i k_x{}^{*} & i k_z{}^{*} & 0 \\ i k_x{}^{*} & 0 & 0 & 0 \\ i k_z{}^{*} & 0 & 0 & 0 \\ 0 & 0 & 0 & 0 \end{bmatrix}, \\
&\boldsymbol{D} \equiv (1-\alpha)/(1+\alpha)\boldsymbol{C},
\end{aligned}\right\} \tag{3-18}$$

where superscript ^{tr} denotes the transposed matrix.

If we use Asselin's time filter

$$S^{*it} = S^{it} + \nu(S^{it+1} - 2S^{it} + S^{*it-1}), \tag{3-19}$$

Eq. (3-17) is modified as follows:

$$\begin{bmatrix} S^{it+1} \\ S^{*it} \end{bmatrix} = \begin{bmatrix} (\boldsymbol{A} + 2\Delta t\boldsymbol{C})^{-1}\boldsymbol{B} & (\boldsymbol{A} + 2\Delta t\boldsymbol{C})^{-1}(\boldsymbol{A} - 2\Delta t\boldsymbol{D}) \\ (1-2\nu)\boldsymbol{I} + \nu(\boldsymbol{A}+2\Delta t\boldsymbol{C})^{-1}\boldsymbol{B} & \nu(\boldsymbol{I} + (\boldsymbol{A}+2\Delta t\boldsymbol{C})^{-1}(\boldsymbol{A}-2\Delta t\boldsymbol{D})) \end{bmatrix} \begin{bmatrix} S^{it} \\ S^{*it-1} \end{bmatrix} \tag{3-20}$$

The amplification factor is the eigenvalue of the (8×8) matrix in Eq. (3-20), and satisfies the 8-th order algebraic equation.

For the case of $N = 0$, $U_m = 0$ and $\nu = 0$ (*i.e.*, only the acoustic mode is considered without Asselin's time filter), the characteristic equation is factorized into $(\lambda^2 - 1)^2$ and the 4-th order algebraic equation with real number coefficients which are given as below:

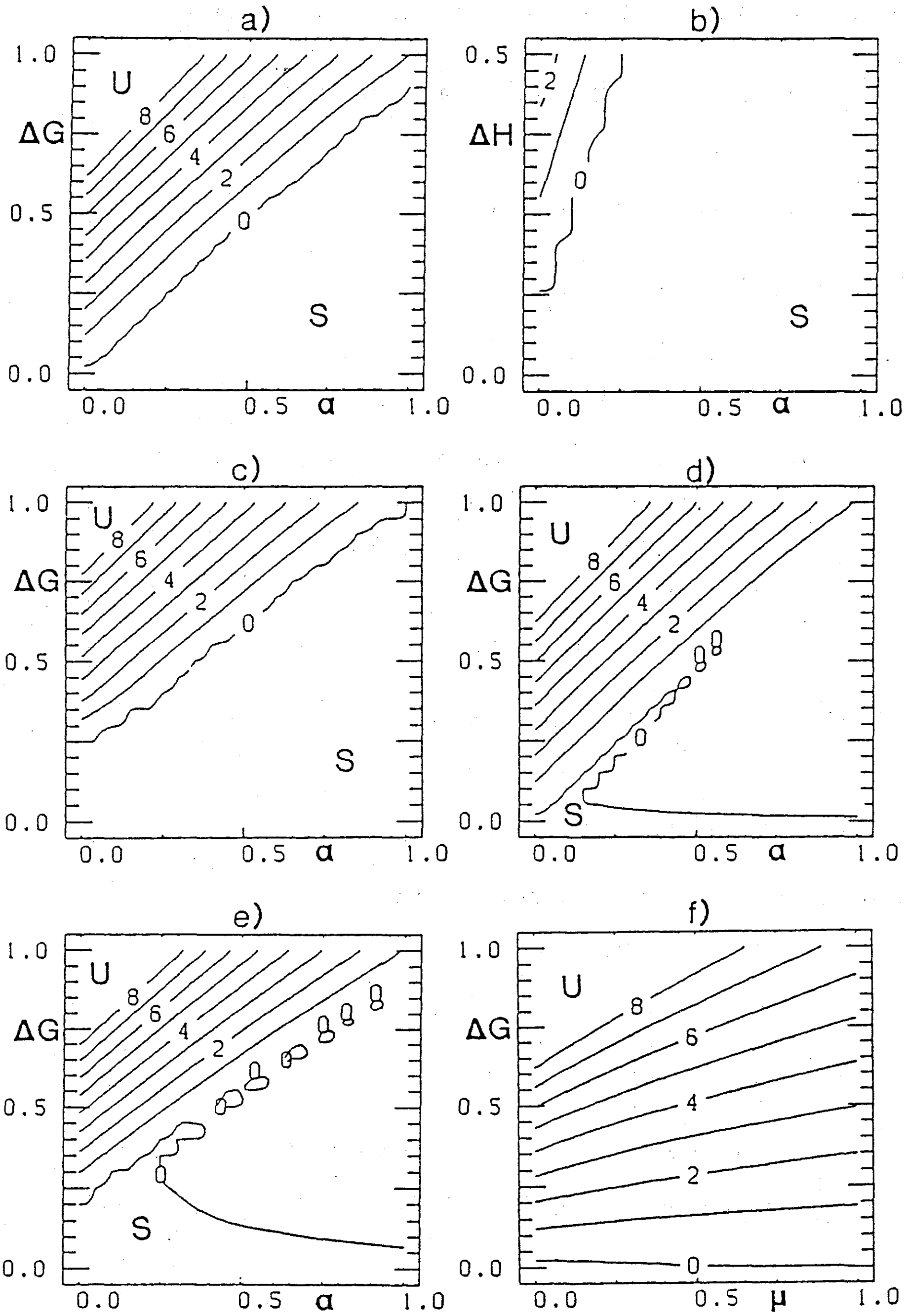

Fig. B-3-1 a, b, c, d, e, f) Amplification factor $|\lambda|$ of E-HI-VI. The horizontal axis indicates α varying from 0 to 1 with intervals of 0.05. The vertical axis indicates $\Delta G = 2\Delta H$ varying from 0 to 1 with intervals of 0.05 unless specifically mentioned. The maximum amplification factor among the cases of $k_x = 2\pi/\Delta x(i/20)$ (from $i = -20$ to 20) and $k_z = 2\pi/\Delta\xi(j/20)$ (from $j = -20$ to 20) is plotted. The contour line numbered by the integer n denotes $|\lambda| = 1 + n \times 0.1$ (the contour interval Δn is 1). The area of $|\lambda| < 1.00009$ is indicated by S. **a)** The case of $N = U_m = 0$,

$\nu = 0$; analytic solution. **b)** The case of $N = U_m = 0$, $\nu = 0$ and $\Delta G = 0$; Vertical axis indicates ΔH, varying from 0 to 0.5; analytic solution. **c)** The same as a) but for $\Delta t = 2$ sec; analytic solution. **d)** The case of $N = 10^{-2}$/s, $U_m = 4$m/s and $\nu = 0$; numerical solution. **e)** The case of $N = 10^{-2}$/s, $U_m = 4$m/s and $\nu = 0.2$; numerical solution. **f)** The case of time averaging by Eq. (3-22), $N = U_m = 0$, $\nu = 0$; numerical solution. The horizontal axis indicates μ varying from 0 to 1 with intervals of 0.05. (adapted from Ikawa, 1988)

$$\left[1+\left(\frac{1+\alpha}{2}\right)^2 X\right]\lambda^4 + (Cs2\Delta t)^2(1+\alpha)(k_x{}^*k_z{}^{**}\Delta G + k_z{}^{*2}\Delta H)\lambda^3$$
$$+2\left[-1+\left(\frac{1+\alpha}{2}\right)\left(\frac{1-\alpha}{2}\right)X + \frac{(\Delta G k_z{}^{**})^2 + (\Delta H k_z{}^*)^2}{2}(Cs2\Delta t)^2\right]\lambda^2$$
$$+(Cs2\Delta t)^2(1-\alpha)(k_x{}^*k_z{}^{**}\Delta G + k_z{}^{*2}\Delta H)\lambda + 1 + \left(\frac{1-\alpha}{2}\right)^2 X = 0, \qquad (3\text{-}21)$$

where $X = (Cs2\Delta t)^2(k_z{}^{*2} + k_x{}^{*2})$. This equation can be solved analytically by Ferrari method†. In case of $\Delta G = \Delta H = 0$ (without orography), we see that the scheme is unconditionally stable; $\alpha > 0$ gives damping of sound wave mode, and $\alpha = 0$ gives neither damping nor amplification.

Now, we examine the dependence of stability on α, ΔH and ΔG. Hereafter, parameters $\Delta\chi$, $\Delta\xi$, Δt, Cs, N and U_m are 1200m, 200m, 12s, 340m/s, 0.01/s, 4m/s, respectively, which are the same as were used in the experiments in section 3 of Ikawa (1988). If orography is included, as shown in Fig. B-3-1a, $\alpha = 0$ gives amplification, and $\alpha > 0$ becomes necessary for stable time integration. When the ($\Delta H = a$, $\Delta G = 0$) case (Fig. B-3-1b) is compared with the ($2\Delta H = 0$, $\Delta G = a$) case (not shown here) or ($2\Delta H = a$, $\Delta G = a$) (Fig. B-3-1a) with $0 \leqq a \leqq 1.0$, the destabilized area of the case of ($2\Delta H = a$, $\Delta G = 0$) is small. So, it might be said that the steepness (ΔG) destabilizes the shcheme more than the height ($2\Delta H$) does. As shown in Fig. B-3-1c, this instability is not suppressed much by a smaller Δt, especially for $\Delta G > 0.5$.

For the case of $N \neq 0$, $U_m \neq 0$ and $\nu \neq 0$ (*i.e.*, both the gravity wave and the acoustic modes are considered with Asselin's time filter), the amplification factor is obtained numerically††. The accuracy of this numerical procedure was checked against the analytical

†HITAC mathematical subprogram library 2: subroutine ¥DNAQM is used.

††HITAC mathematical subprogram library 2: subroutine ¥ZEFIM is used. First, the matrix is similarly transformed in Hessenberg form. Next, eigenvalues of the Hessenberg matrix are solved by the modified LR method with double precision calculation, where 'L' and 'R' denote lower and upper triangular matrices, respectively.

solution by Ferrari method for the case of $N = 0$, $U_m = 0$ and $\nu = 0$. The difference between the two was found to be below 2×10^{-6}. As shown in Fig. B-3-1d, the inclusion of the slow mode gives a small amplification ($|\lambda| \geqq 1.001$) even if $\alpha > 0$ is used. However, as shown in Fig. B-3-1e, an appropriate Asselin's time filter can reduce the amplification factor below $|\lambda| \leqq 1.00009$ which may cause no trouble in practice. It is noted that, for the case of a very high or very steep mountain ($2\Delta H = \Delta G = a,\ 1 \leqq a$), no $\alpha\,(0 \leqq\alpha\leqq 1)$ or $\nu\,(0 \leqq\nu\leqq 1)$ can reduce $|\lambda|$ below 1.01 ($\alpha > 1$ degrades the accuracy, so is not considered here). ΔH can be decreased by increasing the height of the model domain H. Therefore, in principle, E-HI-VI-PI cannot be used for the case of a very steep mountain ($\Delta G \geqq 1$). This imposes a severe limitation on E-HI-VI-PI, as contrasted with E-HE-VI (see B-4-2).

A different time averaging from the present one Eq. (3-4) such as

$$\overline{f}^{t} = \frac{1+\mu}{2}\left(f^{it+1} + f^{it-1}\right) - \mu f^{it} \tag{3-22}$$

was proposed by Simmons *et al.* (1978) in order to prevent the instability of a partially semi-implicit method for primitive equations. However, as shown in Fig. B-3-1f, their time averaging is not applicable to the present case. The time averaging is equivalent to the present case of $N = 0$ and $U_m = 0$, if the parameters are set as follows:

$$\begin{aligned}
&\alpha = 0, \\
&\Delta t \longrightarrow (1+\mu)\Delta t, \\
&\Delta H\ ikz^{*} \longrightarrow ikz^{*}\ (\Delta H - \mu)/(1+\mu) \\
&\Delta G\ ikz^{**} \longrightarrow (\Delta G\ ikz^{**} - i\mu\ kx^{*})/(1+\mu).
\end{aligned}$$

Therefore, the method can reduce ΔH, but not ΔG. The effective ΔG depends on $(kx^{*},\ kz^{**})$ and may have larger values than original ones for some $(kx^{*}\ , kz^{**})$. Usually, at both slopes of an isolated mountain in the model, the sign of ΔG (steepness of a mountain) is opposite to each other and the magnitude of ΔG is almost equal to each other. $\alpha = 0$ and a large ΔG cause instability. This is the reason for the futility of the time averaging Eq. (3-22).

B-3-3. E-HI-VI-PI with $\Delta^2 P$ adopted as an unknown variable

In the program, $\Delta^2 P$, $\Delta^2 U$ and $\Delta^2 W$ are adopted instead of P, U and W as unknown variables in coding E-HI-VI schemes, following Tapp and White (1976). The operator Δ^2 is defined for any predicted variable f as

$$\Delta^2 f = 2\overline{f}^{t} - 2f^{it}, \tag{3-23}$$

$$\overline{f}^t = \frac{1+\alpha}{2} f^{it+1} + \frac{1-\alpha}{2} f^{it-1} = \Delta^2 f/2 + f^{it}, \tag{3-24}$$

$$\begin{aligned}\delta_t f &= \frac{f^{it+1} - f^{it-1}}{2\Delta t} = \frac{\Delta^2 f}{2\Delta t\alpha''} + \frac{(f^{it} - f^{it-1})}{\alpha''\Delta t} \\ &= \frac{2}{\Delta t\alpha''}(\overline{f}^t - f^{it-1}),\end{aligned} \tag{3-25}$$

$$\alpha'' = 1 + \alpha. \tag{3-26}$$

Prognostic equations for U, W and P are given in terms of $\overline{P}^t$, $\overline{U}^t$ and $\overline{W}^t$ as follows:

$$\delta_t U + \frac{\partial}{\partial x}\overline{P}^t = -\mathrm{ADVU} - \frac{\partial}{\partial \xi}(G^{13}P), \tag{3-27}$$

$$\begin{aligned}&\delta_t W + \frac{\tilde{1}}{G^{1/2}}\frac{\partial \overline{P}^t}{\partial \xi} + \frac{\tilde{g}}{\tilde{C}s^2}\overline{P}^t \\ &= \mathrm{BUOY} - \mathrm{ADVW} + \left(\frac{\tilde{1}}{G^{1/2}} - \frac{1}{G^{1/2}}\right)\frac{\partial P}{\partial \xi} + \left(\frac{\tilde{g}}{\tilde{C}s^2} - \frac{g}{Cs^2}\right)P,\end{aligned} \tag{3-28}$$

and

$$\delta_t P + \tilde{C}s^2\mathrm{DIVS}(\overline{U}^t, \overline{W}^t) = Cs^2(\mathrm{PFT} - \mathrm{DIVT}(U, W)) + \tilde{C}s^2\mathrm{DIVS}(U, W). \tag{3-29}$$

Here, the operators DIVT and DIVS are defined by Eqs. (2-3) and (2-2). The above equations are rewritten in terms of $\Delta^2 P$, $\Delta^2 U$ and $\Delta^2 W$ as follows:

$$\frac{\Delta^2 W}{\Delta t\alpha''} + \left(\frac{\tilde{1}}{G^{1/2}}\frac{\partial}{\partial \xi} + \frac{\tilde{g}}{\tilde{C}s^2}\right)\Delta^2 P = -2\mathrm{ADVW}'', \tag{3-30}$$

$$\mathrm{ADVW}'' \equiv \mathrm{ADVW} - \mathrm{BUOY} + \frac{W^{it} - W^{it-1}}{\Delta t\alpha''} + \left(\frac{1}{G^{1/2}}\frac{\partial}{\partial \xi} + \frac{g}{Cs^2}\right)P^{it}. \tag{3-31}$$

$$\frac{\Delta^2 U}{\Delta t\alpha''} + \frac{\partial}{\partial x}\Delta^2 P = -2\mathrm{ADVU}'', \tag{3-32}$$

$$\mathrm{ADVU}'' \equiv \mathrm{ADVU} + \frac{(U^{it} - U^{it-1})}{\Delta t\alpha''} + \frac{\partial P^{it}}{\partial x} + \frac{\partial(G^{13}P^{it})}{\partial \xi}. \tag{3-33}$$

$$\frac{\Delta^2 P}{\tilde{C}s^2\alpha''\Delta t} + \mathrm{DIVS}(\Delta^2 U, \Delta^2 W) = -2\mathrm{ADVP}'', \tag{3-34}$$

$$\mathrm{ADVP}'' \equiv \left(\frac{P^{it} - P^{it-1}}{\Delta t\alpha''} - Cs^2(\mathrm{PFT} - \mathrm{DIVT}(U, W))\right) \Big/ \tilde{C}s^2. \tag{3-35}$$

Helmholtz equation for $\Delta^2 P$ is obtained by eliminating $\Delta^2 U$ and $\Delta^2 W$ in Eq. (3-34) by use of Eqs. (3-30) and (3-32) as follows:

$$\frac{\Delta^2 P}{(\widetilde{C}s\alpha''\Delta t)^2}-\frac{\partial^2}{\partial x^2}\Delta^2 P-\frac{\widetilde{1}}{G^{1/2}}\frac{\partial}{\partial\xi}\left(\frac{\widetilde{1}}{G^{1/2}}\frac{\partial}{\partial\xi}+\frac{\widetilde{g}}{Cs^2}\right)\Delta^2 P$$

$$=\mathrm{FP.HIP.INV}\equiv-2\left(\frac{\mathrm{ADVP}''}{\Delta t\alpha''}-\mathrm{DIVS}\,(\mathrm{ADVU}'',\ \mathrm{ADVW}'')\right). \tag{3-36}$$

It is noted that the forcing term for the pressure equation, FP.HIP.INV, includes no $\Delta^2 P$. Therefore iteration is not needed from this part. Iteration is needed in order to incorporate exactly the upper and lower boundary conditions.

The upper and lower boundary conditions for E-HI-VI-PI are derived as follows. From Eq. (2-7).

$$\Delta^2 W^*=0=\frac{1}{G^{1/2}}\Delta^2 W+G^{13}\Delta^2 U. \tag{3-37}$$

Eliminating $\Delta^2 U$ and $\Delta^2 W$ from Eq. (3-37) by use of Eqs. (3-30) and (3-32) yields

$$\left(\frac{\widetilde{1}}{G^{1/2}}\frac{\partial}{\partial\xi}+\frac{\widetilde{g}}{Cs^2}\right)\Delta^2 P=-2\,(\mathrm{ADVW}''+G^{1/2}G^{13}\mathrm{ADVU}'')-G^{1/2}G^{13}\frac{\partial}{\partial x}\Delta^2 P. \tag{3-38}$$

For the iteration procedure, the above equation is written as

$$\left(\frac{\widetilde{1}}{G^{1/2}}\frac{\partial}{\partial\xi}+\frac{\widetilde{g}}{Cs^2}\right)\Delta^2 P_i=\mathrm{FPB.HIP.INV}+\mathrm{FPB.HIP.VAR}\ (P_{i-1}), \tag{3-39}$$

$$\mathrm{FPB.HIP.INV}=-2\,(\mathrm{ADVW}''+G^{1/2}G^{13}\mathrm{ADVU}''), \tag{3-40}$$

$$\mathrm{FPB.HIP.VAR}\,(P_{i-1})=-G^{1/2}G^{13}\frac{\partial}{\partial x}\Delta^2 P_{i-1}. \tag{3-41}$$

Here, suffix i denotes the value at the i-th iteration. Eqs. (3-36) and (3-39) are solved by an iterative application of the pressure equation solver mentioned in section B-6.

Program Guide

ADVU″, ADVW″ and ADVP″ are set in sub.MODADV in mem.SFXCV. FP.HIP.INV is set in sub.SPFORI in mem.SFXTPG1. FPB.HIP is set in sub.SFPBD and SPFCBD in mem.SFXTPG1.

B-3-4. Implicit treatment of gravity waves in addition to sound waves

Recently, Tanguay *et al.* (1990), Cullen (1990) and Gouda and Kurihara (1991) independently proposed E-HI-VI schemes which treat implicitly not only sound waves but also gravity waves. In these schemes, a longer time step can be taken with little computational overhead than an ordinary E-HI-VI scheme. However, these schemes artificially reduce frequencies of gravity wave oscillations which may be of meteorological interest. Here, this version of an E-HI-VI scheme is formulated, although it is not implemented at present.

Prognostic equations for U, W, P and $\theta' \equiv \Theta - \overline{\Theta}(z)$ are given in terms of $\overline{P}^t$, $\overline{U}^t$ $\overline{W}^t$ and $\overline{\theta}'^t$ as follows:

$$\delta_t U + \frac{\partial}{\partial x}\overline{P}^t = -\mathrm{ADVU} - \frac{\partial}{\partial \xi}(G^{13}P), \tag{3-42}$$

$$\delta_t W + \frac{\tilde{1}}{G^{1/2}}\frac{\partial \overline{P}^t}{\partial \xi} + \sigma_g g\left(\frac{\tilde{1}}{Cs^2}\overline{P}^t - \frac{\rho G^{1/2}\overline{\theta}'^t}{\overline{\Theta}}\right)$$
$$= -gG^{1/2}(\rho - \overline{\rho}) - \mathrm{ADVW} + \left(\frac{\tilde{1}}{G^{1/2}} - \frac{1}{G^{1/2}}\right)\frac{\partial P}{\partial \xi} + \sigma_g g\left(\frac{\tilde{1}}{Cs^2}P - \frac{\rho G^{1/2}\theta'}{\overline{\Theta}}\right) \tag{3-43}$$

$$\rho \equiv \frac{p_0}{R\Theta_m}\left(\frac{\overline{p} + P/G^{1/2}}{p_0}\right)^{C_v/C_p}, \tag{3-44a}$$

$$N^2 \equiv \frac{g}{\overline{\Theta}(z)\partial z}\frac{\partial\overline{\Theta}(z)}{}, \tag{3-44b}$$

$$\rho G^{1/2}\frac{\partial \theta'}{\partial t} + \sigma_g\frac{N^2}{g}\overline{\Theta}(z)\overline{W}^t = -\rho G^{1/2}(\mathrm{ADV}\Theta - \mathrm{DIF}.\Theta - Q/C_p\Pi) + \sigma_g\frac{N^2}{g}\overline{\Theta}(z)W, \tag{3-45}$$

and

$$\delta_t P + \tilde{C}s^2\left(\mathrm{DIVS}\,(\overline{U}^t, \overline{W}^t) + \sigma_g\frac{N^2}{g}\overline{W}^t\right)$$
$$= Cs^2(\mathrm{PFT} - \mathrm{DIVT}\,(U,W)) + \tilde{C}s^2\left(\mathrm{DIVS}\,(U,W) + \sigma_g\frac{N^2}{g}W\right), \tag{3-46}$$

$$\mathrm{PFT} \equiv \frac{\rho G^{1/2}}{\Theta_m}\frac{\partial \Theta'_m}{\partial t} \simeq \frac{\rho G^{1/2}}{\overline{\Theta}}\frac{\partial \theta'}{\partial t} = \frac{\rho G^{1/2}(-\mathrm{ADV}\Theta + \mathrm{DIF}.\Theta + Q/Cp\Pi)}{\overline{\Theta}}$$

σ_g is a switching parameter; $\sigma_g = 1$ for implicit treatment of gravity waves; $\sigma_g = 0$ for explicit treatment of gravity waves. The operators DIVT and DIVS are defined by Eqs. (2-1) and (2-2). It is noted that the exact buoyancy term $-g(\rho - \overline{\rho})$ is employed instead of the approximated term by linearization around the basic state. Replacing $\overline{\rho}$ in Eqs. (1-30)–(1-37) by ρ given by Eq. (3-44) eliminates errors associated with the advection term shown in Eq. (1-24).

The above equations are rewritten in terms of $\Delta^2 P$, $\Delta^2 U$, $\Delta^2 W$ and $\Delta^2\theta'$ as follows:

$$\frac{\Delta^2 W}{\Delta t\alpha''}+\left(\frac{\widetilde{1}}{G^{1/2}}\frac{\partial}{\partial\xi}+\frac{\sigma_g\widetilde{g}}{Cs^2}\right)\Delta^2 P-\frac{\sigma_g g\rho G^{1/2}\Delta^2\theta'}{\overline{\Theta}}=-2\mathrm{ADVW}'' \tag{3-47}$$

$$\mathrm{ADVW}''\equiv\mathrm{ADVW}+gG^{1/2}(\rho-\overline{\rho})+\frac{W^{it}-W^{it-1}}{\Delta t\alpha''}+\frac{1}{G^{1/2}}\frac{\partial}{\partial\xi}P^{it}. \tag{3-48}$$

$$\rho G^{1/2}\frac{\Delta^2\theta'}{\Delta t\alpha''}+\frac{\sigma_g N^2}{g}\overline{\Theta}(z)\Delta^2 W=-2\mathrm{ADV}\theta'' \tag{3-49}$$

$$\mathrm{ADV}\theta''\equiv\rho G^{1/2}\left(\mathrm{ADV}\Theta-\mathrm{DIF.}\Theta-\frac{Q}{Cp\Pi}+\frac{\theta'^{it}-\theta'^{it-1}}{\Delta t\alpha''}\right). \tag{3-50}$$

$$\frac{\Delta^2 U}{\Delta t\alpha''}+\frac{\partial}{\partial x}\Delta^2 P=-2\mathrm{ADVU}'', \tag{3-51}$$

$$\mathrm{ADVU}''\equiv\mathrm{ADVU}+\frac{(U^{it}-U^{it-1})}{\Delta t\alpha''}+\frac{\partial P^{it}}{\partial x}+\frac{\partial(G^{13}P^{it})}{\partial\xi}. \tag{3-52}$$

$$\frac{\Delta^2 P}{\widetilde{C}s^2\alpha''\Delta t}+\mathrm{DIVS}\,(\Delta^2 U,\Delta^2 W)+\frac{\sigma_g N^2}{g}\Delta^2 W=-2\mathrm{ADVP}'' \tag{3-53}$$

$$\mathrm{ADVP}''\equiv\left(\frac{P^{it}-P^{it-1}}{\Delta t\alpha''}-Cs^2(\mathrm{PFT}-\mathrm{DIVT}\,(U,\ W)\right)\Big/\widetilde{C}s^2 \tag{3-54}$$

Eliminating $\Delta^2\theta'$ from Eqs. (3-47) and (3-49) yields

$$\frac{\overline{A}\Delta^2 W}{\Delta t\alpha''}+\left(\frac{\widetilde{1}}{G^{1/2}}\frac{\partial}{\partial\xi}+\frac{\sigma_g\widetilde{g}}{Cs^2}\right)\Delta^2 P=-2\mathrm{ADVW}'''', \tag{3-55}$$

where

$$\overline{A}\equiv 1+\sigma_g(\Delta t\alpha'')^2N^2,$$

$$\mathrm{ADVW}''''\equiv\mathrm{ADVW}''+\frac{\sigma_g g\Delta t\alpha''\mathrm{ADV}\theta''}{\overline{\Theta}}.$$

The Helmholtz equation for $\Delta^2 P$ is obtained by eliminating $\Delta^2 U$ and $\Delta^2 W$ in Eq. (3-53) by use of Eqs. (3-51) and (3-55) as follows:

$$\begin{aligned}&\frac{\Delta^2 P}{(\widetilde{C}s\alpha''\Delta t)^2}-\frac{\partial^2}{\partial x^2}\Delta^2 P-\left(\frac{\widetilde{1}}{G^{1/2}}\frac{\partial}{\partial\xi}+\frac{\sigma_g N^2}{g}\right)\overline{A}^{-1}\left(\frac{\widetilde{1}}{G^{1/2}}\frac{\partial}{\partial\xi}+\frac{\sigma_g\widetilde{g}}{Cs^2}\right)\Delta^2 P\\&\quad=\mathrm{FP.HIP.INV}\\&\quad\equiv-2\left(\frac{\mathrm{ADVP}''}{\Delta t\alpha''}-\mathrm{DIVS}\,(\mathrm{ADVU}'',\overline{A}^{-1}\mathrm{ADVW}'''')-\frac{\sigma_g N^2\overline{A}^{-1}\mathrm{ADVW}''''}{g}\right).\end{aligned} \tag{3-56}$$

It is noted that the forcing term for the pressure equation, FP.HIP.INV, includes no $\Delta^2 P$. Therefore iteration is not needed from this part. Iteration is needed in order to incorporate exactly the upper and lower boundary conditions.

In finite discretization form, $\overline{A}$ is a matrix. Unless W and θ' are placed on the same vertical level, the matrix $\overline{A}$ is not a diagonal matrix, and finite discretization of Eq. (3-56) becomes complex due to the complexity of $\overline{A}^{-1}$, the inverse of $\overline{A}$.

The upper and lower boundary conditions for E-HI-VI-PI are derived as follows. From Eq. (2-7),

$$\Delta^2 W^* = 0 = \frac{1}{G^{1/2}} \Delta^2 W + G^{13} \Delta^2 U. \tag{3-57}$$

Eliminating $\Delta^2 U$ and $\Delta^2 W$ from Eq. (3-57) by use of Eqs. (3-51) and (3-55) yields

$$\begin{aligned} &\left(\frac{\widetilde{1}}{G^{1/2}} \frac{\partial}{\partial \xi} + \frac{\widetilde{g}}{Cs^2} \right) \Delta^2 P \\ &= -2\left(\mathrm{ADVW''''} + \overline{A} G^{1/2} G^{13} \mathrm{ADVU''}\right) - \overline{A} G^{1/2} G^{13} \frac{\partial}{\partial x} \Delta^2 P. \end{aligned} \tag{3-58}$$

For the iteration procedure, the above equation is written as:

$$\left(\frac{\widetilde{1}}{G^{1/2}} \frac{\partial}{\partial \xi} + \frac{\widetilde{g}}{Cs^2} \right) \Delta^2 P_i = \mathrm{FPB.HIP.INV} + \mathrm{FPB.HIP.VAR}\,(P_{i-1}) \tag{3-59}$$

$$\mathrm{FPB.HIP.INV} = -2\left(\mathrm{ADVW''''} + \overline{A} G^{1/2} G^{13} \mathrm{ADVU''}\right) \tag{3-60}$$

$$\mathrm{FPB.HIP.VAR}\,(P_{i-1}) = -\overline{A} G^{1/2} G^{13} \frac{\partial}{\partial x} \Delta^2 P_{i-1}. \tag{3-61}$$

Here, suffix i denotes the value at the i-th iteration. Eqs. (3-56) and (3-58) are solved by an iterative application of the pressure equation solver mentioned in section B-6.

B-4. E-HE-VI (elastic-horizontally explicit-vertically implicit) scheme

In this scheme, sound waves are included, and the equations in B-1-3 with substitution of $\sigma = 1$ and $\rho = \overline{\rho}$ are used. In the time integration, terms related to sound waves are treated explicitly in the horizontal direction and implicitly in the vertical direction. In addition, a time-splitting method is uded for economical computation. There are a variety of so called "time splitting" methods. The time splitting technique used here is illustrated in Fig. B-4-1, and is the same as is used by Durran and Klemp (1983) and Horibata (1986, 1987).

B-4-1. Formulation of E-HE-VI scheme with $\overline{P}^{\tau}$ as unknown

The formulation is as follows:

$$\delta\tau U + \frac{\partial}{\partial x} P + \frac{\partial}{\partial \xi}(G^{13}P) = -\mathrm{ADVU}, \tag{4-1}$$

$$\delta\tau W + \frac{1}{G^{1/2}} \frac{\partial \overline{P}^{\tau\beta}}{\partial \xi} + \frac{g\overline{P}^{\tau\beta}}{Cs^2} = \mathrm{BUOY} - \mathrm{ADVW}, \tag{4-2}$$

$$\frac{1}{Cs^2}\delta\tau P + \frac{\partial}{\partial x}\overline{U}^{\tau\gamma} + \frac{1}{G^{1/2}}\frac{\partial \overline{W}^{\tau\beta}}{\partial \xi} + \frac{\partial}{\partial \xi}(G^{13}\overline{U}^{\tau\gamma}) = \mathrm{PFT}, \tag{4-3}$$

$$\overline{f}^{\tau\beta} = \frac{1+\beta}{2} f^{\tau+\Delta\tau} + \frac{1-\beta}{2} f^{\tau}, \tag{4-4}$$

$$\overline{f}^{\tau\gamma} = \frac{1+\gamma}{2} f^{\tau+\Delta\tau} + \frac{1-\gamma}{2} f^{\tau} \tag{4-5}$$

and

$$\delta\tau f = \frac{f^{\tau+\Delta\tau} - f^{\tau}}{\Delta\tau} = \frac{2}{\Delta\tau(1+\beta)}(\overline{f}^{\tau\beta} - f^{\tau}), \tag{4-6}$$

where τ denotes a small time step.

Small time step integration is made for terms related to sound waves on the left side of Eqs. (4-1)–(4-3), with the other terms fixed which are evaluated at the large time step, t. The leap-frog method is used for the large time step integration. The upper and lower boundary conditions are given by Eq. (2-7). From Eqs. (4-1) through (4-6), the one-dimensional Helmholtz-type elliptic equation for $\overline{P}^{\tau\beta}$ is obtained as follows:

$$\frac{1}{(G^{1/2})^2}\frac{\partial^2 \overline{P}^{\tau\beta}}{\partial \xi^2} + \frac{1}{G^{1/2}}\frac{\partial}{\partial \xi}\left(\frac{g}{Cs^2}\overline{P}^{\tau\beta}\right) - \frac{1}{(Cs\Delta\tau)^2}\left(\frac{2}{1+\beta}\right)^2 \overline{P}^{\tau\beta}$$
$$= \mathrm{FP.HE.INV} + \mathrm{FP.HE.VAR}(\tau), \tag{4-7}$$

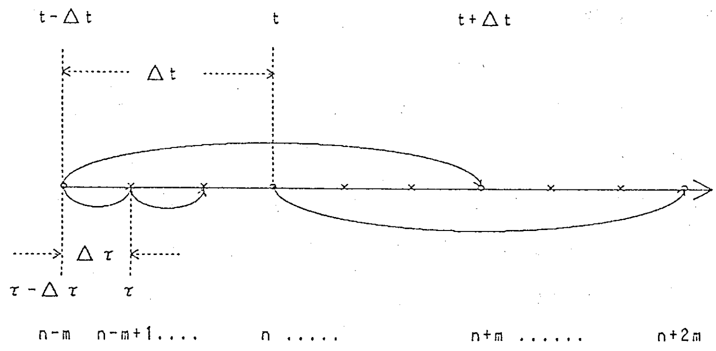

Fig. B-4-1 A schematic illustration of the time "splitting" method used here. $\Delta\tau$ is the time interval of the small time step integration. Δt is the time interval of the large time step integration. $Ns = 2\Delta t/\Delta\tau = 2\mathrm{m}$ is the number of small time step integration during one large leap-frog time integration. (adapted from Ikawa, 1988)

$$\mathrm{FP.HE.INV} = -\frac{2}{\Delta\tau(1+\beta)}\mathrm{PFT} + \frac{1}{G^{1/2}}\frac{\partial}{\partial\xi}(\mathrm{BUOY} - \mathrm{ADVW}) \tag{4-8}$$

$$\mathrm{FP.HE.VAR}(\tau) = \frac{2}{\Delta\tau(1+\beta)}\left(\frac{\partial\overline{U}^{\tau\gamma}}{\partial x} + \frac{\partial G^{13}\overline{U}^{\tau\gamma}}{\partial\xi} + \frac{1}{G^{1/2}}\frac{\partial\overline{W}^{\tau}}{\partial\xi}\right) - \frac{1}{(Cs\Delta\tau)^2}\left(\frac{2}{1+\beta}\right)^2 P^{\tau}. \tag{4-9}$$

The upper and lower boundary conditions are obtained from Eqs. (2-7), (4-1) and (4-2) as:

$$\frac{1}{G^{1/2}}\frac{\partial\overline{P}^{\tau\beta}}{\partial\xi} + \frac{g\overline{P}^{\tau\beta}}{Cs^2} = \mathrm{FPB.INV.HE} + \mathrm{FPB.VAR.HE}(\tau), \tag{4-10}$$

$$\mathrm{FPB.INV.HE} = -\mathrm{ADVW} + \mathrm{BUOY}, \tag{4-11}$$

$$\mathrm{FPB.VAR.HE}(\tau) = \frac{W^{\tau} + G^{1/2}G^{13}U^{\tau+\Delta\tau}}{\Delta\tau}. \tag{4-12}$$

The one-dimensional elliptic equation is solved more easily than 2- or 3-dimensional elliptic equations for AE and E-HI-VI schemes.

A linear stability analysis for the small time step integration is given by Horibata (1986, 1987) with $\gamma = 1$, who emphasized the merit of using $\beta = 1$. That with $\gamma \geqq 1$ for a whole time step integration is given in the next subsection B-4-2. The analysis shows that, even if the small time step integration is stable, the whole time step integration becomes weakly unstable. In order to prevent instability of the whole time step integration, $\gamma > 1$ and Asselin's time filter work well. Using $\gamma > 1$ effectively damps sound waves with infinite or large vertical wavelengths.

B-4-2. A linear stability analysis of a whole time step integration of E-HE-VI with orography

A linear stability analysis of the small time step integration only is given by Horibata (1986, 1987) for $\gamma = 1$. That for the whole time step integration and $\gamma \geqq 1$ is given as follows. We simplify the governing equations (4-1), (4-2), (4-3) as below:

$$\frac{1}{Cs^2}\,\delta\tau P + \frac{\partial}{\partial x}\,\overline{U}^{\tau\gamma} + (1+\varDelta H)\frac{\partial \overline{W}^{\tau\beta}}{\partial \xi} + \Delta G\frac{\partial}{\partial \xi}\overline{\overline{U}}^{x\xi}_{\tau\gamma} = 0, \tag{4-13}$$

$$\delta\tau U + \frac{\partial}{\partial x}\,P + \varDelta G\frac{\partial}{\partial \xi}\,\overline{P}^{x\xi} = -U_m\frac{\partial U}{\partial x}, \tag{4-14}$$

$$\delta\tau W + (1+\varDelta H)\frac{\partial \overline{P}^{\tau\beta}}{\partial \xi} = N\varTheta'' - U_m\frac{\partial W}{\partial x}, \tag{4-15}$$

$$\delta\tau\varTheta'' = -NW - U_m\frac{\partial \varTheta''}{\partial x}. \tag{4-16}$$

For the meaning of symblos, $\varTheta''$, $\varDelta H$ and $\varDelta G$, see B-3-2. Eq. (4-13) should be replaced by

$$\frac{1}{Cs^2}\,\delta\tau P + \frac{\partial}{\partial x}\,\overline{U}^{\tau\gamma} + (1+\varDelta H)\frac{\partial \overline{W}^{\tau\beta}}{\partial \xi} + \varDelta G\frac{\partial}{\partial \xi}\overline{\overline{U}}^{x\xi}_{\tau\gamma} = -\frac{N^2}{g}\left[W + \frac{U_m}{N}\frac{\partial \varTheta''}{\partial x}\right].$$

Ikawa (1988) used Eq. (4-13) by mistake. The additional term is related to slow modes in the program, and this term is expected to bring about little difference in the qualitative conclusion of the linear analysis made by Ikawa (1988) which will be shown below.

The large time step is at every $m = \varDelta t/\varDelta\tau$ small time step, indicated as $n-m$, n, $n+m$, $n+2m$ (see Fig. B-4-1). The terms on the righthand side are evaluated by the values at the large time step n, and kept constant during the small time step integration from $(n-m)$ to $(n+m)$. One small time step integration from $(n-m)$ to $(n-m+1)$ time step is expressed in matrix form using the same symbols defined in subsection B-3-2 as below:

$$S^{n-m+1} = (\boldsymbol{A} + \varDelta\tau\boldsymbol{C})^{-1}\boldsymbol{B}S^{n} + (\boldsymbol{A} + \varDelta\tau\boldsymbol{C})^{-1}(\boldsymbol{A} - \varDelta\tau\boldsymbol{D})S^{n-m} \tag{4-17}$$

where

$$S^{n,tr} \equiv (P^n,\ U^n,\ W^n,\ \varTheta''^{n})$$

$$\boldsymbol{A} \equiv \begin{bmatrix} 1/Cs^2 & 0 & 0 & 0 \\ 0 & 1 & 0 & 0 \\ 0 & 0 & 1 & 0 \\ 0 & 0 & 0 & 1 \end{bmatrix}$$

$$\boldsymbol{B} \equiv \Delta\tau \begin{bmatrix} 0 & 0 & 0 & 0 \\ 0 & -U_m i k_x{}^* & 0 & 0 \\ 0 & 0 & -U_m i k_x{}^* & N \\ 0 & 0 & -N & -U_m i k_x{}^* \end{bmatrix} \tag{4-18}$$

$$\boldsymbol{C} \equiv \begin{bmatrix} 0 & \frac{1+\gamma}{2} i(k_x{}^* + \Delta G k_z{}^{**}) & \frac{1+\beta}{2} \widetilde{H} i k_z{}^* & 0 \\ 0 & 0 & 0 & 0 \\ \frac{1+\beta}{2} \widetilde{H} i k_z{}^* & 0 & 0 & 0 \\ 0 & 0 & 0 & 0 \end{bmatrix} \tag{4-19}$$

$$\boldsymbol{D} \equiv \begin{bmatrix} 0 & \frac{1-\gamma}{2} i(k_x{}^* + \Delta G k_z{}^{**}) & \frac{1-\beta}{2} \widetilde{H} i k_z{}^* & 0 \\ i(k_x{}^* + \Delta G k_z{}^{**}) & 0 & 0 & 0 \\ \frac{1-\beta}{2} \widetilde{H} i k_z{}^* & 0 & 0 & 0 \\ 0 & 0 & 0 & 0 \end{bmatrix}$$

$$\widetilde{H} = 1 + \Delta H = 1/G^{1/2}.$$

First, we consider only the linear stability of the small time step of the acoustic mode by setting $\boldsymbol{B} = \boldsymbol{0}$. The amplification factor λ is the eigenvalue of the (4×4) matrix $(\boldsymbol{A} + \Delta\tau\boldsymbol{C})^{-1}(\boldsymbol{A} - \Delta\tau\boldsymbol{D})$. The characteristic equation for λ is factorized into $(\lambda - 1)^2$ and the following equation:

$$\begin{aligned} &\left[\frac{1}{(Cs\Delta\tau)^2} + (kz^*\widetilde{H})^2 \left(\frac{1+\beta}{2}\right)^2\right] \lambda^2 \\ &\quad + \left[\frac{1+\gamma}{2}(k_x{}^* + Gk_z{}^{**})^2 - \frac{2}{(Cs\Delta\tau)^2} + \frac{1-\beta^2}{2}(k_z{}^*\widetilde{H})^2\right] \lambda \\ &\quad + \frac{1}{(Cs\Delta\tau)^2} + (k_z{}^*\widetilde{H})^2 \left(\frac{1-\beta}{2}\right)^2 + \frac{1-\gamma}{2}(k_x{}^* + \Delta G k_z{}^{**})^2 = 0. \end{aligned} \tag{4-20}$$

The necessary and sufficient condition for $|\lambda| \leqq 1$ is

$$\begin{gathered} \beta \geqq 0, \ \gamma \geqq 1, \\ \frac{1}{(Cs\Delta\tau)^2} \geqq \frac{(k_x{}^* + \Delta G k_z{}^{**})^2}{4}\gamma - \frac{(k_z{}^*\widetilde{H})^2}{4}\beta^2. \end{gathered} \tag{4-21}$$

Under this condition, a measure of the amplification factor is given as

$$|\lambda_1\lambda_2| = \frac{\frac{1}{(Cs\Delta\tau)^2} + (k_z{}^*\widetilde{H})^2\left(\frac{1-\beta}{2}\right)^2 + \frac{1-\gamma}{2}(k_x{}^* + \Delta G k_z{}^*)^2}{\frac{1}{(Cs\Delta\tau)^2} + (k_z{}^*\widetilde{H})^2\left(\frac{1+\beta}{2}\right)^2}, \tag{4-22}$$

where λ_1 and λ_2 are the two roots of Eq. (4-20).

Neutral amplification for all $k_z{}^*$, $k_z{}^{**}$ and $k_x{}^*$ is given only by $\beta = 0$ and $\gamma = 1$. When $\beta > 0$ and $\gamma = 1$, sound waves of $k_z{}^* \neq 0$ are damped, but sound waves of $k_z{}^* = 0$ are not. In order to damp sound waves of $k_z{}^* = 0$, $\gamma > 1$ becomes necessary. As pointed out by Horibata (1987), inclusion of orography requires the time step interval $\Delta\tau$ to be restrictive. The condition of $\beta > 0$ relaxes the criterion of $\Delta\tau$ for stability of the scheme in addition to damping sound waves, but the condition of $\gamma > 1$ requires a smaller $\Delta\tau$ for stability of the scheme than $\gamma = 1$.

Using the eigen-vector matrix of $(\boldsymbol{A}+\Delta\tau\boldsymbol{C})^{-1}(\boldsymbol{A}-\Delta\tau\boldsymbol{D})$ which is obtained analytically, we simplify the equation (4-17) as below.

$$T^{n-m+1} = \boldsymbol{F}T^n + \boldsymbol{E}T^{n-m} \tag{4-23}$$

$$T^n = \boldsymbol{X}^{-1}S^n; \quad \boldsymbol{F} = \boldsymbol{X}^{-1}(\boldsymbol{A}+\Delta\tau\boldsymbol{C})^{-1}\boldsymbol{B}\boldsymbol{X}$$

$$(\boldsymbol{A}+\Delta\tau\boldsymbol{C})^{-1}(\boldsymbol{A}-\Delta\tau\boldsymbol{D})\boldsymbol{X} = \boldsymbol{X}\boldsymbol{E} \tag{4-24}$$

$\boldsymbol{X}$: (4×4) eigen-vector matrix;

$\boldsymbol{E}$: (4×4) diagonal matrix with diagonal elements of eigen-values.

This transformation makes the numerical computation more accurate as well as making clear the relation between the small and the large time step integration. A whole time step integration from $(n-m)$ to $(n+m)$ is expressed as

$$T^{n+m} = (\boldsymbol{I}+\boldsymbol{E}+\cdots+\boldsymbol{E}^{2m-1})\boldsymbol{F}T^n + \boldsymbol{E}^{2m}T^{n-m}. \tag{4-25}$$

The linear stability analysis of the case $\boldsymbol{F} = \boldsymbol{0}$ (sound wave modes only) is modified by $\boldsymbol{F}$ and $Ns = 2m$ in a large time step integration. If Asselin's time filter is applied at every large time step integration, the whole equation is given as below:

$$\begin{bmatrix} T^{n+m} \\ T^{*n} \end{bmatrix} = \begin{bmatrix} (\boldsymbol{I}+\boldsymbol{E}+\cdots+\boldsymbol{E}^{2m-1})\boldsymbol{F} & \boldsymbol{E}^{2m} \\ (1-2\nu)\boldsymbol{I}+\nu(\boldsymbol{I}+\boldsymbol{E}+\cdots+\boldsymbol{E}^{2m-1})\boldsymbol{F} & \nu(\boldsymbol{I}+\boldsymbol{E}^{2m}) \end{bmatrix} \begin{bmatrix} T^n \\ T^{*n-m} \end{bmatrix}, \tag{4-26}$$

where

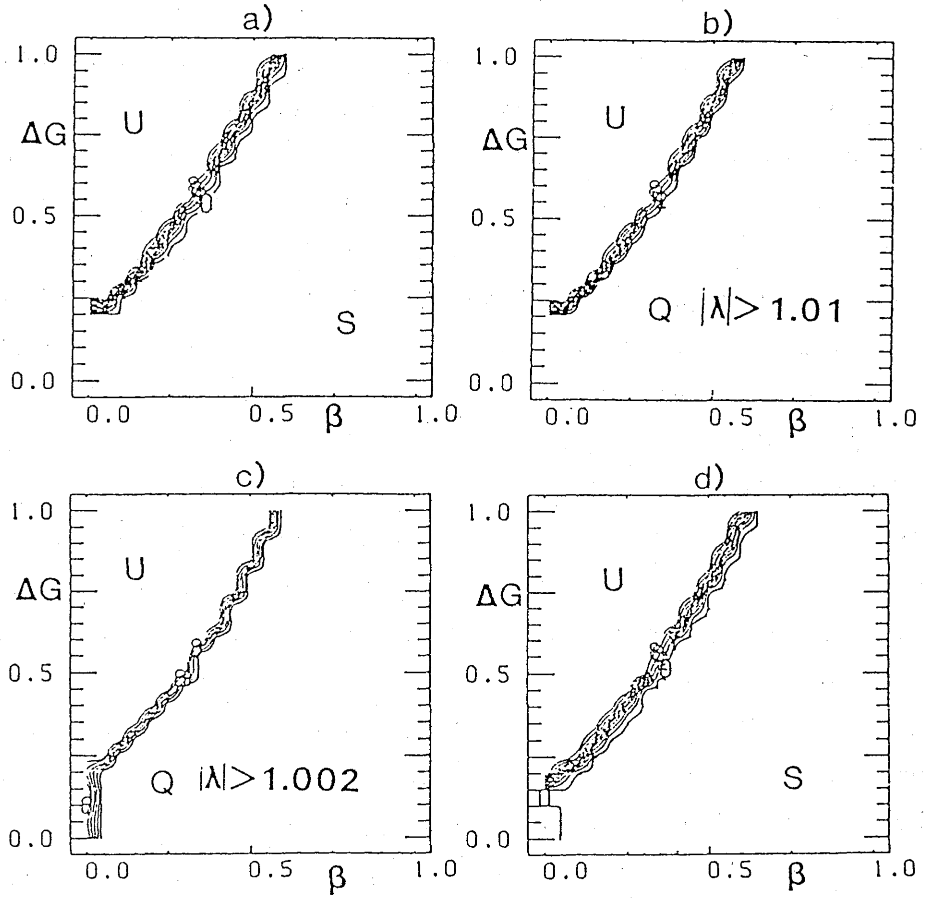

Fig. B-4-2 a, b, c, d) Amplification factor $|\lambda|$ of E-HE-VI. The horizontal axis indicates β, varying from 0 to 1. The vartical axis indicates $\Delta G = 2\Delta H$ varying from 0 to 1 with an interval of 0.05. The maximum amplification factor among the cases of $kx = 2\pi/\Delta x(i/20)$ (from $i = -20$ to 20) and $kz = 2\pi/\Delta\xi(j/20)$ (from $j = -20$ to 20) is plotted. The contour line numbered by n denotes $|\lambda| = 1 + n \times 0.1$ (the contour interval Δn is 1), except for c). The area of $|\lambda| > 1.8$ is indicated by U except for c); the area of $|\lambda| < 1.00009$ is indicated by S. **a)** The case of $F = 0$ ($N = U_m = 0$) and (γ, ν) = (1, 0); analytic solution. **b)** The case of $F \neq 0$ ($N = 10^{-2}$/s, U_m = 4m/s) and (γ, ν) = (1, 0); numerical solution; the area of $1.01 < |\lambda| < 1.1$ is indicated by Q. **c)** The case of $F \neq 0$ ($N = 10^{-2}$/s, U_m = 4m/s) and (γ, ν) = (1, 0.2); numerical solution; The contour line numbered by n denotes $|\lambda| = 1 + n \times 0.001$ (the contour interval Δn is 1). The area of $|\lambda| > 1.008$ is indicated by U; the area of $1.002 < |\lambda| < 1.003$ is indicated by Q. **d)** The case of $F \neq 0$ ($N = 10^{-2}$/s, U_m = 4m/s) and (γ, ν) = (1.1, 0.2); numerical solution. (adapted from Ikawa, 1988)

$$T^{*n} = T^n + \nu(T^{n+m} - 2T^n + T^{*n-m}).$$

The amplification factor is the eigenvalue of the (8×8) matrix in Eq. (4-26), and solved numerically by the same procedure mentioned in the subsection B-3-2.

Next, the dependence of stability on β, γ, ν, ΔH and ΔG is examined for the parameters $(\Delta x, \Delta\xi, \Delta t, \Delta\tau, Cs, N, U_m) =$ (1200m, 200m, 12s, 3s, 340m/s, 0.01/s, 4m/s), which are the same as used in the experiments in section 3 of Ikawa (1988), unless specifically mentioned. Fig. B-4-2a shows the amplification factor for the case of $\boldsymbol{F} = \boldsymbol{B} = \boldsymbol{0}$ (acoustic mode only; U_m = 0m/s and N = 0/s) with $\gamma = 1$ and $\nu = 0$, which is obtained analytically. The unstable area at $(0 \leqq \beta \leqq 0.2,\ 0.4 \leqq 2\Delta H = \Delta G)$ is due to the violation of the stability criterion Eq. (4-21) for $\Delta\tau$. This area can be removed by a smaller $\Delta\tau$. An appropriate choice of β reduces $|\lambda|$ below 1.00009, which would practically result in no instability. Fig. B-4-2b shows the amplification factor for the case of $\boldsymbol{F} \neq \boldsymbol{0}$ with $\gamma = 1$ and $\nu = 0$, which is obtained numerically. It is found that, even if a small time step integration is stable, a whole time step integration becomes unstable, even though it is weak $(1.006 \leqq |\lambda| \leqq 1.007)$. Fig. B-4-2c shows the amplification factor of the case of $\boldsymbol{F} \neq \boldsymbol{0}$ with $\gamma = 1$ and $\nu = 0.2$. As compared with Fig. B-4-2b, $|\lambda|$ becomes small, but the minimum $|\lambda|$ is above 1.003. This remaining weak instability comes from sound waves with $kz^* = 0$. Fig. B-4-2d shows the amplification factor of the case of $\boldsymbol{F} \neq \boldsymbol{0}$ with $\gamma = 1.1$ and $\nu = 0.2$. An appropriate choice of β reduces $|\lambda|$ below 1.0009. As shown by these figures, in order to be stable in a whole time step integration, $\beta > 0$, $\gamma > 1$ and Asselin's time filter work well.

B-5. Grid structure, variable grid and finite discretization form

B-5-1. Grid structure

The staggered grid shown in Fig. B-5-1 is adopted (see Clark, 1977). Prognostic variables other than velocity components are located on the grid point indexed by integer $(i,\ j,\ k)$. Velocity components, U, V and W, are located on the grid points indexed by the half integer $(i+1/2,\ j,\ k)$, $(i,\ j+1/2,\ k)$ and $(i,\ j,\ k+1/2)$, respectively. The density of the reference atmosphere $\overline{\rho}$ is located on the grid point $(i,\ j,\ k)$. $G^{1/2}$ and Z_s are located on the grid point $(i,\ j)$, independent of k.

As shown in Figs. B-5-2 and B-5-3, boundaries of the model domain are located at $(1+1/2,\ j,\ k)$ and $(nx-1/2,\ j,\ k)$ for the y-z boundaries, at $(i,\ 1+1/2,\ k)$ and $(i,\ ny-1/2,\ k)$ for the x-z boundaries and at $(i,\ j,\ 1+1/2)$ and $(i,\ j,\ nz-1/2)$ for the x-y boundaries. On these boundary planes, velocity components normal to the planes are placed.

Program Guide

In the program, the array index (IX,JY,KZ) is used instead of the logical index, such as $(i,\ j+1/2,\ k)$. Hereafter, the array index is expressed by the capital letters (IX,JY,KZ), while the logical index is expressed by small letters, such as $(i,\ j,\ k)$ or $(i+1/2,\ j,\ k)$. In Figs. B-5-2, B-5-3, B-5-4 and B-5-5, the array index is also shown. The dimension of the array in program is (NX,NY,NZ) = (nx,ny,nz).

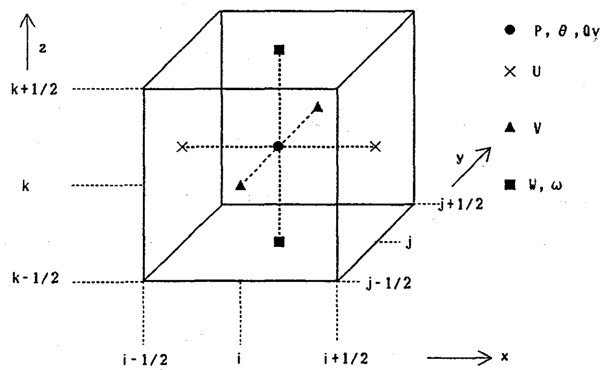

Fig. B-5-1 Staggered grid.

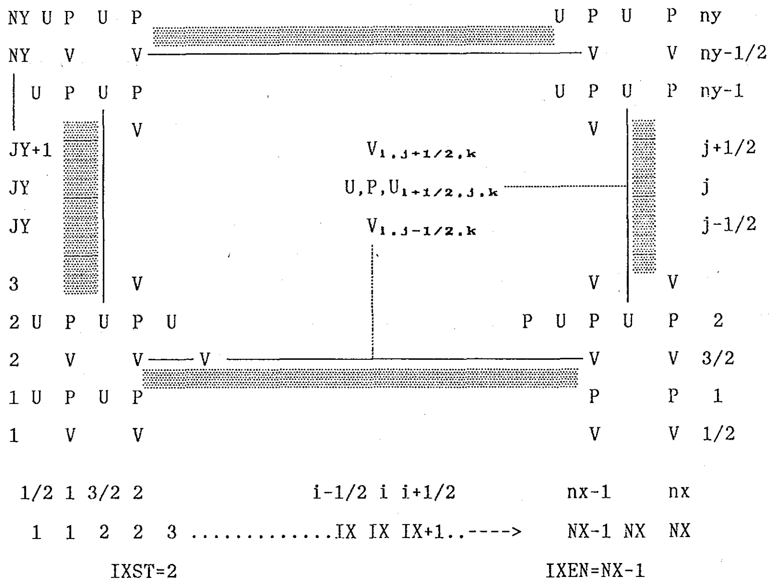

Fig. B-5-2 Horizontal plane (x-y cross section, k is integer) of the grid mesh and the domain boundary. The logical index for P at the center of this figure is (i, j, k). The array index in the program code is expressed by (IX, JY, KZ) for $P_{i,j,k}$.

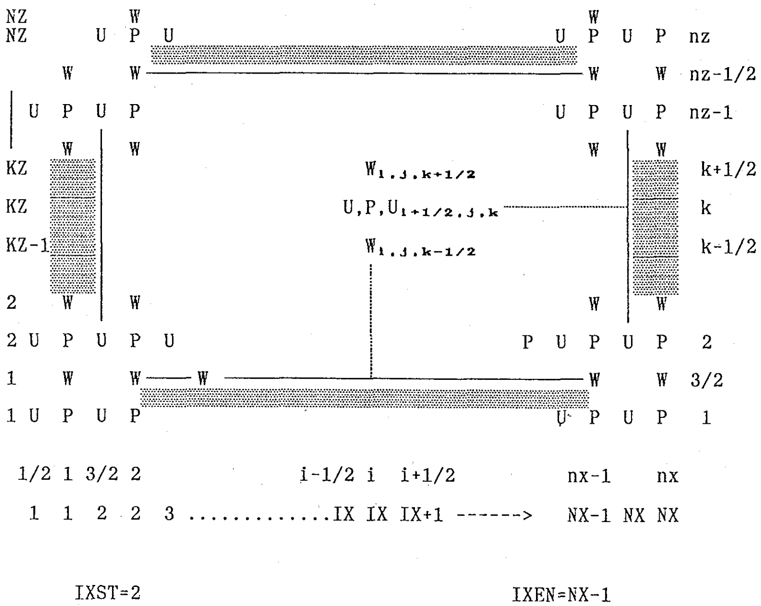

Fig. B-5-3 Vertical plane (x-z cross section, j is integer) of the grid mesh and the domain boundary. The logical index for P at the center of this figure is (i, j, k). The array index in the program code is expressed by (IX, JY, KZ) for $P_{i,j,k}$.

B-5-2. Variable grid

Figure B-5-4 shows the variable grid structure in the z-direction. Two kinds of grid intervals are defined. Δz_k represents the grid interval between the two grid points $(i,\ j,\ k-1/2)$ and $(i,\ j,\ k+1/2)$; $\Delta z_{k-1/2}$ represents the grid interval between the two grid points $(i,\ j,\ k-1)$ and $(i,\ j,\ k)$. As shown in Fig. B-5-4, the following relation between grid intervals Δz_k and $\Delta z_{k-1/2}$ exists:

$$\Delta z_k = 0.5(\Delta z_{k-1/2} + \Delta z_{k+1/2}). \tag{5-1}$$

The horizontal plane indexed by $k = 1 + 1/2$ is assumed to be the lower boundary. The height of the grid point $(i,\ j,\ k+1/2)$ is given as

for $k = 1$

$$z(k+1/2) = 0, \tag{5-2}$$

for $k \geqq 2$

$$z(k+1/2) = \sum_{m=2}^{k} \Delta z_m.$$

The height of the grid point $(i,\ j,\ k)$ is given as

for $k = 1$

$$z(k) = -\Delta z_{1+1/2}/2, \tag{5-3}$$

for $k \geqq 2$

$$z(k) = \sum_{m=1}^{k-1} \Delta z_{m+1/2} - \Delta z_{1+1/2}/2. \tag{5-4}$$

The variable grid structure in the x- and y-directions is similar to that in the z-direction. As shown in Fig. B-5-5, the following relations exist:

$$\Delta x_i = 0.5(\Delta x_{i-1/2} + \Delta x_{i+1/2}), \tag{5-5}$$

$$\Delta y_j = 0.5(\Delta y_{j-1/2} + \Delta y_{j+1/2}). \tag{5-6}$$

B-5-3. Finite discretization form on the variable staggered grid

Averaging operator $-x$ in the x-direction is, for any variable F placed on the grid point indexed by integer, defined by

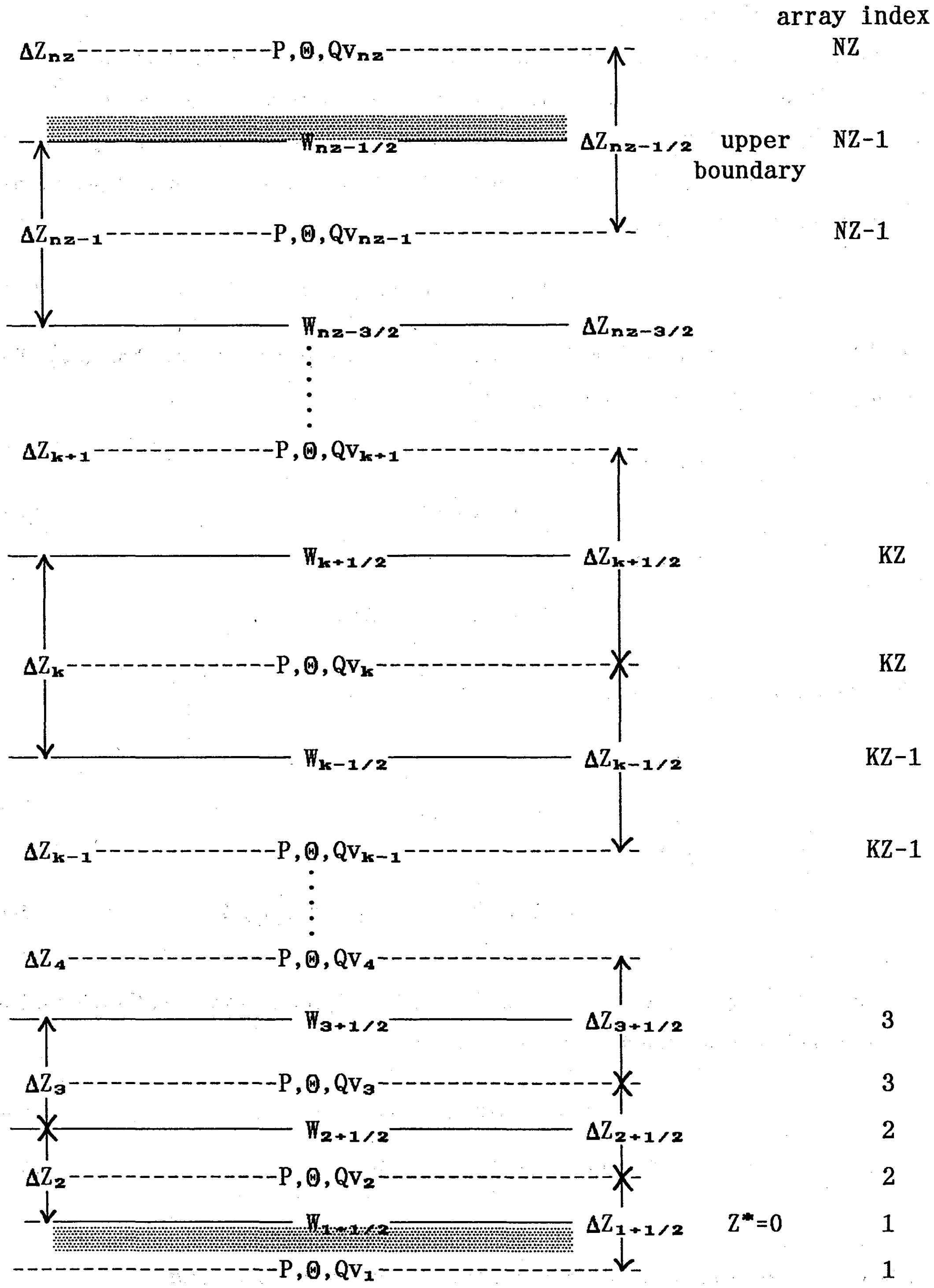

Fig. B-5-4 Variable grid structure in the z-direction.

```
<----- Δx_{i-1/2}     ---><--------- Δx_{i+1/2}     ---><-----Δx_{i+3/2}

--P_{i-1} -----U_{i-1/2} -----P_i--------- U_{i+1/2} -----P_{i+1/2}---U_{i+3/2}

Δx_{i-1}   ---><---------Δx_i---------><--------Δx_{i+1}------>

DX(i-1)---><---------DX(i)-------><--------DX(i+1)---->

<----- DX2(i-1/2)---><-------- DX2(i+1/2)----><-- DX2(i+3/2)

array index  IX        IX        IX+1        IX+1        IX+2
```

Fig. B-5-5 Variable grid in the x-direction. Grid interval and grid indexing.

$$\overline{F}^{x}]_{i+1/2} = \frac{F_i + F_{i+1}}{2}, \tag{5-7}$$

and, for any variable U placed on the grid point indexed by half integer, by

$$\overline{U}^{x}]_i = \frac{\Delta x_{i+1/2} U_{i-1/2} + \Delta x_{i-1/2} U_{i+1/2}}{2\Delta x_i}. \tag{5-8}$$

Averaging operators in the y and z directions, $-y$ and $-z$, are defined in the same way.

Finite difference operator ∂_x (∂_y, ∂_z is defined in the same way) is defined by

$$\partial_x F]_{i-1/2} = \frac{F_i - F_{i-1}}{\Delta x_{i-1/2}}, \tag{5-9a}$$

$$\partial_x U]_i = \frac{U_{i+1/2} - U_{i-1/2}}{\Delta x_i}. \tag{5-9b}$$

Using these operators, terms in governing equations are expressed in finite discretization form as follows (see Clark (1977), p. 193 for more detail):

G^{13} and G^{23} (Eq. (1-27)) are

$$G^{13}]_{i+1/2,j,k+1/2} = \frac{\overline{1}^{x}}{G^{1/2}} \left(\frac{\xi}{H} - 1\right) \frac{\partial Z_s}{\partial x} \tag{5-10a}$$

$$G^{23}]_{i,j+1/2,k+1/2} = \frac{\overline{1}^{y}}{G^{1/2}} \left(\frac{\xi}{H} - 1\right) \frac{\partial Z_s}{\partial y} \tag{5-10b}$$

Pressure gradient terms (Eqs. (1-28) and (1-29)) are expressed in discretized form as

$$\mathrm{PFX}]_{i+1/2,j,k} = \partial_x P + \partial_z(G^{13}\overline{P}^{xz}), \tag{5-11}$$

$$\mathrm{PFZ}]_{i,j,k+1/2} = \frac{1}{G^{1/2}}\,\partial_z P + \frac{g\overline{P}^z}{Cs^2}. \tag{5-12}$$

The operators DIVT and DIVS (see Eqs. (2-3) and (2-2)) are expressed in discretized form as

$$\mathrm{DIVT}(U,W)]_{i,j,k} = \partial_x U + \partial_z\left(\overline{G^{13}\overline{U}^z}^x\right) + \partial_y V + \partial_z\left(\overline{G^{23}\overline{V}^z}^y\right) + \frac{1}{G^{1/2}}\,\partial_z W, \tag{5-13}$$

$$\mathrm{DIVS}(U,V,W)]_{i,j,k} = \partial_x U + \partial_y V + \frac{\tilde{1}}{G^{1/2}}\,\partial_z W. \tag{5-14}$$

Eq. (1-31) is expressed in discretized form as

$$U]_{i+1/2,j,k} \equiv \overline{\overline{\rho}G^{1/2}}^x u, \qquad V]_{i,j+1/2,k} \equiv \overline{\overline{\rho}G^{1/2}}^y v, \tag{5-15}$$

$$W]_{i,j,k+1/2} = \overline{\overline{\rho}G^{1/2}}^z w, \qquad P]_{i,j,k} \equiv G^{1/2}p'.$$

Eqs. (1-32) and (1-33) are expressed in discretized form as

$$\mathrm{ADVU}]_{i+1/2,j,k} = \partial_x(\overline{U}^x\overline{u}^x) + \partial_y(\overline{V}^x\overline{v}^y) + \partial_z(\overline{W^*}^x\overline{u}^z), \tag{5-16}$$

$$\mathrm{ADVV}]_{i,j+1/2,k} = \partial_x(\overline{U}^y\overline{v}^x) + \partial_y(\overline{V}^y\overline{v}^y) + \partial_z(\overline{W^*}^y\overline{v}^z), \tag{5-17}$$

$$\mathrm{ADVW}]_{i,j,k+1/2} = \partial_x(\overline{U}^z\overline{w}^x) + \partial_y(\overline{V}^z\overline{w}^y) + \partial_z(\overline{W^*}^z\overline{w}^z). \tag{5-18}$$

Eq. (1-34) is expressed in discretized form as

$$W^* = \overline{\rho}G^{1/2}\omega]_{i,j,k+1/2} = \frac{1}{G^{1/2}}W + \overline{G^{13}\overline{U}^z}^x + \overline{G^{23}\overline{V}^z}^y, \tag{5-19}$$

Eqs. (1-35), (1-36) and (1-37) are expressed in discretized form as

$$\mathrm{BUOY}]_{i,j,k+1/2} = g\frac{\overline{\rho G^{1/2}}^z\,\overline{\theta'_m}^z}{\overline{\Theta}_m}, \tag{5-20}$$

$$\mathrm{ADV}\theta]_{i,j,k} = \frac{1}{\overline{\rho}G^{1/2}}\{\partial x(U\overline{\theta}^x) + \partial y(V\overline{\theta}^y) + \partial z(W^*\overline{\theta}^z)\}, \tag{5-21}$$

$$\mathrm{PFT}]_{i,j,k} = \frac{1}{g}\frac{\partial\overline{\mathrm{BUOY}}^z}{\partial t}. \tag{5-22}$$

Program Guide (hereafter, abbreviated as P.G.)

PFX is computed by sub.CPFX where "sub" denotes subroutine.

PFZ is computed by sub.CPFZ.

Conversion from $W(w)$ to OMW $= W^*$ (or ω) is made by sub. WCVOMW.

Conversion from OMW $= W^*$ (or ω) to $W(w)$ is made by sub. OMWCVW.

Conversion from U (or V) to $u(v)$ is made by sub.UCVDNU.

ADVU and ADVW are computed by CADVC3.

ADVθ or ADVF ($F = Qv,\ Qc\ldots$) is computed by sub.CADVET.

DIVT is computed by sub.SFDIVT in mem.SFXTPG1, where "men" denotes member name in the FORTRAN source file.

DIVS is computed by sub.SFDIV in mem.SFXTPG1.

BUOY is computed by sub.CBUOY3 in mem.SFXTPG1.

B-6. Pressure equation solver on variable grid

Pressure equation is an elliptic equation (Helmholtz equation for E-HI-VI and Poisson equation for AE) with Neumann type boundary conditions. The solving method of the equation by a direct method (Dimension Reduction Method; e.g., Ogura (1969)) is presented for a non-orographic case here. The elliptic equation to be solved is expressed as

$$\partial_{xx}P + \partial_{yy}P + d\partial_z(d\partial_z P + hP) + eP = F, \tag{6-1}$$

$$d = \frac{\widetilde{1}}{G^{1/2}}, \quad h = \frac{\widetilde{g}}{Cs^2}, \quad e = \frac{\sigma}{(Cs\alpha''\Delta t)^2}. \tag{6-2}$$

Here, σ is the switching parameter; $\sigma = 0$ for AE scheme (Eq. (2-5)) and $\sigma = 1$ for E-HI-VI scheme (Eq. (3-36)). Hereafter, $d = 1$ is assumed for simplicity. h and e are assumed to be dependent on z but independent of x and y.

Lateral boundary conditions are given as

$$\partial_x P = Bx \equiv -\frac{\partial U}{\partial t} - \mathrm{ADVU}, \tag{6-3}$$

$$\partial_y P = By \equiv -\frac{\partial V}{\partial t} - \mathrm{ADVV}. \tag{6-4}$$

Upper and lower boundary conditions are given as

$$\partial_z P + hP = Bz \equiv -\frac{\partial W}{\partial t} - \mathrm{ADVW} + \mathrm{BUOY}. \tag{6-5}$$

B-6-1. The case of open (noncyclic) lateral boundary conditions

a) Finite discretized equation in matrix form

Finite discretization form of Eq. (6-1) on variable grid at $(i,\ j,\ k)$ is as follows:

$$\begin{aligned}
&\frac{P_{i+1,j,k}}{\Delta x_{i+1/2}\Delta x_i} - \frac{P_{i,j,k}}{\Delta x_i}\left(\frac{1}{\Delta x_{i+1/2}} + \frac{1}{\Delta x_{i-1/2}}\right) + \frac{P_{i-1,j,k}}{\Delta x_i \Delta x_{i-1/2}} \\
&+ \frac{P_{i,j+1,k}}{\Delta y_{i+1/2}\Delta y_i} - \frac{P_{i,j,k}}{\Delta y_i}\left(\frac{1}{\Delta y_{i+1/2}} + \frac{1}{\Delta y_{i-1/2}}\right) + \frac{P_{i,j-1,k}}{\Delta y_i \Delta y_{i-1/2}} \\
&+ \frac{1}{\Delta z_k}\left(\frac{1}{\Delta z_{k-1/2}} - \frac{h_{k-1/2}}{2}\right) P_{i,j,k-1} \\
&- \frac{1}{\Delta z_k}\left(\frac{1}{\Delta z_{k-1/2}} + \frac{1}{\Delta z_{k+1/2}} - \frac{h_{k+1/2} - h_{k-1/2}}{2}\right) P_{i,j,k} \\
&+ \frac{1}{\Delta z_k}\left(\frac{1}{\Delta z_{k+1/2}} + \frac{h_{k+1/2}}{2}\right) P_{i,j,k+1} + eP_{i,j,k} \\
&= F_{i,j,k}.
\end{aligned} \tag{6-6}$$

Finite discretization of boundary conditions Eqs. (6-3)–(6-5) are for $2 \leqq j \leqq ny-1$ and $2 \leqq k \leqq nz-1$

$$\frac{P_{2,j,k}-P_{1,j,k}}{\Delta x_{1+1/2}} = Bx_{;1,j,k}\,, \quad \frac{P_{nx,j,k}-P_{nx-1,j,k}}{\Delta x_{nx-1/2}} = Bx_{;nx,j,k}\,, \tag{6-7a}$$

for $2 \leqq i \leqq nx-1$ and $2 \leqq k \leqq nz-1$

$$\frac{P_{i,2,k}-P_{i,1,k}}{\Delta y_{1+1/2}} = By_{;i,1,k}\,, \quad \frac{P_{i,ny,k}-P_{i,ny-1,k}}{\Delta y_{ny-1/2}} = By_{;i,ny,k}\,, \tag{6-7b}$$

for $2 \leqq i \leqq nx-1$ and $2 \leqq j \leqq ny-1$

$$\frac{P_{i,j,nz}-P_{i,j,nz-1}}{\Delta z_{k-1/2}} + h_{nz-1/2}\,\frac{P_{i,j,nz}+P_{i,j,nz-1}}{2} = Bz_{;i,j,nz}\,, \tag{6-8}$$

$$\frac{P_{i,j,2}-P_{i,j,1}}{\Delta z_{i+1/2}} + h_{1+1/2}\,\frac{P_{i,j,2}+P_{i,j,1}}{2} = Bz_{;i,j,1}\,.$$

The element outside the lateral boundary $P_{1,j,k}$ is eliminated for the practical reason that the same dimension for the matrix A (see Eq. (6-13)) is applicable to open and cyclic boundary cases as below: At the point $(2,\ j,\ k)$

$$F_{2,j,k} \longleftarrow F_{2,j,k} + \frac{P_{2,j,k}-P_{1,j,k}}{\Delta x_{1+1/2}\Delta x_2} = F_{2,j,k} + \frac{Bx_{;1,j,k}}{\Delta x_2}$$

$$\frac{P_{3,j,k}}{\Delta x_{2+1/2}\Delta x_2} - \frac{P_{2,j,k}}{\Delta x_2 \Delta x_{2+1/2}} \longleftarrow \frac{P_{3,j,k}}{\Delta x_{2+1/2}\Delta x_2} - \frac{P_{2,j,k}}{\Delta x_2}\left(\frac{1}{\Delta x_{2+1/2}} + \frac{1}{\Delta x_{1+1/2}}\right) + \frac{P_{1,j,k}}{\Delta x_2 \Delta x_{1+1/2}}.$$

For other points next to the lateral boundary such as $(nx-1,\ j,\ k)$ $(i,\ 2,\ k)$ and $(i,\ ny-1, k)$, the equations are changed in the same manner.

The above equations are written in matrix form as follows:

$$[\boldsymbol{I} \otimes \boldsymbol{Y}_A^{-1}\boldsymbol{A} + \boldsymbol{Y}_B^{-1}\boldsymbol{B} \otimes \boldsymbol{I}]\Pi_{,,k} + r_k \Pi_{,,k+1} + (s_k+e_k)\Pi_{,,k} + t_k \Pi_{,,k-1} = \Phi_{,,k} \tag{6-9}$$

for $2 \leqq k \leqq nz-1$.

Here r_k, s_k and t_k are given by Eqs. (6-27)–(6-29) and

$$\Pi_{,,k}{}^{tr} \equiv (\Pi_{,2,k}{}^{tr};\ \Pi_{,3,k}{}^{tr};\ \cdots\cdots\cdots\ \Pi_{,ny-1,k}{}^{tr}), \tag{6-10a}$$

$$\Pi_{,j,k}{}^{tr} \equiv (P_{2,j,k};\ P_{3,j,k};\ \cdots\cdots\cdots\ P_{nx-1,j,k}), \tag{6-10b}$$

$$\Phi_{,,k}{}^{tr} \equiv (\Phi_{,2,k}{}^{tr};\ \Phi_{,3,k}{}^{tr};\ \cdots\cdots\cdots\ \Phi_{,ny-1,k}{}^{tr}), \tag{6-11a}$$

$$\boldsymbol{\Phi}_{,j,k}{}^{tr} \equiv (F_{2,j,k};\ F_{3,j,k};\ \cdots\cdots\ F_{nx-1,j,k}). \tag{6-11b}$$

Superscript ^{tr} denotes the transposed matrix.

$$\boldsymbol{Y}_A \equiv \begin{bmatrix} \Delta x_2 & 0 & 0 & & \text{\Large 0} \\ 0 & \Delta x_3 & 0 & & \\ 0 & 0 & \Delta x_4 & & \\ & & \vdots & & \\ & & & & 0 \\ \text{\Large 0} & & & 0 & \Delta x_{nx-1} \end{bmatrix} \tag{6-12}$$

$$\boldsymbol{A} \equiv$$

$$\begin{bmatrix} \frac{1}{\Delta x_{2+1/2}}, & \frac{-1}{\Delta x_{2+1/2}}, & & 0, & & \text{\Large 0} \\ \frac{-1}{\Delta x_{2+1/2}}, & \frac{1}{\Delta x_{2+1/2}} + \frac{1}{\Delta x_{3+1/2}}, & -\frac{1}{\Delta x_{3+1/2}}, & & 0, & 0 \\ & & & \vdots & & \\ 0, & -\frac{1}{\Delta x_{i+1/2}}, & \frac{1}{\Delta x_{i+1/2}} + \frac{1}{\Delta x_{i+3/2}}, & -\frac{1}{\Delta x_{i+3/2}}, & 0, & 0 \\ & & & \vdots & & \\ 0, & 0, & \frac{1}{\Delta x_{nx-5/2}}, & \frac{1}{\Delta x_{nx-5/2}} + \frac{1}{\Delta x_{nx-3/2}}, & -\frac{1}{\Delta x_{nx-3/2}} & \\ \text{\Large 0} & & 0, & \frac{-1}{\Delta x_{nx-3/2}}, & \frac{1}{\Delta x_{nx-3/2}} & \end{bmatrix} \tag{6-13}$$

The matrices, $\boldsymbol{Y}_B$ and $\boldsymbol{B}$, which are associated with finite discretization operators in the y direction, are defined in a similar way to $\boldsymbol{Y}_A$ and $\boldsymbol{A}$ which are associated with finite discretization operators in the x direction. The symbol $\otimes$ indicates the tensor product operation, *i.e.*, for the (m, m) matrix $\boldsymbol{M}$ and (n, n) matrix $\boldsymbol{N}$,

$$\boldsymbol{M} \otimes \boldsymbol{N} = \begin{bmatrix} m_{1,1}\boldsymbol{N} & m_{1,2}\boldsymbol{N} & \ldots & m_{1,m}\boldsymbol{N} \\ m_{2,1}\boldsymbol{N} & m_{2,2}\boldsymbol{N} & & \\ & & & \\ m_{m,1}\boldsymbol{N} & \ldots\ldots & & m_{m,m}\boldsymbol{N} \end{bmatrix},\ (mn,\ mn) \text{ matrix.} \tag{6-14}$$

Upper and lower boundary conditions are expressed as

$$-\partial z \Pi_{,,k}]_{k=1+1/2} - h_{1+1/2}\overline{\Pi}^{z}_{,,k}]_{k=1+1/2} = \Phi_{b,,1} \tag{6-15a}$$

$$\partial z \Pi_{,,k}]_{k=nz-1/2} + h_{nz-1/2}\overline{\Pi}^{z}_{,,k}]_{k=nz-1/2} = \Phi_{b,,nz}, \tag{6-15b}$$

where

$$\Phi_{b,,1}{}^{tr} = [\Phi_{b,2,1}{}^{tr};\ \Phi_{b,3,1}{}^{tr};\ \ldots\ldots\ \Phi_{b,ny-1,1}{}^{tr}] \tag{6-15c}$$

$$\Phi_{b,j,1}{}^{tr} = [-Bz_{,2,j,1};\ -Bz_{,3,j,1};\ \ldots\ldots\ -Bz_{,nx-1,j,1}] \tag{6-15d}$$

$$\Phi_{b,,nz}{}^{tr} = [\Phi_{b,2,nz}{}^{tr};\ \Phi_{b,3,nz}{}^{tr};\ \ldots\ldots\ \Phi_{b,ny-1,nz}{}^{tr}] \tag{6-15e}$$

$$\Phi_{b,j,nz}{}^{tr} = [Bz_{,2,j,nz};\ Bz_{,3,j,nz};\ \ldots\ldots\ Bz_{,nx-1,j,nz}]. \tag{6-15f}$$

b) Eigenvector and eigenvalue matrixes

In order to solve Eqs. (6-9) and (6-15) for a variable grid mesh, the generalized eigen-vectors for the matrix $\boldsymbol{Y}_A{}^{-1}\boldsymbol{A}$ and $\boldsymbol{Y}_B{}^{-1}\boldsymbol{B}$ are used. They are defined as follows:

$$\boldsymbol{AP} = \boldsymbol{Y}_A\boldsymbol{P}\Lambda(\boldsymbol{A}), \qquad \boldsymbol{BQ} = \boldsymbol{Y}_B\boldsymbol{Q}\Lambda(\boldsymbol{B}): \tag{6-16a}$$

$\boldsymbol{P}$ and $\boldsymbol{Q}$: generalized eigen-vector matrixes normalized as

$$\boldsymbol{P}^{tr}\boldsymbol{Y}_A\boldsymbol{P} = \boldsymbol{I} \text{ and } \boldsymbol{Q}^{tr}\boldsymbol{Y}_B\boldsymbol{Q} = \boldsymbol{I} \quad (\text{note } \boldsymbol{P}^{-1} = \boldsymbol{P}^{tr}\boldsymbol{Y}_A \text{ and } \boldsymbol{Q}^{-1} = \boldsymbol{Q}^{tr}\boldsymbol{Y}_B)$$

$\Lambda(\boldsymbol{A})$ and $\Lambda(\boldsymbol{B})$: generalized eigenvalue matrixes for $\boldsymbol{A}$ and $\boldsymbol{B}$ with only diagonal elements.

$\boldsymbol{P}$ is obtained by a standard procedure, say, Jacobi method, because $\boldsymbol{A}$ is a symmetric matrix and $\boldsymbol{Y}_A$ is a positive definite symmetric matrix and written as $\boldsymbol{Y}_A = \boldsymbol{L}^{tr}\boldsymbol{L}$ for a certain non-singular matrix $\boldsymbol{L}$. For the symmetric matrix $\boldsymbol{A}^* = \boldsymbol{L}^{-1}\boldsymbol{A}(\boldsymbol{L}^{tr})^{-1}$, the eigen-vector matrix $\boldsymbol{P}^*$ can be obtained by a standard procedure as

$$\boldsymbol{A}^*\boldsymbol{P}^* = \boldsymbol{P}^*\Lambda(\boldsymbol{A}^*),$$

where $\Lambda(\boldsymbol{A}^*)$ is the eigen-value matrix of $\boldsymbol{A}^*$.

$\boldsymbol{P}$ is calculated from $\boldsymbol{P}^*$ as

$$\boldsymbol{P} = (\boldsymbol{L}^{tr})^{-1}\boldsymbol{P}^*. \tag{6-16b}$$

Note the following relations:

$$\boldsymbol{P}^* = \boldsymbol{L}^{tr}\boldsymbol{P};\ \boldsymbol{A}\boldsymbol{P} = \boldsymbol{L}\boldsymbol{L}^{tr}\boldsymbol{P}\Lambda(\boldsymbol{A}^*);$$

$$\boldsymbol{L}^{-1}\boldsymbol{A}(\boldsymbol{L}^{tr})^{-1}\boldsymbol{L}^{tr}\boldsymbol{P} = \boldsymbol{L}^{tr}\boldsymbol{P}\boldsymbol{A};\ \Lambda(\boldsymbol{A}) = \Lambda(\boldsymbol{A}^*). \tag{6-16c}$$

For a uniform grid mesh, ${\boldsymbol{Y}_A}^{-1}\boldsymbol{A}$ is equivalent to the $(n_x-2,\ n_x-2)$ matrix $\boldsymbol{Au}$

$$\boldsymbol{Au} = \begin{bmatrix} 1 & -1 & & & & & 0 \\ -1 & 2 & -1 & & & & \\ & -1 & 2 & -1 & & & \\ & & & \cdot & & & \\ & & & \cdot & & & \\ & & & & -1 & 2 & -1 \\ 0 & & & & & -1 & 1 \end{bmatrix}. \tag{6-17a}$$

The eigenvector matrix $\boldsymbol{Pu}$ and eigenvalue matrix $\Lambda(\boldsymbol{Au})$ for $\boldsymbol{Au}$ are

$$\boldsymbol{Pu} = \frac{1}{\sqrt{M}} \begin{bmatrix} 1 & \dots & \cos\frac{k\pi}{M}\left(1-\frac{1}{2}\right) & \dots & \cos\frac{(M-1)\pi}{M}\left(1-\frac{1}{2}\right) \\ 1 & & \cdot & & \cdot \\ 1 & & \cdot & & \cdot \\ 1 & \dots & \cos\frac{k\pi}{M}\left(m-\frac{1}{2}\right) & \dots & \cos\frac{(M-1)\pi}{M}\left(m-\frac{1}{2}\right) \\ 1 & & \cdot & & \cdot \\ 1 & & \cdot & & \cdot \\ 1 & \dots & \cos\frac{k\pi}{M}\left(M-\frac{1}{2}\right) & \dots & \cos\frac{(M-1)\pi}{M}\left(M-\frac{1}{2}\right) \end{bmatrix} \tag{6-17b}$$

$$\Lambda(\boldsymbol{Au}) = \begin{bmatrix} 0 & & & & & & 0 \\ & \cdot & & & & & \\ & & \cdot & & & & \\ & & & -4\sin^2\left(\frac{k\pi}{2M}\right) & & & \\ & & & & \cdot & & \\ & & & & & \cdot & \\ 0 & & & & & & -4\sin^2\left(\frac{(M-1)\pi}{2M}\right) \end{bmatrix} \tag{6-17c}$$

where $M = n_x - 2$, k is the integer ranging from 0 to $M-1$ and m is the integer ranging from 1 to M.

c) Derivation of dimension-reduced equations

By operating $\boldsymbol{Q}^{-1}\otimes\boldsymbol{P}^{-1}$ from left side on Eqs. (6-9) and (6-15) (forward transformation;

analogue to taking the Fourier transform of $\boldsymbol{P}$ in Eq. (6-1)), the following equations are obtained:

$$\begin{aligned}
&\boldsymbol{Q}^{-1}\otimes\boldsymbol{P}^{-1}[\boldsymbol{I}\otimes\boldsymbol{Y}_A^{-1}\boldsymbol{A}+\boldsymbol{Y}_B^{-1}\boldsymbol{B}\otimes\boldsymbol{I}]\Pi_{,,k}+\boldsymbol{Q}^{-1}\otimes\boldsymbol{P}^{-1}(r_k\Pi_{,,k+1}+s_k\Pi_{,,k}+t_k\Pi_{,,k-1})\\
&=\boldsymbol{Q}^{-1}\otimes\boldsymbol{P}^{-1}[\boldsymbol{I}\otimes\boldsymbol{Y}_A^{-1}\boldsymbol{A}+\boldsymbol{Y}_B^{-1}\boldsymbol{B}\otimes\boldsymbol{I}](\boldsymbol{Q}\otimes\boldsymbol{P})\boldsymbol{Q}^{-1}\otimes\boldsymbol{P}^{-1}\Pi_{,,k}\\
&\qquad+\boldsymbol{Q}^{-1}\otimes\boldsymbol{P}^{-1}(r_k\Pi_{,,k+1}+s_k\Pi_{,,k}+t_k\Pi_{,,k-1})\\
&=[\boldsymbol{Q}^{-1}\boldsymbol{Q}\otimes\boldsymbol{P}^{-1}\boldsymbol{Y}_A^{-1}\boldsymbol{A}\boldsymbol{P}+\boldsymbol{Q}^{-1}\boldsymbol{Y}_B^{-1}\boldsymbol{B}\boldsymbol{Q}\otimes\boldsymbol{P}^{-1}\boldsymbol{P}]\boldsymbol{Q}^{-1}\otimes\boldsymbol{P}^{-1}\Pi_{,,k}\\
&\qquad+\boldsymbol{Q}^{-1}\otimes\boldsymbol{P}^{-1}(r_k\Pi_{,,k+1}+s_k\Pi_{,,k}+t_k\Pi_{,,k-1})\\
&=[\boldsymbol{I}\otimes\Lambda(\boldsymbol{A})+\Lambda(\boldsymbol{B})\otimes\boldsymbol{I}]\boldsymbol{Q}^{-1}\otimes\boldsymbol{P}^{-1}\Pi_{,,k}\\
&\qquad+(r_k\boldsymbol{Q}^{-1}\otimes\boldsymbol{P}^{-1}\Pi_{,,k+1}+s_k\boldsymbol{Q}^{-1}\otimes\boldsymbol{P}^{-1}\Pi_{,,k}+t_k\boldsymbol{Q}^{-1}\otimes\boldsymbol{P}^{-1}\Pi_{,,k-1})\\
&=\boldsymbol{Q}^{-1}\otimes\boldsymbol{P}^{-1}\Phi_{,,k}
\end{aligned}\tag{6-18}$$

Upper and lower boundary conditions are

$$\begin{aligned}
&-\partial z\boldsymbol{Q}^{-1}\otimes\boldsymbol{P}^{-1}\Pi]_{k=1+1/2}-0.5h_{1+1/2}(\boldsymbol{Q}^{-1}\otimes\boldsymbol{P}^{-1}\Pi_{,,1}+\boldsymbol{Q}^{-1}\otimes\boldsymbol{P}^{-1}\Pi_{,,2})\\
&\qquad=\boldsymbol{Q}^{-1}\otimes\boldsymbol{P}^{-1}\Phi_{b,,1}\\
&\partial z\boldsymbol{Q}^{-1}\otimes\boldsymbol{P}^{-1}\Pi]_{k=nz}+0.5h_{nz-1/2}(\boldsymbol{Q}^{-1}\otimes\boldsymbol{P}^{-1}\Pi_{,,nz-1}+\boldsymbol{Q}^{-1}\otimes\boldsymbol{P}^{-1}\Pi_{,,nz})\\
&\qquad=\boldsymbol{Q}^{-1}\otimes\boldsymbol{P}^{-1}\Phi_{b,,nz}.
\end{aligned}\tag{6-19}$$

Define the vectors with $(nx-2)\times(ny-2)$ elements as

$$S_{,,k}\equiv\boldsymbol{Q}^{-1}\otimes\boldsymbol{P}^{-1}\Pi_{,,k},\tag{6-20}$$

$$R_{,,k}\equiv\boldsymbol{Q}^{-1}\otimes\boldsymbol{P}^{-1}\Phi_{,,k}.\tag{6-21}$$

Let the $[(nx-2)\ (j-1)+i]$-th elements of $S_{,,k}$ and $R_{,,k}$ be expressed as $S_{i,j,k}$ and $R_{i,j,k}$, respectively, and introduce vectors $S_{i,j,;}$ and $R_{i,j,;}$ as

$$S_{i,j,;}{}^{tr}\equiv(S_{i,j,1};\ S_{i,j,2};\ \ldots\ldots\ S_{i,j,nz}),\tag{6-22}$$

$$R_{i,j,;}{}^{tr}\equiv(R_{i,j,1};\ R_{i,j,2};\ \ldots\ldots\ R_{i,j,nz}).\tag{6-23}$$

Here, the dimension-reduced equations for Eqs. (6-9) and (6-5) (analogue to the vertical structure equation of (6-1)) are given as below:

$$C_{i,j}S_{i,j},; = R_{i,j}, \quad \text{for} \quad 1 \leqq i \leqq nx-2 \quad \text{and} \quad 1 \leqq j \leqq ny-2, \tag{6-24}$$

$$C_{i,j} \equiv \begin{bmatrix} b_1, & b_2, & & 0 & & 0 \\ t_2, & s_2+e_2+\lambda_i(A)+\lambda_j(B), & & r_2 & & \\ & \cdot & & \cdot & & \\ & \cdot & & \cdot & & \\ 0 & t_k, & & s_k+e_k+\lambda_i(A)+\lambda_j(B), & r_k, & 0 \\ & & & & \cdot & \\ & & & & \cdot & \\ 0 & & & 0 & b_{nz-1}, & b_{nz} \end{bmatrix} \tag{6-25}$$

$$b_1 = \frac{1}{\Delta z_{1+1/2}} - \frac{h_{1+1/2}}{2}, \qquad b_2 = -\frac{1}{\Delta z_{1+1/2}} - \frac{h_{1+1/2}}{2} \tag{6-26}$$

$$t_k = -\frac{1}{\Delta z_k}\left(\frac{1}{\Delta z_{k-1/2}} - \frac{h_{k-1/2}}{2}\right) \tag{6-27}$$

$$s_k = \frac{1}{\Delta z_k}\left(\frac{1}{\Delta z_{k-1/2}} + \frac{1}{\Delta z_{k+1/2}} - \frac{h_{k+1/2}-h_{k-1/2}}{2}\right) \tag{6-28}$$

$$r_k = -\frac{1}{\Delta z_k}\left(\frac{1}{\Delta z_{k+1/2}} + \frac{h_{k+1/2}}{2}\right) \tag{6-29}$$

$$b_{nz-1} = -\frac{1}{\Delta z_{nz-1/2}} + \frac{h_{nz-1/2}}{2}, \qquad b_{nz} = \frac{1}{\Delta z_{nz-1/2}} + \frac{h_{nz-1/2}}{2}. \tag{6-30}$$

$\lambda_i(\boldsymbol{A})$ and $\lambda_j(\boldsymbol{B})$ are the i-th and j-th diagonal elements of eigenvalue matrixes $\Lambda(\boldsymbol{A})$ and $\Lambda(\boldsymbol{B})$, respectively.

d) Solving method of dimension-reduced equations and backward transformation

The matrix $\boldsymbol{C}_{i,j}$ is a tridiagonal $(nz,\ nz)$ matrix, and Eq. (6-24) can be solved easily, say, by Gaussian elimination method, unless $\boldsymbol{C}_{i,j}$ is singular.

$\boldsymbol{C}_{i,j}$ becomes singular with rank of $(nz-1)$ if $e=0$ and $\lambda_{i_0}(\boldsymbol{A})=0$ and $\lambda_{j_0}(\boldsymbol{B})=0$, *i.e.*, for the case of Poisson equation and for the horizontally uniform mode ($i=i_0$ and $j=j_0$). This corresponds to the non-uniqueness of the solution of the Poisson equation with

Neumann boundary condition. In this case, the constraint of

$$S_{i_0,j_0,nz-1} + S_{i_0,j_0,nz} = 0 \tag{6-31}$$

is imposed, and the solution is uniquely obtained.

Once $S_{i,j,;}$ for all i and j is obtained, $\Pi_{,,k}$ is calculated (backward transformation) as

$$\Pi_{,,k} = \boldsymbol{Q} \otimes \boldsymbol{P} S_{,,k} \quad \text{(for all } k\text{)}. \tag{6-32}$$

$P_{i,j,k}$ outside the domain ($i = 1$ or nx; $j = 1$ or ny) are determined from Eqs. (6-7) and (6-8).

The alternative method of solving Eq. (6-24) using the eigen vector matrix $\boldsymbol{U}$ for a singular $\boldsymbol{C}$ is given as below.

$$\boldsymbol{CU} = \boldsymbol{U}\Lambda(\boldsymbol{C}); \tag{6-33}$$

$$\boldsymbol{U}^{-1}\boldsymbol{CUU}^{-1}S_{i,j,;} = \Lambda(\boldsymbol{C})\boldsymbol{U}^{-1}S_{i,j,;} = \boldsymbol{U}^{-1}R_{i,j,;} \tag{6-34}$$

$$S_{i,j,;} = \boldsymbol{U}\Lambda^{-1} * (\boldsymbol{C})\boldsymbol{U}^{-1}R_{i,j,;} \tag{6-35}$$

where $\Lambda^{-1} * (\boldsymbol{C})$ is the quasi-inverse of $\Lambda(\boldsymbol{C})$ defined by

$$\Lambda^{-1} * (\boldsymbol{C}) = \begin{bmatrix} 0 & 0 & & & & 0 \\ 0 & 1/\lambda_2 & & & & \\ & & 1/\lambda_2 & & & \\ & & & & & \\ & & & 1/\lambda_k & & \\ & & & & & \\ 0 & & & & & 1/\lambda_{nz} \end{bmatrix} \tag{6-36}$$

with the eigen value $\lambda_1 = 0$. This method is not yet implemented.

B-6-2. The solvability condition and the constraint of mass conservation

The matrix $\boldsymbol{C}$ (Eq. (6-25)) becomes singular with rank of $(nz-1)$ if $e = 0$, $\lambda_i(\boldsymbol{A}) = 0$ and $\lambda_j(\boldsymbol{B}) = 0$, *i.e.*, for the case of Poisson equation (AE scheme) and for the horizontally uniform modes. Here, the singular case ($e = 0$ case; AE scheme) is considered in detail. Let $i = 1$ and $j = 1$ denote the uniform horizontal mode of $\lambda_i(\boldsymbol{A}) = 0$ and $\lambda_j(\boldsymbol{B}) = 0$. For simplicity, no mountain is included. For a singular matrix $\boldsymbol{C}$, there exists a nullifying vector Z such as

$$Z^{tr}\boldsymbol{C} = 0, \tag{6-37}$$

where 0 is the row vector with all elements being zero.

As a result, the following must be satisfied:

$$Z^{tr}CS_{1,1,;} = 0 = Z^{tr}R_{1,1,;} \tag{6-38}$$

$$Z^{tr} = (1,\ \Delta z_2,\ \Delta z_3,\ \ldots\ldots\ \Delta z_{nz-1},\ 1). \tag{6-39}$$

Unless $Z^{tr}R_{1,1,;} = 0$, Eq. (6-24) is ill-posed, and insolvable. Solvability condition, $Z^{tr}R_{1,1,;} = 0$, is related to the mass conservation as delineated below.

Horizontally uniform modes correspod to horizontally averaged modes. Taking horizontal average of Eq. (6-1) yields

$$\begin{aligned}&\iint [\partial_{xx}P + \partial_{yy}P + \partial_{zz}P + \partial_z hP]\, dxdy \\ &\quad = \iint [-\partial_x \mathrm{ADVU} - \partial_y \mathrm{ADVV} - \partial_z(\mathrm{ADVW} - \mathrm{BUOY})]\, dxdy\end{aligned} \tag{6-40}$$

By use of lateral boundary conditions Eqs. (6-3) and (6-4), it is rewritten as below.

$$\begin{aligned}\iint [\partial_{zz}P + \partial_z hP]\, dxdy = \int \left[\frac{\partial U_{\mathrm{out}}}{\partial t} - \frac{\partial U_{\mathrm{in}}}{\partial t}\right] dy + \int \left[\frac{\partial V_{\mathrm{out}}}{\partial t} - \frac{\partial V_{\mathrm{in}}}{\partial t}\right] dx \\ - \partial_z\left(\iint [\mathrm{ADVW} - \mathrm{BUOY}]\, dxdy\right).\end{aligned} \tag{6-41}$$

Note that the lefthand side of Eq. (6-41) corresponds to $CS_{1,1,;}$ the the righthand side corresponds to $R_{1,1,;}$. Roughly speaking, operation of the vector Z from the left side on Eq. (6-24) corresponds to taking the vertical integration of the above relation, considering upper and lower boundary conditions Eq. (6-5). This yields

$$\int \left(\int \left[\frac{\partial U_{\mathrm{out}}}{\partial t} - \frac{\partial U_{\mathrm{in}}}{\partial t}\right] dy + \int \left[\frac{\partial V_{\mathrm{out}}}{\partial t} - \frac{\partial V_{\mathrm{in}}}{\partial t}\right] dx\right) dz = 0. \tag{6-42}$$

This is the constraint of the mass conservation over the entire domain. In section B-7, the adjustment to satisfy this constraint on the time derivative of U and V on the lateral boundary will be shown. This adjustment is found to be necessary for stable run of the numerical model using both AE and E-HI-VI schemes.

B-6-3. The case of cyclic lateral boundary conditions

The equation is almost similar to that of the noncyclic case except that the matrix $\boldsymbol{A}$ (or $\boldsymbol{B}$) is changed as

$$
\boldsymbol{A} \equiv
$$

$$
\begin{bmatrix}
\frac{1}{\Delta x_{1+1/2}} + \frac{1}{\Delta x_{2+1/2}}, & \frac{-1}{\Delta x_{2+1/2}}, & 0, & 0, & \cdots & 0, & \frac{-1}{\Delta x_{1+1/2}} \\
\frac{-1}{\Delta x_{2+1/2}}, & \frac{1}{\Delta x_{2+1/2}} + \frac{1}{\Delta x_{3+1/2}}, & & -\frac{1}{\Delta x_{3+1/2}}, & & 0, & 0 \\
 & & & \vdots & & & \\
0, & -\frac{1}{\Delta x_{i+1/2}}, & \frac{1}{\Delta x_{i+1/2}} + \frac{1}{\Delta x_{i+3/2}}, & -\frac{1}{\Delta x_{i+3/2}}, & & 0, & 0 \\
 & & & \vdots & & & \\
\frac{-1}{\Delta x_{1+1/2}}, & 0, & \cdots & 0, & \frac{-1}{\Delta x_{nx-3/2}}, & \frac{1}{\Delta x_{nx-3/2}} + \frac{1}{\Delta x_{nx-1/2}} &
\end{bmatrix}
\tag{6-43}
$$

Note that $\Delta x_{1+1/2} = \Delta x_{nx-1/2}$ for the cyclic case.

The solving method of the pressure equation for the case of uniform grid and the cyclic boundary conditions is described in detail in Ikawa (1981).

B-7. Lateral boundary conditions

The model can handle four kinds of lateral boundary conditions as below:

1. Open in the x-direction and wall in the y-direction.
2. Open in both x- and y-directions.
3. Open in the x-direction and cyclic in the y-direction.
4. Cyclic in both x- and y-directions.

B-7-1. Cyclic boundary conditions

For all field varibles, F,

$$F_{1,j,k} = F_{nx-1,j,k}; \quad F_{nx,j,k} = F_{2,j,k}; \quad \text{for all } j \text{ and } k$$

$$F_{i,1,k} = F_{i,ny-1,k}; \quad F_{i,ny,k} = F_{i,2,k}; \quad \text{for all } i \text{ and } k$$

are imposed.

B-7-2. Open boundary conditions

a) For Θ, Qv, $Qc\ldots$ and velocity components non-normal to the boundary plane

The boundary is divided into two cases, *i.e.*, inflow and outflow boundaries. The inflow boundary is the boundary where the velocity normal to the boundary plane is directed into the model domain. The outflow boundary is the boundary where the velocity normal to the boundary plane is directed out of the model domain. Let us consider the one dimensional case shown in Fig. B-7-1. In the case of $U > 0$, the inflow boundary is the left boundary ($i = 3/2$) and the outflow boundary is the right boundary ($i = nx - 1/2$).

```
           Fb     U    F    U   F...   U    F      U    Fb
       outside    |  inner domain                  | outside
index      1     3/2   2             ....   nx-1 nx-1/2 nx
           b          b+1   b+2
```

Fig. B-7-1 Grid index used in B-7-2 a).

a-1) At the inflow boundary

Boundary values F_b are specified as below.

$$F_b{}^{it+1} = \mu F.\mathrm{ext} + (1-\mu) F_b{}^{it-1} \tag{7-1}$$

F_b: the value just outside the boundary

F.ext: external value specified from outside

a-2) At the outflow boundary

If the left boundary ($i = 3/2$) is the outflow boundary, boundary values are extrapolated from the values of the inner domain as below:

$$F_b^{it+1} = 2F_{b+1}^{it} - F_{b-2}^{it-1} \tag{7-2}$$

For the right boundary case, boundary values are extrapolated in a similar way.

b) Velocity components normal to the boundary plane

For simplicity, the one-dimensional case shown in Fig. B-7-2 is considered. First, the phase speed, Cp, of waves at the boundary is estimated. Next, it is determined whether waves are outgoing or incoming from the sign of the phase speed. For the outgoing case, a radiation condition is applied.

b-1) At the left boundary (at $i = JS$)

The basic equation adopted by Orlanski (1976) is

$$\frac{U^{it}(JS) - U^{it-2}(JS)}{2\Delta t} = \frac{Cp}{\Delta x}\left[\frac{U^{it}(JS) + U^{it-2}(JS)}{2} - U^{it-1}(JS+1)\right], \tag{7-3}$$

where Cp is the phase velocity of waves radiating into outer region. Cp is estimated as follows: First $Cp(it-1)$ is calculated from values at it, $it-1$ and $it-2$ on the inside grid points as

	U	U	U		U	U	U	
outside	|			inner domain			|	outside
index	JS	JS+1	JS+2	....	JM-2	JM-1	JM	

Fig. B-7-2 Grid index used in B-7-2 b).

$$Cp(it-1) = \frac{\Delta x}{\Delta t} \frac{[U^{it}(JS+1) - U^{it-2}(JS+1)]}{[U^{it}(JS+1) + U^{it-2}(JS+1) - 2U^{it-1}(JS+2)]}. \tag{7-4}$$

Next, $Cp(it-1)$ is modified as

$$Cp*(it) = \text{MIN}\left(0,\ \text{MAX}\left(-\frac{\Delta x}{\Delta t},\ Cp(it-1)\right)\right). \tag{7-5}$$

This $Cp*(it)$ is an estimator of C. Substitution of C by $Cp*(t)$ in Eq. (7-3) yields

$$U^{it+1}(JS) = U^{it-1}(JS) + \frac{2\Delta t}{\Delta x} Cp*(it) \frac{U^{it-1}(JS) - U^{it}(JS+1)}{\left(1 - \frac{\Delta t}{\Delta x} Cp*(it)\right)}. \tag{7-6}$$

b-2) At the right boundary (at $i = JM$ in Fig. B-7-2)

In a similar way to the left boundary, the basic equation is

$$\frac{U^{it}(JM) - U^{it-2}(JM)}{2\Delta t} = -\frac{Cp}{\Delta x}\left[\frac{U^{it}(JM) + U^{it-2}(JM)}{2} - U^{it-1}(JM-1)\right]. \tag{7-7}$$

Cp is estimated as below:

$$Cp(it-1) = -\frac{\Delta x}{\Delta t} \frac{[U^{it}(JM-1) - U^{it-2}(JM-1)]}{[U^{it}(JM-1) + U^{it-2}(JM-1) - 2U^{it-1}(JM-2)]}. \tag{7-8}$$

Modification of $Cp(it)$ gives $Cp*(it)$ as

$$Cp*(it) = \text{MAX}\left(0,\ \text{MIN}\left(\frac{\Delta x}{\Delta t},\ Cp(it-1)\right)\right). \tag{7-9}$$

This $Cp*(it)$ is an estimator of Cp. Substitution of Cp by $Cp*(it)$ in Eq. (7-7) yields

$$U^{it+1}(JM) = U^{it-1}(JM) + \frac{2\Delta t}{\Delta x} Cp*(it) \frac{U^{it}(JM-1) - U^{it-1}(JM)}{\left(1 + \frac{\Delta t}{\Delta x} Cp*(it)\right)}, \tag{7-10}$$

b-3) Setting of the time tendency of U at the boundary

Computed phase velocities $Cp*$'s are smoothed by taking average of $Cp*$'s on the adjacent grid points. Judging from the sign of $Cp*$, it is determined whether waves are outgoing or incoming at the boundary.

In an outgoing case, the time tendency of U at the boundary, DUDTBC, is computed as follows:

at the left boundary (at $i = JS$), $Cp* < 0$

$$\text{DUDTBC}(y,\ z,\ 1) \equiv \left.\frac{\partial U}{\partial t}\right)_{b.\text{left}}$$

$$= \frac{U^{it+1}(JS) - U^{it-1}(JS)}{2\Delta t} = \frac{1}{\Delta x} Cp * (it) \frac{U^{it-1}(JS) - U^{it}(JS+1)}{\left(1 - \frac{\Delta t}{\Delta x} Cp * (it)\right)} \tag{7-11a}$$

at the right boundary (at $i = JM$), $Cp* > 0$

$$\mathrm{DUDTBC}(y,\ z,\ 2) \equiv \left.\frac{\partial U}{\partial t}\right)_{b.\mathrm{right}}$$

$$= \frac{U^{it+1}(JM) - U^{it-1}(JM)}{2\Delta t} = \frac{1}{\Delta x} Cp * (it) \frac{-U^{it-1}(JM) + U^{it}(JM-1)}{\left(1 + \frac{\Delta t}{\Delta x} Cp * (it)\right)} \tag{7-11b}$$

In an incoming case, *i.e.*,

at the left boundary (at $i = JS$), $Cp * \geqq 0$

or at the right boundary (at $i = JM$), $Cp * \leqq 0$,

the time tendency of U at the boundary, DUDTBC, is computed in order to restore the boundary value to the external value, U.ext, to a certain degree as follows:

$$\mathrm{DUDTBC} \equiv \left.\frac{\partial U}{\partial t}\right)_b = [\mu U.\mathrm{ext} + (1-\mu)U^{it-1} - U^{it-1}]/2\Delta t. \tag{7-11c}$$

Note that $\mu = 1$ makes U^{it+1} at the boundary equal to U.ext.

b-4) Adjustment of the time tendency of U and V at the boundary

In order to satisfy mass conservation in the entire domain,

$$\iiint \{\partial x U + \partial y V + \partial z W^*\}\, dx\, dy\, dz = \iint (U_{\mathrm{in}} - U_{\mathrm{out}})\, dz\, dy + \iint (V_{\mathrm{in}} - V_{\mathrm{out}})\, dz\, dx = 0,$$

the adjustment to the time tendencies of U and V at the boundaries, DUDTBC and DVDTBC, is needed. The constant value of adjustment, ADJ, is derived from the equation below:

$$\iint \{[\mathrm{DUDTBC}(y,\ z,\ 1) - \mathrm{ADJ}] - [\mathrm{DUDTBC}(y,\ z,\ 2) + \mathrm{ADJ}]\}\, dz\, dy$$
$$+ \iint \{[\mathrm{DVDTBC}(x,\ y,\ 1) - \mathrm{ADJ}] - [\mathrm{DVDTBC}(x,\ y,\ 2) + \mathrm{ADJ}]\}\, dz\, dx = 0. \tag{7-12}$$

This equation yields

$$\mathrm{ADJ} = 0.5 \times \mathrm{error}/(\iint dz dx + \iint dz\, dy), \tag{7-13}$$

where

$$\text{error} = \iint [\text{DUDTBC}(y,\ z,\ 1) - \text{DUDTBC}(y,\ z,\ 2)]\, dz\, dy$$
$$+ \iint [\text{DVDTBC}(x,\ z,\ 1) - \text{DVDTBC}(x,\ z,\ 2)]\, dz\, dx \tag{7-14}$$

and index 1 for DUDTBC (or DVDTBC) denotes the value at $i = 1 + 1/2$ (or $j = 1 + 1/2$) and index 2 denotes the value at $i = nx - 1/2$ (or $j = ny - 1/2$).

The adjustments on DUDTBC and DVDTBC are

$$\left.\begin{aligned}
\text{DUDTBC}(y,\ z,\ 1) &\longleftarrow \text{DUDTBC}(y,\ z,\ 1) - \text{ADJ},\\
\text{DUDTBC}(y,\ z,\ 2) &\longleftarrow \text{DUDTBC}(y,\ z,\ 2) + \text{ADJ},\\
\text{DVDTBC}(x,\ z,\ 1) &\longleftarrow \text{DVDTBC}(x,\ z,\ 1) - \text{ADJ},\\
\text{DVDTBC}(x,\ z,\ 2) &\longleftarrow \text{DVDTBC}(x,\ z,\ 2) + \text{ADJ}.
\end{aligned}\right\} \tag{7-15}$$

As discussed in B-6-2, the requirement of mass conservation in the entire domain is related to the solvability condition of the pressure equation. Adjustment on DUDTBC and DVDTBC is necessary for the realization of the solvability condition of the pressure equation.

P.G.

Cp is set in arrays CPHU and CPHV by subs.ORUCPH and ORVCPH, respectively, which are called in sub.SVELC. The setting of DUDTBC and adjustment is done by sub. SUVPBD in mem.SFXHEI. Array DUDTBC and DVDTBC are used in setting lateral boundary condition for pressure and computing boundary values of U and V.

c) For the pressure equation of AE and E-HI-VI

c-1) For the pressure equation of AE

Neumann boundary condition for pressure is obtained from Eq. (1-28):

$$\frac{\partial}{\partial x}(P) = -\text{ADVU} - \left.\frac{\partial U}{\partial t}\right)_b - \frac{\partial}{\partial \xi}(G^{13}P) = -\text{ADVU} - \text{DUDTBC} - \frac{\partial}{\partial \xi}(G^{13}P). \tag{7-16}$$

The time tendency of U at the boundary, DUDTBC is computed as discussed in B-7-2, b-4).

c-2) For the pressure equation of E-HI-VI

Neumann boundary condition for pressure is obtained from Eq. (3-32):

$$\frac{\partial}{\partial x}(\Delta^2 P) = -2\text{ADVU}'' - \frac{\Delta^2 U}{\Delta t\alpha''} = -2\left[\text{ADVU}'' + \text{DUDTBC} - \frac{U^{it} - U^{it-1}}{\Delta t\alpha''}\right] \tag{7-17}$$

P.G.

The righthand side of Eqs. (7-16) and (7-17) are evaluated by sub.SUVPBD in mem.SFXHEL and provided as the lateral boundary condition by sub.SFPBD.

B-7-3. Wall lateral boundary conditions

The wall is free-slip, and thermally insulated. This condition imposed at $j = 1+1/2$ and $ny-1/2$ is described below. For all field variables except for V, the (mirror image) condition

$$F_{i,1,k} = F_{i,2,k}; \quad F_{i,ny,k} = F_{i,ny-1,k} \tag{7-18}$$

is imposed.

For the velocity component V, normal to the wall boundary,

$$\left.\begin{array}{ll} V_{i,1/2,k} = -V_{i,2+1/2,k}; & V_{i,1+1/2,k} = 0; \\ V_{i,ny+1/2,k} = -V_{i,ny-3/2,k}; & V_{i,ny-1/2,k} = 0; \end{array}\right\} \tag{7-19}$$

are imposed.

In the evaluation of ADVV at $j = 1+1/2$, which is necessary for the boundary condition to pressure,

$$\mathrm{ADVV} \equiv \partial_x(\overline{U}^y\overline{v}^x) + \partial_y(\overline{V}^y\overline{v}^y) + \partial_z(\overline{W^*}^y\overline{v}^z), \tag{7-20}$$

the following term must be adopted:

$$\partial y(\overline{V}^y\overline{v}^y) = \frac{\overline{V}^y\overline{v}^y]_2 - \overline{V}^y\overline{v}^y]_1}{\Delta y_{1+1/2}} = \frac{2\overline{V}^y\overline{v}^y]_2}{\Delta y_{1+1/2}}, \tag{7-21}$$

where the following relation is virtually used such as

$$\overline{V}^y\overline{v}^y]_{j=2} + \overline{V}^y\overline{v}^y]_{j=1} = 0. \tag{7-22}$$

This makes dynamic pressure at the wall boundary to be properly calculated (see also Eqs. (8-11), (8-12)).

B-7-4. Sponge layer

Rayleigh damping near the lateral boundary, $D_{r\ell}$, is imposed to prevent the false reflection of internal gravity waves from the lateral boundary, enforce the environmental external conditions (designated by f.ext below) and suppress noises.

$$D_{r\ell}(f) = -\frac{1}{2m_{r\ell}\Delta t}\left(1+\cos\left(\frac{\pi(LX-x)}{x_d}\right)\right)(f - f.\mathrm{ext}) \tag{7-23}$$

for $x > LX - x_d$.

$$D_{r\ell}(f) = -\frac{1}{2m_{r\ell}\Delta t}\left(1+\cos\left(\frac{\pi x}{x_d}\right)\right)(f - f.\mathrm{ext}) \tag{7-24}$$

for $x < x_d$.

B-8. Lower boundary conditions

B-8-1. For velocity

For W, the kinematical condition,

$$\frac{1}{G^{1/2}} W + \overline{G^{13}\overline{U}^{z}}^{x} + \overline{G^{23}\overline{V}^{z}}^{y} \equiv W^* = \overline{\rho} G^{1/2}\omega = \overline{\rho} G^{1/2}\frac{d\xi}{dt} = 0 \tag{8-1}$$

at $k = 1 + 1/2$ is imposed.

For the case of no friction (free-slip; no subgrid scale momentum flux),

$$\overline{\rho u'' w''} = 0 \ (\text{at } k = 1 + 1/2), \quad U_{k=1} = U_{k=2}, \quad V_{k=1} = V_{k=2}, \tag{8-2}$$

is imposed.

For the case of friction (non-slip; subgrid scale momentum flux is present; see B-10-2),

$$\overline{\rho u'' w''} = -\overline{\rho} C_{dm} V_a \frac{(U^* + U_{k=2})}{\overline{\rho} G^{1/2}}, \tag{8-3}$$

$$V_a \equiv \frac{((U^* + U_{k=2})^2 + (V^* + V_{k=2})^2)^{1/2}}{\overline{\rho} G^{1/2}} \tag{8-4}$$

is imposed. The suffix $k = 2$ denote the lowest level above the ground. U^* and V^* are the translation velocity components of the numerical model frame relative to the earth surface. It is noted that U and V are velocity components of air relative to the model frame, and those relative to the earth surface are given by $U^* + U$ and $V^* + V$, respectively.

$\overline{\rho v'' w''}$ is formulated in a similar way to $\overline{\rho u'' w''}$.

B-8-2. For Θ and Qv

For the case of no flux condition,

$$\overline{\rho \theta'' w''} = 0 \quad \text{and} \quad \Theta_{k=1} = \Theta_{k=2}, \tag{8-5}$$

$$\overline{\rho Qv'' w''} = 0 \quad \text{and} \quad Qv_{k=1} = Qv_{k=2}. \tag{8-6}$$

For the case of flux condition (see B-10-2),

$$\overline{\rho \theta'' w''} = -\overline{\rho} C_{dh} V_a (\Theta_2 - \Theta s) \quad \text{and} \quad \Theta_{k=1} = \Theta s \tag{8-7}$$

$$\overline{\rho Qv'' w''} = -\overline{\rho} C_{dh} V_a (Qv_2 - Qv_s) \quad \text{and} \quad Qv_{k=1} = Qv_s, \tag{8-8}$$

where Θs and Qv_s are the potential temperature and mixing ratio of water vapor at the (sea or ground) surface. Over the land, C_{dm} and C_{dh} are determined from Monin and Obukhov's similarity law (see Sommeria, 1976). Over the sea, they are determined from the formula by Kondo (1975).

P.G.

For the case of no friction (free-slip; no subgrid-scale momentum flux), MSW(1) $=0$ must be specified to the program.

For the case of friction (non-slip), MSW(1) $=1$ must be specified to the program.

For the case of no heat flux condition, MSW(1) $=0$ or (MSW(1) $=1$ and MSW(13) $=0$) must be specified to the program.

For the case of heat flux condition, MSW(1) $=1$ and MSW(13) $=1$ must be specified to the program.

B-8-3. For pressure

$$\mathrm{PFZ}]_{1+1/2} = \frac{1}{G^{1/2}}\partial zP + \frac{g\overline{P}^{z}}{Cs^2} = -\frac{\partial W}{\partial t} - \mathrm{ADVW} + \mathrm{BUOY} \tag{8-9}$$

is specified so as to be consistent with the kinematic condition Eq. (8-1). The estimation of ADVW and BUOY at $k=1+1/2$ is somewhat ambiguous for the case of non-slip (flux) condition.

$$\mathrm{ADVW} \equiv \partial_x(\overline{U}^z\overline{w}^x) + \partial_y(\overline{V}^z\overline{w}^y) + \partial_z(\overline{W^*}^z\overline{w}^z), \tag{8-10}$$

where

$$\partial_z(W^*w) = \frac{\overline{W^*}^z\overline{w}^z]_2 - \overline{W^*}^z\overline{w}^z]_1}{\Delta z_{1+1/2}} = \frac{2\overline{W^*}^z\overline{w}^z]_2}{\Delta z_{1+1/2}}. \tag{8-11}$$

The above equation comes from the following relation:

$$\overline{W^*}^z\overline{w}^z]_{k=1} + \overline{W^*}^z\overline{w}^z]_{k=2} = 0, \tag{8-12}$$

which is required from the vertical momentum conservation (see Clark, 1977. Eq. (3-33)).

Buoyancy term is computed as

$$\mathrm{BUOY} \equiv g\frac{\overline{\overline{\rho}G^{1/2}}^z\,\overline{\Theta'_m}^z}{\overline{\Theta}_m},$$

$$\Theta'_{m,k=1+1/2} = 0.5(\Theta_{m,k=2} + \Theta_{m,k=1}) - \overline{\Theta}_m.$$

In the case where heat flux is present, currently $\Theta_{m,k=1} = \Theta_{m,s}$ is used. However, the use of

$$\Theta'_{m,k=1+1/2} = 0.5(\Theta_{m,k=2} + \overline{\Theta}_{m,k=1}) - \overline{\Theta}_{m,k=1+1/2}$$

might be better in this case.

B-9. Upper boundary conditions

The upper boundary is the slip, thermally insulated rigid wall. Currently, radiation conditions (Klemp and Durran, 1983) is not implemented. Instead, sponge layer (absorption of waves by Rayleigh friction) (see B-12-3) is introduced to realize quasi-radiation conditions.

B-9-1. For velocity

For W, the kinematical condition,

$$\frac{1}{G^{1/2}} W + \overline{G^{13}\overline{U}^{z}}^{x} + \overline{G^{23}\overline{V}^{z}}^{y} \equiv W^{*} = \overline{\rho} G^{1/2} \omega = \overline{\rho} G^{1/2} \frac{d\xi}{dt} = 0 \tag{9-1}$$

at $k = nz - 1/2$ is imposed (note ${G^{13}}_{k=nz-1/2} = 0$, *i.e.*, Eq. (9-1) is equivalent to $W = 0$).

No friction (free-slip; no subgrid scale momentum flux) condition, such as

$$\overline{u''w''} = 0 \text{ (at } k = nz - 1/2), \quad U_{k=nz} = U_{k=nz-1}, \; V_{k=nz} = V_{k=nz-1}, \tag{9-2}$$

is imposed.

B-9-2. For Θ and Qv

No flux condition, such as

$$\overline{\overline{\rho}\theta''w''} = 0 \quad \text{and} \quad \Theta_{k=nz-1} + \Theta_{k=nz} = \overline{\Theta}, \tag{9-3}$$

$$\overline{\overline{\rho}Qv''w''} = 0 \quad \text{and} \quad Qv_{k=nz-1} = Qv_{k=nz}. \tag{9-4}$$

Note that $\Theta_{k=nz-1} + \Theta_{k=nz} = \overline{\Theta}$ guarantees $\mathrm{BUOY}_{k=nz-1/2} = 0$.

B-9-3. For pressure

$$\mathrm{PFZ}]_{nz-1/2} = \frac{1}{G^{1/2}} \partial z P + \frac{g\overline{P}^{z}}{Cs^2} = -\frac{\partial W}{\partial t} - \mathrm{ADVW} + \mathrm{BUOY} \tag{9-5}$$

is specified so as to be consistent with the kinematic condition Eq. (9-1). The first term of the righthand side of Eq. (9-5) is zero due to $W_{k=nz-1/2} = 0$.

$$\mathrm{ADVW} \equiv \partial x(\overline{U}^{z}\overline{w}^{x}) + \partial y(\overline{V}^{z}\overline{w}^{y}) + \partial z(\overline{W^{*}}^{z}\overline{w}^{z}) = \partial z(\overline{W^{*}}^{z}\overline{w}^{z})$$

$$= \frac{\overline{W^{*}}^{z}\overline{w}^{z}]_{nz} - \overline{W^{*}}^{z}\overline{w}^{z}]_{nz-1}}{\Delta z_{nz-1/2}} = \frac{-2\overline{W^{*}}^{z}\overline{w}^{z}]_{nz-1}}{\Delta z_{nz-1/2}},$$

where the following relation is used:

$$\overline{W^*}^z\overline{w}^z]_{k=nz} + \overline{W^*}^z\overline{w}^z]_{k=nz-1} = 0.$$

The above relation comes from the vertical momentum conservation (see Clark, 1977, Eq. (3-33)).

B-9-4. Absorption layer

Rayleigh damping near the upper boundary, D_{ru}, is added for a field variable $f(f = u,\ v,\ w,\ \theta)$ in the upper part of the domain $(z > z_d)$ to prevent the false reflection of internal gravity waves from the upper right wall.

$$D_{ru}(f) = -\frac{1}{2m_{ru}\Delta t}\left(1 + \cos\left(\frac{\pi(LZ - z)}{LZ - z_d}\right)\right)(f - f.\text{ext}) \tag{9-6}$$

for $z > z_d$. Here, LZ is the height of the domain.

B-10. Subgrid-scale turbulence

B-10-1. Turbulent closure model

To determine the diffusion coefficients, the turbulent closure model is used. The formulation is based on that by Klemp and Wilhelmson (1978) and Deardorff (1980).

The prognostic equation for subgrid-scale turbulent kinetic energy E is given as follows:

$$\frac{dE}{dt} = \mathrm{BUOYP} - \overline{u_i'' u_j''}\frac{\partial u_i}{\partial x_j} + \frac{\partial}{\partial x_j}\left(K_e \frac{\partial E}{\partial x_j}\right) - \frac{C_e}{\ell} E^{3/2}, \tag{10-1}$$

where

$$E = (\overline{u''^2 + v''^2 + w''^2})/2, \tag{10-2}$$

$$\overline{u_i'' u_j''} = -K_m \left(\frac{\partial u_i}{\partial x_j} + \frac{\partial u_j}{\partial x_i}\right) + \frac{2}{3}\delta_{i,j} E. \tag{10-3}$$

The subgrid-scale perturbation is denoted by the superscript $''$, and the overbar denotes the average of the subgrid-scale quantities in one grid box.

The buoyancy production term BUOYP in Eq. (10-1) is calculated taking account of the cloud water loading and the release of latent heat as

$$\mathrm{BUOYP} = \overline{gw''\left(\frac{\theta''}{\overline{\Theta}} + 0.61 Qv''\right)} = \frac{gK_h}{G^{1/2}}\left(-\frac{1}{\overline{\Theta}}\frac{\partial \Theta}{\partial \xi} - 0.61\frac{\partial Qv}{\partial \xi}\right) \tag{10-4a}$$

for the unsaturate case ($Qc = 0$),

and

$$\mathrm{BUOYP} = \overline{gw''\left(\frac{\theta''}{\overline{\Theta}} + 0.61 Qv'' - Qc''\right)} = \frac{gK_h}{G^{1/2}}\left(-A\frac{\partial \Theta_e}{\partial \xi} + \frac{\partial Qc}{\partial \xi}\right) \tag{10-4b}$$

for the saturate case ($Qc > 0$).

Here

$$A = \frac{1}{\overline{\Theta}}\left(\frac{1 + \dfrac{1.61\varepsilon L Qv}{R_d T}}{1 + \dfrac{\varepsilon L^2 Qv}{C_p R_d T^2}}\right), \tag{10-5}$$

$\varepsilon = 0.622$, Θ_e is the equivalent potential temperature, L the latent heat of vaporization, and R_d the gas constant for dry air. The last two terms in Eq. (10-1) are evaluated at $(it - 1)$ time step in order to maintain numerical stability.

The subgrid-scale mixing length ℓ is determined depending on the thermal stratification. Near the ground surface, it approaches to the product of Karman constant κ $(= 0.4)$ and height from the surface $(z - Z_s)$ when the surface friction exists;

$$\frac{1}{\ell} = \frac{1}{\kappa(z - Z_s)} + \frac{1}{\ell_\infty}, \tag{10-6}$$

where

$$\ell_\infty = \Delta s \qquad \text{for the unstable case } (N_\ell \leqq 0), \tag{10-7a}$$

$$\ell_\infty = \min(\Delta s,\ 0.76E^{1/2}N_\ell{}^{-1}) \qquad \text{for the stable case } (N_\ell > 0), \tag{10-7b}$$

Δs is the typical grid distances, N_ℓ is the local stability and Θ_ℓ is the liquid water potential temperature defined by

$$\Delta s = (\Delta x \Delta z)^{1/2} \qquad \text{for 2-dimensional model,} \tag{10-8a}$$

$$\Delta s = (\Delta x \Delta y \Delta z)^{1/3} \qquad \text{for 3-dimensional model,} \tag{10-8b}$$

$$N_\ell = \frac{g}{\Theta}\frac{\partial \Theta_\ell}{\partial z}, \tag{10-9}$$

$$\Theta_\ell = \Theta - \frac{L}{Cp\Pi}Qc. \tag{10-10}$$

The eddy diffusion coefficients for velocity components, turbulent energy and other predicted variables $(\theta,\ Qv,\ Qc, \ldots)$ are given as

$$K_m = C_m \ell E^{1/2} \quad (C_m = 0.2 \text{ is used}), \tag{10-11}$$

$$K_e = 2K_m, \tag{10-12}$$

$$K_h = P_r^{-1} K_m. \tag{10-13}$$

The coefficient of the viscosity dispersion term in Eq. (10-1) and the inverse Prandtl number P_r^{-1} are given as

$$C_e = 0.19 + 0.51\ell/\Delta s, \tag{10-14}$$

$$P_r^{-1} = 1 + 2\ell/\Delta s. \tag{10-15}$$

The diffusion term by subgrid-scale turbulence for turbulent energy E is given as

$$\text{DIF.}E = -\frac{\partial \overline{u_j{}''E''}}{\partial x_j} = \frac{\partial}{\partial x_j}\left(K_e \frac{\partial E}{\partial x_j}\right), \tag{10-16a}$$

and for other scalar variables $f(\theta,\ Qv,\ Qc, \ldots)$ as

$$\mathrm{DIF}.f = -\frac{\partial \overline{u_j''f''}}{\partial x_j} = \frac{\partial}{\partial x_j}\left(K_h \frac{\partial f}{\partial x_j}\right). \tag{10-16b}$$

The diffusion term by subgrid-scale turbulence for each velocity component ($u = u_1,\ v = u_2,\ w = u_3$) is given as

$$\mathrm{DIF}.u_i = \frac{\partial \overline{u_j''u_i''}}{\partial x_j}. \tag{10-17}$$

The above diffusion terms are evaluated using the values at $(it-1)$ time step to maintain numerical stability.

P.G.

E, K_m and K_h are computed by sub.CTURB5 and CNVED3 in mem.CVTURB, respectively. DIF.f is computed by sub.CDIFE1, and DIF.u is computed by sub.CRSTUV. DIF.f and DIF.u are added to array ADVF and ADVU in which advection terms for f and u have been stored by sub.CADVET and CADVC3, respectively.

B-10-2. Surface fluxes

They are given from the resistance law as follows:

for momentum fluxes,

$$\overline{\overline{\rho}u''w''} = -\overline{\rho}C_{dm}\,V_a\frac{(U^* + U_{k=2})}{\overline{\rho}G^{1/2}}, \tag{10-18a}$$

$$\overline{\overline{\rho}v''w''} = -\overline{\rho}C_{dm}\,V_a\frac{(V^* + V_{k=2})}{\overline{\rho}G^{1/2}}; \tag{10-18b}$$

for sensible heat and water vapor fluxes,

$$\overline{\overline{\rho}\theta''w''} = -\overline{\rho}C_{dh}\,V_a\,(\Theta_2 - \Theta_s), \tag{10-19}$$

$$\overline{\overline{\rho}Qv''w''} = -\overline{\rho}C_{dh}\,V_a\,(Qv_2 - Qv_s), \tag{10-20}$$

where V_a is given by Eq. (8-4). U^* and V^* are translation velocity components of the numerical model frame relative to the earth surface. It is noted that U and V are the velocity components of air relative to the model frame, not to the earth surface. Suffix 2 and s denotes the values at the lowest grid points above the surface and those at the surface, respectively.

Over the sea, C_{dm} and C_{dh} are determined from the formula by Kondo (1975). Over the land, C_{dm} and C_{dh} are determined from Monin and Obukhov's similarity law (see Sommeria,

1976) for a given roughness length of the ground, $z*$. The C_{dm} and C_{dh} are functions of $z_a/z*$ and z_a/L, where $z_a = (\Delta z_{1+1/2})/2$ and L is the local Monin-Obukhov length:

$$L = -\frac{\Theta_s(-\overline{u''w''})^{3/2}}{\kappa g \overline{\theta'' w''}}, \tag{10-21}$$

where κ is 0.4 (Karman constant).

From similarity theory, the drag coefficients can be written as

$$C_{dm} = \frac{1}{\phi^2}, \qquad C_{dh} = \frac{1}{\phi\psi}, \tag{10-22}$$

where ϕ and ψ are universal functions (Businger *et al.* 1971) defined as,

for unstable cases,

$$\left.\begin{aligned} \phi &= \frac{1}{\kappa}\left\{\log\left(\frac{z_a}{z*}\right) - \left[2\log\left(\frac{1+\xi}{2}\right) + \log\left(\frac{1+\xi^2}{2}\right) - 2\arctan(\xi) + \left(\frac{\pi}{2}\right)\right]\right\}, \\ \psi &= \frac{1}{1.35\kappa}\left[\log\left(\frac{z_a}{z*}\right) - 2\log\left(\frac{1+\eta}{2}\right)\right], \end{aligned}\right\} \tag{10-23a}$$

$$\text{with} \quad \xi = \left(1 - 15\frac{z_a}{L}\right)^{1/2} \quad \text{and} \quad \eta = \left(1 - 9\frac{z_a}{L}\right)^{1/2},$$

and,

for neutral or stable cases,

$$\left.\begin{aligned} \phi &= \frac{1}{\kappa}\left\{\log\left(\frac{z_a}{z*}\right) + 4.7\frac{z_a}{L}\right\}, \\ \psi &= \frac{1}{\kappa}\left\{0.74 \log\left(\frac{z_a}{z*}\right) + 4.7\frac{z_a}{L}\right\}. \end{aligned}\right\} \tag{10-23b}$$

Eqs. (10-18)–(10-23) can be solved by iteration (a three-time iteration is sufficient) to yield the converged C_{dm} and C_{dh}.

P.G.

See sub.CRSTUV in mem.CVTURBXZ. If MSW(1) = 0, no surface fluxes are assumed (free-slip, thermally insulated). If MSW(1) = 1 and MSW(13) = 0, only momentum flux is calculated on the assumption of no heat fluxes and neutral stratification. If MSW(1) = 1 and MSW(13) = 1, both momentum flux and heat fluxes are calculated. Sub.KONDOH and sub.GRDFXH give C_{dm} on the sea and land, respectively, both of which are called in sub.CRSTUV.

B-11. Cloud microphysics

The model can incorporate 5 kinds of parameterization of cloud microphysics:

1. Dry model (no water vapor).
2. Warm rain model (water vapor Qv, cloud water Qc and rain Qr)
3. Cold rain model with the mixing ratios of cloud water, rain, cloud ice Qi, snow Qs and graupel Qg and the number concentration of cloud ice Ni predicted.
4. Cold rain model with the mixing ratios of cloud water, rain, cloud ice, snow and graupel and the number concentrations of cloud ice Ni and snow Ns predicted.
5. Cold rain model with the mixing ratios of cloud water, rain, cloud ice, snow and graupel and the number concentrations of cloud ice Ni, snow Ns and graupel Ng predicted.

In the following, the most sophisticated version of parameterization will be described.

B-11-1. General features of cloud microphysics

In the model, water substance is categorized into 6 forms (water vapour, Qv; cloud

Table B-11-1

Variable Qx(kg/kg) Nx(m^{-3})	Size distribution $Nx(D)$ (m^{-4})	Fall velocity Udx(m/s)	Density ρ_x(kg/m^3)
Qr	$Nr(D) = Nr_0 \exp(-\lambda D)$ $Nr_0 = 8 \times 10^6$	$a_r Dr^{b_r} \left(\frac{\rho_0}{\rho}\right)^{1/2}$ $a_r = 842$ $b_r = 0.8$	$\rho_w = 1 \times 10^3$
Qs Ns	$Ns(D) = Ns_0 \exp(-\lambda D)$ $(Ns_0 = 1.8 \times 10^6)$	$a_s Ds^{b_s} \left(\frac{\rho_0}{\rho}\right)^{1/2}$ $a_s = 17$ $b_s = 0.5$	$\rho_s = 8.4 \times 10$ $r_{s0} = r_0 = 75\,\mu$m $m_{s0} = (4\pi/3)\rho_s r_{0s}^3$
Qg Ng	$Ng(D) = Ng_0 \exp(-\lambda D)$ $(Ng_0 = 1.1 \times 10^6)$	$a_g Dg^{b_g} \left(\frac{\rho_0}{\rho}\right)^{1/2}$ $a_g = 124$ $b_g = 0.64$	$\rho_g = 3 \times 10^2$ $r_{g0} = r_0 = 75\,\mu$m $m_{g0} = (4\pi/3)\rho_g r_{0g}^3$
Qc	mono $Di = \left(\frac{6\rho Qc}{\pi \rho_w Nc}\right)^{1/3}$ $Nc = 1 \times 10^8$m^{-3}	$a_c Dc^{b_c}$ $a_c = 3 \times 10^7$ $b_c = 2.0$	$\rho_c = 1.0 \times 10^3$
Qi Ni	mono $Di = \left(\frac{6\rho Qi}{\pi \rho_i Ni}\right)^{1/3}$	$a_i Di^{b_i} \left(\frac{\rho_0}{\rho}\right)^{0.35}$ $a_i = 7 \times 10^2$ $b_i = 1.0$	$\rho_i = 1.5 \times 10^2$ $m_{i0} = 1 \times 10^{-12}$kg

water, Qc; rain, Qr; cloud ice, Qi; snow, Qs and graupel, Qg) as shown in Table B-11-1. Values in Table B-11-1 are determined referring to observational studies by Locatelli and Hobbs (1974), Kajikawa (1976, 1978), Yagi *et al.* (1979) and Harimaya (1978). For cloud ice, snow and graupel, the number concentrations are predicted in addition to their mixing ratios. For rain, snow and graupel, the inverse exponential functions are hypothesized for their size distribution functions. For cloud water and cloud ice, mono-dispersive distribution is hypothesized, and their precipitation is not taken into account explicitly. Cloud ice designates pristine ice crystal smaller than r_0 in radius, and snow designates snow crystals and aggregates of snow crystals larger than r_0 in radius. As will be shown in C-3, r_0 has a large infuluence on the number and mass of cloud ice, and r_0 is treated as a tuning parameter ranging from 50 to 100μm.

The cloud microphysical processes simulated in the model are illustrated in Fig. B-11-1

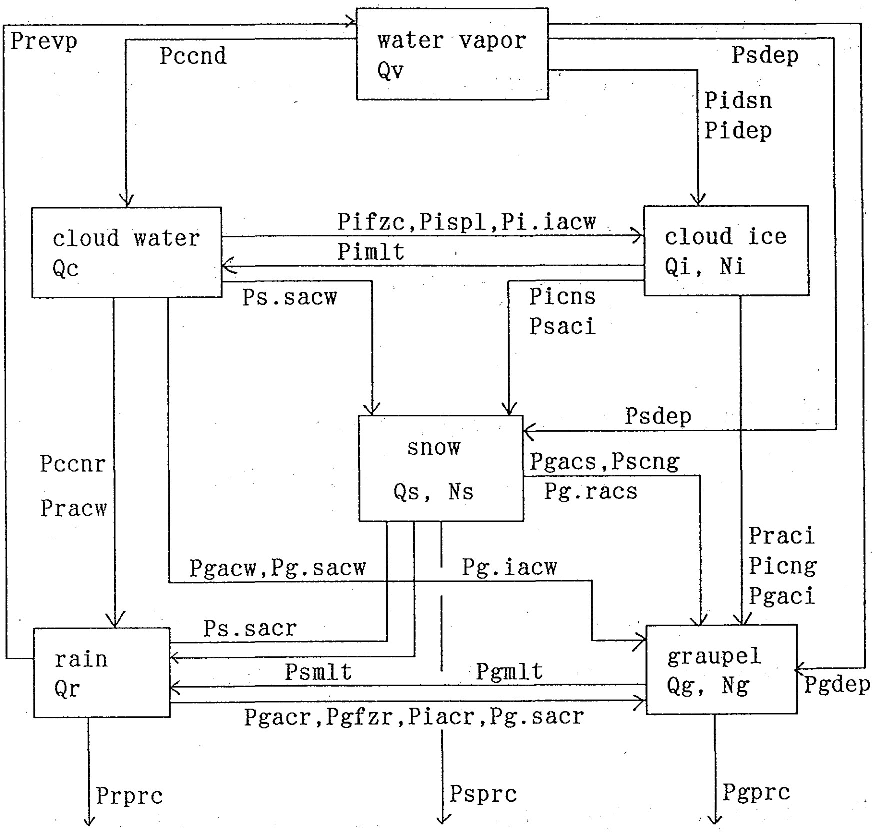

Fig. B-11-1 Cloud microphysical processes in the model. For explanation of the symbols, see Appendix B-11-1.

and the meaning of symbols is explained in the Appendix. Unless specifically mentioned, the parameterizations of microphysical processes are the same as in Ikawa *et al.* (1987). Newly incorporated and revised parts of parameterizatons are described below, which are mainly based upon Murakami (1990) and Cotton *et al.* (1986). In the following, (L-nn), (CT-nn) and (M-nn) denote the number of equation appearing in Lin *et al.*, Cotton *et al.* and Murakami, respectively.

The prognostic equations for mixing ratios of 6 water species and potential temperature are as follows:

$$\frac{\partial Qv}{\partial t}+\mathrm{ADV}(Qv)-D(Qv)=\mathrm{PRD}(Qv)\equiv \mathrm{Prevp}-\mathrm{Pidep}-\mathrm{Psdep}-\mathrm{Pgdep}-\mathrm{Pidsn}-\mathrm{Pccnd}, \tag{11-1}$$

$$\begin{aligned}\frac{\partial Qc}{\partial t}+\mathrm{ADV}(Qc)-D(Qc)=\mathrm{PRD}(Qc)\equiv&-\mathrm{Pccnr}-\mathrm{Pracw}+\mathrm{Pccnd}-\mathrm{Pifzc}\\&-\mathrm{Pispl}-(\mathrm{Ps.sacw}+\mathrm{Pg.sacw})-\mathrm{Pgacw}-(\mathrm{Pi.iacw}+\mathrm{Pg.iacw})+\delta\mathrm{Pimlt},\end{aligned} \tag{11-2}$$

$$\begin{aligned}\frac{\partial Qr}{\partial t}+\mathrm{ADV}(Qr)-D(Qr)=\mathrm{PRD}(Qr)\equiv&-\mathrm{Prprc}+\mathrm{Pracw}+\mathrm{Pccnr}-\mathrm{Prevp}\\&-\mathrm{Pgfzr}-\mathrm{Piacr}-(\mathrm{Ps.sacr}+\mathrm{Pg.sacr})-\mathrm{Pgacr}+\delta(\mathrm{Psmlt}+\mathrm{Pgmlt}),\end{aligned} \tag{11-3}$$

$$\begin{aligned}\frac{\partial Q_i}{\partial t}+\mathrm{ADV}(Q_i)-D(Q_i)=\mathrm{PRD}(Qi)\equiv&\ \mathrm{Pidsn}+\mathrm{Pifzc}+\mathrm{Pispl}+\mathrm{Pidep}\\&+\mathrm{Pi.iacw}-\mathrm{Picng}-\mathrm{Praci}-\mathrm{Psaci}-\mathrm{Pgaci}-\mathrm{Picns}-\delta\mathrm{Pimlt},\end{aligned} \tag{11-4}$$

$$\begin{aligned}\frac{\partial Qs}{\partial t}+\mathrm{ADV}(Qs)-D(Qs)=\mathrm{PRD}(Qs)\equiv&-\mathrm{Psprc}+\mathrm{Psdep}+\mathrm{Picns}+\mathrm{Ps.sacw}\\&-\mathrm{Pscng}+\mathrm{Psaci}+\mathrm{Ps.sacr}-\mathrm{Pg.racs}-\mathrm{Pgacs}-\delta\mathrm{Psmlt},\end{aligned} \tag{11-5}$$

$$\begin{aligned}\frac{\partial Qg}{\partial t}+\mathrm{ADV}(Qg)-D(Qg)=\mathrm{PRD}(Qg)\equiv&-\mathrm{Pgprc}+\mathrm{Pgdep}+(\mathrm{Pscng}+\mathrm{Pg.sacw})\\&+\mathrm{Pgacr}+\mathrm{Pgacw}+\mathrm{Pgaci}+(\mathrm{Piacr}+\mathrm{Praci})+(\mathrm{Pg.sacr}+\mathrm{Pg.racs})\\&+\mathrm{Pgfzr}+(\mathrm{Picng}+\mathrm{Pg.iacw})-\delta\mathrm{Pgmlt}\end{aligned} \tag{11-6}$$

$$
\begin{aligned}
&\frac{\partial\theta}{\partial t} + \mathrm{ADV}(\theta) - D(\theta) = \mathrm{PRD}(\theta) \equiv -\frac{L_v}{C_p \Pi}(\mathrm{Prevp} - \mathrm{Pccnd}) \\
&\quad + \frac{L_s}{C_p \Pi}(\mathrm{Pidep} + \mathrm{Pidsn} + \mathrm{Psdep} + \mathrm{Pgdep}) \\
&\quad + \frac{L_f}{C_p \Pi}((\mathrm{Pi.iacw} + \mathrm{Pg.iacw}) + (\mathrm{Ps.sacw} + \mathrm{Pg.sacw}) + \mathrm{Pgacw} + \mathrm{Piacr} + \mathrm{Pifzc} \\
&\quad + \mathrm{Pgfzr} + \mathrm{Psacr} + \mathrm{Pgacr} - \delta(\mathrm{Pimlt} + \mathrm{Psmlt} + \mathrm{Pgmlt})). \qquad (11\text{-}7)
\end{aligned}
$$

In addition to the prognostic equations for the mixing ratios of water species, prognostic equations for the number concentrations of cloud ice, snow and graupel are also formulated as follows:

$$
\begin{aligned}
&\frac{\partial}{\partial t}[Ni] + \bar{\rho}\mathrm{ADV}\left[\frac{Ni}{\bar{\rho}}\right] - D[Ni] = \mathrm{PRD}(Ni) \\
&\equiv -\mathrm{Niag} + \mathrm{Nifzc} + \frac{\mathrm{Pidsn} + \mathrm{Pispl}}{m_{i0}} - \frac{Ni}{Qi}(\delta\mathrm{Pimlt} + \mathrm{Praci} + \mathrm{Psaci} + \mathrm{Pgaci}) - \frac{\mathrm{Picns}}{m_{s0}}, \quad (11\text{-}8)
\end{aligned}
$$

$$
\begin{aligned}
&\frac{\partial}{\partial t}[Ns] + \bar{\rho}\mathrm{ADV}\left[\frac{Ns}{\bar{\rho}}\right] - D[Ns] = \mathrm{PRD}(Ns) \\
&\equiv -\mathrm{Nsprc} - \mathrm{Nscng} - \mathrm{Ng.sacr} - \mathrm{Nsag} + \frac{\mathrm{Picns}}{m_{s0}} - \frac{Ns}{Qs}(\delta\mathrm{Psmlt} + \mathrm{Pssub}), \qquad (11\text{-}9)
\end{aligned}
$$

$$
\begin{aligned}
&\frac{\partial}{\partial t}[Ng] + \bar{\rho}\mathrm{ADV}\left[\frac{Ng}{\bar{\rho}}\right] - D[Ng] = \mathrm{PRD}(Ng) \\
&\equiv -\mathrm{Ngprc} + \mathrm{Niacr} + \mathrm{Nscng} + \mathrm{Ng.sacr} - \frac{Ng}{Qg}(\delta\mathrm{Pgmlt} + \mathrm{Pgsub}). \qquad (11\text{-}10)
\end{aligned}
$$

Here L_f, L_v, L_s are latent heats of fusion, vaporization and sublimation, respectively. δ is 0 or 1 below or above the freezing temperature, respectively. The ADV term in Eqs. (11-1) to (11-10) represent the advection term defined as

$$
\mathrm{ADV}(f) = \frac{1}{\bar{\rho}G^{1/2}}\left[\frac{\partial}{\partial x}(\bar{\rho}G^{1/2}uf) + \frac{\partial}{\partial y}(\bar{\rho}G^{1/2}vf) + \frac{\partial}{\partial \xi}(\bar{\rho}G^{1/2}\omega f)\right].
$$

The D terms represent the summation of the diffusion due to subgrid scale turbulence (B-10) and artificial computational diffusion (B-12).

The subscripts V, C(or W), R, I, S, and G refer to vapor, cloud water, rain, cloud ice, snow and graupel. Source and sink terms for mass and number are designated by Pqqqq and Nqqqq, respectively. "qqqq" denotes elementary cloud microphysical processes, defined as "xdep(−xsub)" for depositional growth of x, "xsub" for sublimation from x, "xmlt" as

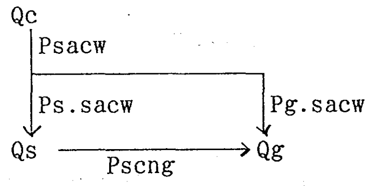

a) Collision between snow and cloud water

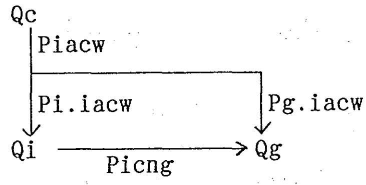

b) Collision between cloud ice and cloud water

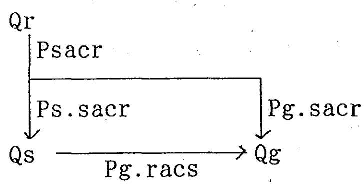

c) Collision between rain and snow

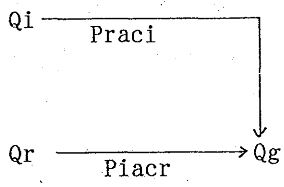

d) Collision between cloud ice and rain

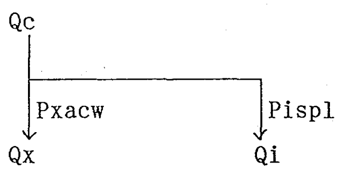

e) Collision between cloud water and Qx(snow,graupel)

Fig. B-11-2 Three component accretion processes.

melting of x, "xprc" for precipitation of x, "xag" for aggregation of x, "xcny" for conversion of x into y, "xfzy" for freezing of y to form x, "xacy" for the accretion of y by x, "x.yacz" for generation of x as a result of accretion of z by y (three-component accretion process, see Fig. B-11-2), "idsn" for deposition/sorption nucleation of cloud ice and "ispl" for ice multiplication process by ice splinters ejected during riming.

For the exchange between water vapor and cloud water (Pccnd), the instant adjustment procedure used by Klemp and Wilhelmson (1978) was adopted. Cloud ice is assumed to melt into cloud water instantaneously above the freezing point (Pimlt).

For water substance, x, whose size distribution function is expressed by the inverse exponential function, the following basic relations hold:

$$Nx = \frac{N_{0x}}{\lambda x}, \quad \rho Qx = \int_0^\infty \rho_x \frac{\pi}{6} Dx^3 N_{0x} \exp(-\lambda x Dx) dDx = \frac{\pi \rho_x N_{0x}}{\lambda x^4},$$

$$\lambda x = \left(\frac{\pi \rho_x Nx}{\rho Qx}\right)^{1/3}, \quad N_{0x} = Nx \left(\frac{\pi \rho_x Nx}{\rho Qx}\right)^{1/3}. \tag{11-11}$$

The change in the number concentration of the precipitable hydrometeor x due to precipitation is given as

$$\text{Nxprc} = -\frac{\partial(\overline{U}nxNx)}{\partial z}, \tag{11-12}$$

where $\overline{U}nx$ is the number-weighted mean terminal velocity defined as

$$\overline{U}nx = \frac{\int U_{dx}(D) N_{0x} \exp(-\lambda x Dx) dDx}{Nx} = \frac{a_x \Gamma(1+b_x)}{\lambda x^{bx}} \lambda x^{-bx} \left(\frac{\rho_0}{\rho}\right)^{1/2}. \tag{11-13}$$

The change in the mixing ratio of the precipitable hydrometeor x due to precipitation is given as

$$\text{Pxprc} = -\frac{\partial(\rho \overline{U}xQx)}{\rho \partial z}, \tag{11-14}$$

where $\overline{U}x$ is the mass-weighted mean terminal velocity defined as

$$\overline{U}x = \frac{\int \frac{\pi}{6}\rho_x Dx^3 U_{dx}(Dx) N_{0x} \exp(-\lambda x Dx) dDx}{\rho Qx} = \frac{a_x \Gamma(4+b_x)}{6\lambda x^{bx}} \left(\frac{\rho_0}{\rho}\right)^{1/2}. \tag{11-15}$$

B-11-2. Production terms for cloud ice

a) Ice Nucleation

In the model cloud, cloud ice is produced through deposition/sorption nucleation (Pidsn: M-29), freezing of cloud droplets (Pifrc; heterogeneous (M-30) and homogeneous freezing of cloud droplets above and below −40°C, respectively) and the secondary ice crystal production term (Pispl: Hallett and Mossop, 1974).

a-1) Deposition/sorption nucleation

The temperature dependency of deposition/sorption nucleation is given by Fletcher's (1962) empirical equation,

$$N_i^* = N_{i0} \exp(\beta_2 T_s). \tag{M-26}$$

The supersaturation dependency of ice nucleation is given by Huffmann and Vali (1973),

$$Ni = A \left(\frac{S_i - 1}{S_0 - 1} \right)^B. \tag{M-27}$$

Replacing A with N_i^*, we obtain

$$Ni = N_{i0} \exp(\beta_2 T_s) \left(\frac{S_i - 1}{S_0 - 1} \right)^B, \tag{M-28}$$

where $N_{i0} = 1.0 \times 10^{-2}(\mathrm{m}^{-3})$, $\beta_2 = 0.6(K^{-1})$, $B = 4.5$. $(S_0 - 1)$ represents the ice supersaturation of a water satureted cloud $(Qvsw/Qvsi - 1)$. It may be reasonable to assume that ice nucleation by deposition/sorption occurs in an ascending air parcel in clouds. Assuming that the vertical change in humidity is negligibly small, we get the following equation for ice nucleaton rate in ascending cloud air:

$$\begin{aligned} \mathrm{Pidsn} &= m_{i0} \frac{dNi}{dt} \approx m_{i0} \frac{\partial Ni}{\partial T_s} \frac{\partial T_s}{\partial z} \frac{dz}{dt} \\ &= m_{i0} \beta_2 N_{i0} \exp(\beta_2 T_s) \left(\frac{S_i - 1}{S_0 - 1} \right)^B \frac{\partial T_s}{\partial z} w, \end{aligned} \tag{11-16}$$

$$\mathrm{Nidsn} = \frac{\mathrm{Pidsn}}{m_{i0}}. \tag{11-17}$$

a-2) Freezing of cloud droplets

For heterogeneous freezing of cloud droplets ($T_c > -40°\mathrm{C}$), we obtain the following equation by extrapolating Bigg's (1953) equation down to the cloud droplet size (M-30):

$$\mathrm{Pifrc} = B'[\exp\{A'(T_0 - T)\} - 1] \frac{\rho Qc^2}{\rho_w Nc}, \tag{11-18}$$

$$\mathrm{Nifzc} = \mathrm{Pifzc} \frac{Nc}{Qc}, \tag{11-19}$$

where $A' = 0.66(\mathrm{K}^{-1})$, $B' = 100.0(\mathrm{m}^{-3}\mathrm{s}^{-1})$ is used. ρ_w is the density of liquid water, Nc the number concentration of cloud droplets which is preset in this model.

For homogeneous freezing of cloud droplets ($T_c < -40°\mathrm{C}$), cloud drops are turned into cloud ice instantaneously:

$$\text{Pifzc} = \frac{Qc}{2\Delta t}, \qquad \text{Nifzc} = \frac{Nc}{2\Delta t}, \tag{11-20}$$

where Δt is the time interval of the leap-frog time integration.

a-3) Ice multiplication process

Hallet and Mossop (1974) reported that approximately 350 ice splinters are produced for every 10^{-6}kg of rime accretion on graupel particles at $-5°$C. Based on their report, ice splinters associated with riming process is parameterized (CT-71) as

$$\text{Nispl} = \rho \times 3.5 \times 10^8 f(T_c)(\text{Ps.sacw} + \text{Pg.sacw} + \text{Pgacw}), \tag{11-21}$$

$$f(T_c) = \begin{cases} 0 & \text{for } T_c > T_1 = -3°\text{C} \\ \dfrac{T_c - T_1}{T_2 - T_1} & \text{for } T_1 \geq T_c \geq T_2 = -5°\text{C} \\ 1 & \text{for } T_2 \geq T_c \geq T_3 = -5°\text{C} \\ \dfrac{T_c - T_4}{T_3 - T_4} & \text{for } T_3 \geq T_c \geq T_4 \\ 0 & \text{for } T_c < T_4 = -8°\text{C} \end{cases} \tag{11-22}$$

The increase in mass of cloud ice associated with this process is given as

$$\text{Pispl} = \text{Nispl} \times m_{i0}. \tag{11-23}$$

b) Depositional growth of cloud ice

Depositional growth of cloud ice is given as

$$\text{Pidep} = \frac{Qv - Qvsi}{Qvsw - Qvsi} a_1 (m_i)^{a_2} Ni/\rho, \tag{11-24}$$

where a_1 and a_2 are temperature-dependent parameters taken from Köenig (1971).

c) Riming growth of cloud ice

The amount of rime on cloud ice is given as

$$\text{Piacw} = Ni\frac{\pi}{4}(Di + Dc)^2 Eic|U_{di} - U_{dc}|Qc. \tag{11-25a}$$

The portion of Piacw consumed for riming growth of cloud ice is given as

$$\text{Pi.iacw} = \min(\text{Piacw}, \beta \times \text{Pidep}). \tag{11-25b}$$

The amount of riming greater than $\beta \times$ Pidep is consumed to form graupel (Pg.iacw). In this study, $\beta = 1.0$ is tentatively used. Collection efficiency, Eic, is given as follows (Fletcher, 1962; Mizuno and Matuo, 1980):

$$\psi = \left(\frac{\rho_w U_{di}}{18\eta Di}\right)^{1/2} \cdot Dc = (Stk/2)^{1/2} \qquad (Stk: \text{Stokes number}) \qquad (11\text{-}26)$$

$$\eta = (1.718 + 0.049T_c - 1.2 \times 10^{-5} T_c^2) \times 10^{-5} \qquad (\text{viscosity}: \mathrm{Nsm^{-2}})$$

in case of $\psi > 0.25$:

for disk ($-4°\mathrm{C} < T_c < 0°\mathrm{C}$ or $-20°\mathrm{C} < T_c < -10°\mathrm{C}$)

$$Eic = 0.572 \times \log_{10}(\psi - 0.25) + 0.967$$

for column ($-10°\mathrm{C} < T_c < -4°\mathrm{C}$ or $T_c < -20°\mathrm{C}$)

$$Eic = 0.556 \times \log_{10}(\psi - 0.25) + 0.632$$

in case of $\psi < 0.25$:

$$Eic = 0.$$

B-11-3. Production terms for snow

a) Conversion from cloud ice to snow (Picns)

The conversion from cloud ice (pristine ice crystals) to snow takes place through three processes; depositional and riming growth of ice crystals and aggregation between pristine ice crystals. The time needed for an ice crystal to grow from m_i to m_{s0} in mass via depositional and riming growth is

$$\Delta\tau = \frac{Ni(m_{s0} - m_i)}{\mathrm{Pidep} + \mathrm{pi.iacw}}; \qquad m_i = \frac{\rho Qi}{Ni}; \qquad m_{s0} = (4\pi/3)\rho_s r_{s0}^3. \qquad (11\text{-}27)$$

Therefore, cloud ice converted into snow in unit time is given as (in case of $m_i < 0.5m_{s0}$)

$$\mathrm{CN}_{\mathrm{is}}^{\mathrm{dep+ac}} = \frac{1}{\Delta\tau}\rho Qi = \frac{m_i}{m_{s0} - m_i}(\mathrm{Pidep} + \mathrm{Pi.iacw}). \qquad (11\text{-}28)$$

This term becomes very large for the case of $m_i \approx m_{s0}$ to yield erroneous results. To prevent this, Eq. (11-28) is applied only to the case of $m_i < 0.5m_{s0}$. To the case of $m_i > 0.5m_{s0}$, the following is applied:

(in case of $m_i > 0.5m_{s0}$)

$$\mathrm{CN}_{\mathrm{is}}^{\mathrm{dep+ac}} = (\mathrm{Pidep} + \mathrm{Pi.iacw}) + \left(1 - \frac{0.5m_{s0}}{m_i}\right)\frac{Qi}{2\Delta t}. \qquad (11\text{-}29)$$

The conversion from cloud ice to snow due to aggregation is parameterized, following Murakami (Eqs. (M-34)....(M-41)). The rate of collision-coalescene among a homogeneous population of ice crystals may be written by

$$\left.\frac{dNi}{dt}\right|_{\mathrm{aggr}} = \frac{1}{2}K_I Ni^2, \tag{M-34}$$

where

$$K_I = \frac{\pi}{6}\overline{Di}^2\overline{U}_I E_{II} X. \tag{M-35}$$

Here $\overline{Di}$ represents the mean diameter of ice crystals, $\overline{U}_I$ the fall velocity of ice crystals, E_{II} the collection efficiency between ice crystals, and X the dispersion of the fall velocity spectrum of ice crystals. Using the following equation for the fall velocity

$$\overline{U}_I = a_I \overline{Di}\left(\frac{\rho_0}{\rho}\right)^{\frac{1}{3}}, \tag{M-36}$$

Eq. (M-35) is rewritten as

$$K_I = \frac{C_1}{Ni}, \tag{M-37}$$

where

$$C_1 = \frac{\rho Qi a_I E_{II} X}{\rho_I}\left(\frac{\rho_0}{\rho}\right)^{\frac{1}{3}}. \tag{M-38}$$

Combining Eq. (M-34) and Eq. (M-37), we obtain

$$\left.\frac{dNi}{dt}\right|_{\mathrm{aggr}} = -\frac{C_1}{2}Ni. \tag{M-39}$$

The time needed for cloud ice to grow by aggregation from $\overline{r}_I$ to r_{s0} in radius is equal to the time needed for the cloud ice concentration to decrease form Ni to $Ni(\overline{r}_I/\overline{r}_{s0})^3$. Assuming that ρ_I is constant yields

$$\Delta\tau_2 = -\frac{2}{C_1}\log\left(\frac{\overline{r}_I}{r_{s0}}\right)^3. \tag{M-40}$$

The conversion rate from cloud ice to snow is given by

$$\mathrm{CN}_{\mathrm{IS}}^{\mathrm{Ag}} = \frac{Qi}{\Delta\tau_2}. \tag{M-41}$$

The total conversion rate in mass from cloud ice to snow is given by the sum of

$$\mathrm{Picns} = \mathrm{CN}_{\mathrm{IS}}^{\mathrm{dep+ac}} + \mathrm{CN}_{\mathrm{IS}}^{\mathrm{Ag}}. \tag{11-30}$$

The total conversion rate in number from cloud ice to snow is given by

$$\text{Nicns} = \frac{\text{Picns}}{m_{s0}}. \tag{11-31}$$

b) Aggregation among snow particles(Nsag)

The decrease in number concentration of snow due to aggregation among snow crystals (or aggregates)(M-44) is obtained using an equation based on the analytical model of aggregational growth by Passarelli (1978).

$$\text{Nsag} = \left.\frac{dNs}{dt}\right|_{\text{aggr}} = -\frac{a_s EssI(b_s)}{4 \times 720}\pi^{\frac{1-b_s}{3}}\rho^{\frac{2+b_s}{3}}\rho_s^{\frac{-2-b_s}{3}}Qs^{\frac{2+b_s}{3}}Ns^{\frac{4-b_s}{3}}, \tag{11-32}$$

where

$$I(d) = \int_0^\infty \int_0^\infty x^3 y^3 (x+y)^2 |x^d - y^d| e^{-(x+y)} dx dy.$$

For $d = 0.6$, 0.5 and 0.4, $I(d) = 2566$, 1610 and 1108 (Mizuno, 1990).

c) Depositional growth and melting of snow

Depositional growth of snow (L-52) for $T_c < T_0$ is modified in order to incorporate the warming of the surface temperature of a snow particle due to riming as follows (Cotton and Anthes, 1989, Eq. 4-37)

$$\text{Psdep (or } -\text{Pssub)} = \frac{2\pi(Si-1)}{\rho(A''+B'')}\text{VENT}(a_s, b_s, \lambda_s, N_{s0}) - \frac{L_s L_f}{\kappa_a R_w T^2 (A''+B'')}\text{Psacw}, \tag{11-33a}$$

where

$$A'' = \frac{L_s^2}{\kappa_a R_w T^2}, \qquad B'' = \frac{1}{\rho Qvsi\,\psi},$$

$$\text{VENT}(a_s, b_s, \lambda_s, N_{s0})$$
$$= N_{s0}\left[0.78\lambda_s^{-2} + 0.31 S_c^{1/3}\Gamma\left(\frac{b_s+5}{2}\right)a_s^{1/2}\left(\frac{\rho_0}{\rho}\right)^{1/4}\nu^{-1/2}\lambda_{bs}^{-(b_s+5)/2}\right].$$

The first term on R.H.S of Eq. (11-33a) is the same as Psdep without modification, (L-52). Similar modification is made for the depositional growth of graupel (Pgdep). Generally, modification for graupel is much larger than that for snow.

The melting of snow for $T_c > T_0$ is formulated on heat balance considerations. The cooling associated with the melting is balanced by the combined effects of conduction and convection of heat to the particle surface, the latent heat of condensation and evaporation of water to or from the particle surface, and the sensible heat associated with the accreted water. The rate of melting of snow to form rain can be expressed as

$$\mathrm{Psmlt} = \frac{2\pi}{\rho L_f}(K_a T_c - L_v \psi \rho (Qvsw - Qv)) \times \mathrm{VENT}(a_s, b_s, \lambda_s, N_{s0}) + \frac{C_w T_c}{L_f}(\mathrm{Psacw} + \mathrm{Psacr}), \tag{L-32}$$

If Psmlt is positive, melting occurs, and Psdep (−Pssub) is calculated (see Ikawa *et al.*, 1987, Eq. (2-12)) by

$$\mathrm{Psdep} = -2\pi\psi(Qvs(T = T_0) - Qv) \times \mathrm{VENT}(a_s, b_s, \lambda_s, N_{s0}). \tag{11-33b}$$

If Psmlt is negative for $T_c > T_0$, melting does not occur. In a dry air, evaporative cooling is large enough to prevent melting. Psdep (−Pssub) is calculated in a similar way to Prevp (L-52) by

$$\mathrm{Psdep(or - Pssub)} = \frac{2\pi(S_w - 1)}{\rho(A'' + B'')}\mathrm{VENT}(a_s, b_s, \lambda_s, N_{s0}), \tag{11-34}$$

where

$$A'' = \frac{L_s^2}{K_a R_w T^2}, \qquad B'' = \frac{1}{\rho Qvsw\, \psi}.$$

Pgdep for $T > T_0$ is formulated in a similar way to Psdep for $T > T_0$.

B-11-4. Production terms for graupel

a) Conversion from cloud ice to graupel (Picng; see Fig. B-11-2b)

This occurs via riming on ice crystals, and is parameterized as follows. The mass required for an ice crystal to be converted into a graupel particle of minimum weight, m_{g0}, is

$$\Delta m_{gi} = m_{g0} - m_i,$$

where

$$m_{g0} = (4\pi/3)\rho_g r_{g0}^3; \quad m_i = \frac{\rho Qi}{Ni}; \quad r_{g0} = r_0 = 75\mu\mathrm{m}.$$

On the other hand, it is assumed that the portion of the amount of rime on an ice crystal greater than $\beta \times$ Pidep,

$$\text{CLic} = \max\left(\frac{\pi}{4}(Di + Dc)^2 Eic|U_{di} - U_{dc}|\rho Qc - \beta\frac{\text{Pidep}}{Ni},\quad 0\right), \tag{11-35}$$

is consumed to form a graupel particle. The time needed for an ice crystal to be convented into a graupel is $\Delta m_{gi}/\text{CLic}$. The amount of cloud ice in mass converted into graupel in unit time is given as

$$\text{Picng} = \frac{\text{CLic}}{\Delta m_{gi}}\rho Qi = \text{Nicng}\, m_i \tag{11-36}$$

The number of ice crystals to be converted into graupel is given as

$$\text{Nicng} = \frac{\text{CLic}}{\Delta m_{gi}} Ni = \frac{\text{Picng} + \text{Pg.iacw}}{m_{g0}}. \tag{11-37}$$

The amount of rime converted into graupel in unit time is given as

$$\text{Pg.iacw} = Ni\, \text{CLic} = \text{Nicng}\Delta m_{gi}. \tag{11-38}$$

b) Conversion from snow to graupel (Pscng; see Fig. B-11-2a)

Snow is converted into graupel through the collection of supercooled cloud droplets (riming process). All of the accreted cloud water is not converted into graupel; some is consumed for the riming growth of snow itself. The point of the parameterization is how to determine the dispatcher function $\eta(D)$ which specifies the portion of the accreted cloud water to be converted into graupel. The remainder $(1-\eta(D))$ is consumed for the riming growth of snow. Following Murakami (1990) who assumed that the change of snow particle size due to riming is negligibly small, the amount of riming needed for snow with diameter D to be converted into graupel with diameter D through the riming process is given by

$$\Delta m_{sg} = (\rho_g - \rho_s)\pi D^3/6. \tag{11-39}$$

The amount of riming by snow with the diameter D is given by

$$CL(D) = \frac{\pi}{4}D^2 EscU_{ds}\,\rho Qc, \tag{11-40}$$

$$U_{ds} = a_s D^{b_s}(\rho_0/\rho)^{0.5} \qquad (a_s = 17, \quad b_s = 0.5) \tag{11-41}$$

The time needed for a snow particle with diameter D to be converted into graupel with diameter D through the riming process (Murakami, 1990, M-42) is given by

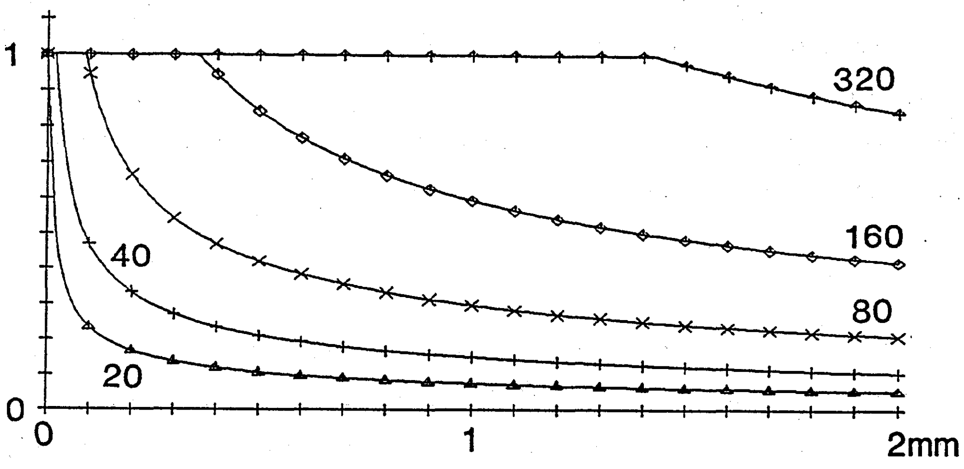

Fig. B-11-3 The dispatcher function (Eq. (11-43)) as a function of the diameter of a snow particle, D, with the parameters $\rho_0 = \rho = 1$ kgm^{-3}, $\rho Qc = 10^{-3}$ kgm^{-3} and $Esc = 1$ for the case of $\alpha 2\Delta t = 20$, 40, 80, 160 and 320.

$$\Delta\tau = \frac{\Delta m_{sg}}{CL(D)} = \frac{2(\rho_g - \rho_s)D^{1-b_s}}{3a_s Esc\,\rho Qc}\left(\frac{\rho}{\rho_0}\right)^{1/2}. \tag{11-42}$$

$\Delta\tau$ is small for small D, and small snow particles are more likely converted into graupel than large snow particles. Therefore the dispatcher function is assumed to be

$$\eta(D) = \min\left(1, \frac{\alpha 2\Delta t}{\Delta\tau}\right) = \min\left(1, \frac{\alpha 2\Delta t CL(D)}{\Delta m_{sg}}\right), \tag{11-43}$$

where α is a tuning parameter and Δt is the time step of the leap-frog time integration. The amount of riming to be consumed for graupel generation is $\eta(D)CL(D)$, while that for riming growth of a snow particle is $(1-\eta(D))CL(D)$. Hereafter, the diameter which yields $\alpha 2\Delta t = \Delta\tau$ is designated by Dsc:

$$Dsc = \left(\alpha 2\Delta t \frac{3a_s Esc\,\rho Qc}{2(\rho_g - \rho_s)}\right)^2. \tag{11-44}$$

All the amount of riming on snow particles smaller than Dsc in diameter is assumed to form graupel. For the case of $\alpha 2\Delta t = 80s$, $\rho Qc = 10^{-3}$kg/m^3, $Dsc = 100\mu$m (see Fig. B-11-3).

Figure B-11-3 shows the dispatcher function with the parameters $\rho_0 = \rho = 1$kgm^{-3}, $\rho Qc = 10^{-3}$kgm^{-3} and $Esc = 1$ for the case of $\alpha 2\Delta t = 20, 40, 80, 160$ and 320.

As will be shown in C-3, in the 3-dimensional simulation of convective snow clouds observed over the Sea of Japan in winter, it is found that $\alpha = 2 \sim 5$ for $2\Delta t = 8$ sec gives rise to the observed ratio of the precipitation amount of graupel over that of snow which is about $0.3 \sim 1.0$.

In the 2-dimensional simulation of convective snow clouds observed over the Sea of Japan in winter, Ikawa (1988) used Matsuo's method (1986),

$$\eta(D) = \begin{cases} 1 & \text{for } D < Dcr \\ 0 & \text{for } D > Dcr. \end{cases} \tag{11-45}$$

He found $Dcr = 1 \times 10^{-3}$m gives rise to the reasonable ratio of the precipitation amount of graupel over that of snow. As can been seen from Fig. B-11-3, the dispatcher function of the form Eq. (11-45) with $Dcr = 1 \times 10^{-3}$m is larger than the dispatcher function given by Eq. (11-43) with $\alpha\Delta t = 32$. This difference comes from the differences of the dimension of the model (2-D or 3-D) and two parameterizations; his previous parameterization incorporates Pg.sacw, but not Pscng explicitly. This dispatcher funciton is simple enough, but overestimates the number of graupel particles generated, and may cause imbalance between number and mass of graupel.

The amount of rime on snow particles converted into graupel is given as

$$\begin{aligned} \mathrm{Pg.sacw} &= \int \eta(D) CL(D) f(D) dD \\ &= \alpha 2\Delta t \frac{3\rho_0 \pi N_{s0} (\rho Qc)^2 Esc^2 a_s^2 \Gamma(2b_s + 2)}{8\rho(\rho_g - \rho_s)\lambda_s^{2b_s+2}}. \end{aligned} \tag{11-46}$$

The probability for a snow particle of the diameter D to be converted into a graupel particle in unit time is given by

$$\mathrm{Prob}(D) = \frac{1}{2\Delta t} \min\left(1, \frac{2\Delta t \eta(D) CL(D)}{\Delta m_{sg}}\right) \simeq \frac{\eta(D) CL(D)}{\Delta m_{sg}}. \tag{11-47}$$

The approximate expression holds for most D ($D > Dsc/\alpha^2$).

The number generation of graupel due to riming of snow is given as

$$\mathrm{Nscng} = \int \mathrm{Prob}(D) f(D) dD \simeq \int \frac{\eta(D) CL(D)}{\Delta m_{sg}} f(D) dD. \tag{11-48}$$

In evaluating the above integral,

$$f(D) = N_{s0} D \exp(-\lambda_s D) \tag{11-49}$$

is used instead of

$$f(D) = N_{s0}\exp(-\lambda_s D), \tag{11-50}$$

in order to avoid over-estimation of the number concentration for small D (snow particles of $D < 100\mu$m are categorized into pristine ice crystals, and should not be counted).

Nscng is approximated as

$$\begin{aligned}
\text{Nscng} &= \int_0^{Dsc} \frac{CL(D)}{\Delta m_{sg}} f(D)dD + 2\alpha\Delta t \int_{Dsc}^{\infty} \frac{CL(D)^2}{\Delta m_{sg}^2} f(D)dD \\
&= \text{coef}\frac{N_{s0}}{\lambda_s^{3/2}}\left[-z\exp(-z^2) + \int \exp(-z^2)dz\right]_0^{(\lambda Dsc)^{1/2}} \\
&\qquad + (\alpha 2\Delta t)\text{coef}^2 \frac{N_{s0}\exp(-\lambda_s Dsc)}{\lambda_s},
\end{aligned} \tag{11-51}$$

where

$$\text{coef} = \left(\frac{\rho_0}{\rho}\right)^{1/2} \frac{3a_s Esc\,\rho Qc}{2(\rho_g - \rho_s)}. \tag{11-52}$$

The equation might be further simplified as

$$\text{Nscng} = \frac{\rho_0}{\rho}\left(\frac{3\pi a_s \rho Qc Ecs}{2(\rho_g - \rho_s)}\right)^2 \frac{N_{s0}}{\lambda_s}\alpha 2\Delta t, \tag{11-53}$$

for the case of small λDsc (small $\alpha 2\Delta t$, small Qc, large Qs and small Ns). For example, Eq. (11-53) gives only 10% overestimation of Nscng for the case of ($\lambda Dsc = 0.37$, $\alpha 2\Delta t =$ 100sec, $Qc = 10^{-3}$kg/kg, $Qs = 0.5\times 10^{-3}$kg/kg, $Ns = 3.4\times 10^3\text{m}^{-3}$), while this gives 50% overestimation of Nscng for the case of ($\lambda Dsc = 1.5$, $\alpha 2\Delta t = 100$sec, $Qc = 2\times 10^{-3}$kg/kg, $Qs = 0.5\times 10^{-3}$kg/kg, $Ns = 3.4\times 10^3\text{m}^{-3}$).

The amount of snow converted into graupel as embryo is given as (see Murakami, 1990, (M-43))

$$\text{Pscng} = \int \frac{\pi}{6} D^3 \rho_s \text{Prob}(D) f(D)dD \simeq \frac{\rho_s}{\rho_g - \rho_s}\text{Pg.sacw}. \tag{11-54}$$

The amount of riming consumed for the growth of snow itself is

$$\text{Ps.sacw} = \text{Psacw} - \text{Pg.sacw},$$

where Psacw is given by (L-24).

Dependency of Pg.sacw and Pscng on $\alpha 2\Delta t$ is shown in Figs. B-11-6. and B-11-8.

c) Collision between rain and snow (see Fig. B-11-2c)

For collision between rain and snow, the accretion rate of rain by snow is

$$\text{Psacr} = \frac{1}{\rho}\int_0^\infty\int_0^\infty \frac{\pi}{4}(Dr+Ds)^2 Ers|U_{dr}-U_{ds}|\rho_w\frac{\pi}{6}Dr^3 N_{r0}\exp(-\lambda_r Dr)N_{s0} \times \exp(-\lambda_s Ds)dDrdDs. \tag{11-55}$$

In most of models so far, the following approximation is used for the differential velocity;

$$|U_{dr}-U_{ds}| \approx |\overline{U}_r - \overline{U}_s|.$$

This approximation underestimates Pracs when the value of $\overline{U}_r$ is close to $\overline{U}_s$. To remedy this underestimation, we used the following approximation proposed by Mizuno (1990a) who obtained the exact value of the intergral of Eq. (11-55) analytically for the case of $b_r = b_s = 0.5$,

$$|U_{dr}-U_{ds}| \approx \sqrt{(\alpha\overline{U}_r - \beta\overline{U}_s)^2 + \gamma\overline{U}_r - \overline{U}_s} \tag{11-56}$$

wiht $\alpha = 1.2$, $\beta = 0.95$ and $\gamma = 0.08$. The approximation expressed by Eq. (11-56) yields

$$\text{Psacr} = \pi^2 Ers\sqrt{(\alpha\overline{U}_r - \beta\overline{U}_s)^2 + \gamma\overline{U}_r\overline{U}_s}\,\frac{\rho_w}{\rho}N_{r0}N_{s0}\left(\frac{5}{\lambda_r^6\lambda_s} + \frac{2}{\lambda_r^5\lambda_s^2} + \frac{0.5}{\lambda_r^4\lambda_s^3}\right), \tag{11-57}$$

where the collection efficiency of snow for rain (or that of rain for snow), Ers, is assumed to be unity. Eq. (11-57) is used for the case shown in C-3 where b_r is not equal to 0.5 but 0.8.

The accretion rate of snow by rain is

$$\text{Pracs} = \pi^2 Ers\sqrt{(\alpha\overline{U}_r - \beta\overline{U}_s)^2 + \gamma\overline{U}_r\overline{U}_s}\,\frac{\rho_s}{\rho}N_{s0}N_{r0}\left(\frac{5}{\lambda_s^6\lambda_r} + \frac{2}{\lambda_s^5\lambda_r^2} + \frac{0.5}{\lambda_s^4\lambda_r^3}\right) \tag{11-58}$$

with $\alpha = 1.2$, $\beta = 0.95$ and $\gamma = 0.08$.

The number of collisions between snow and rain particles in unit time is given as

$$\text{Nsacr} = \text{Nracs} = \int_0^\infty\int_0^\infty \frac{\pi}{4}(Dr+Ds)^2 Ers|U_{dr}-U_{ds}| \times N_{r0}\exp(-\lambda_r Dr)N_{s0}\exp(-\lambda_s Ds)dDrdDs. \tag{11-59}$$

Mizuno (1990b) obtained the exact value of the above integral analytically, and he proposed the following approximation for the case of $b_r = b_s = 0.5$ to Eq. (11-59):

$$\begin{aligned}\text{Nsacr} &= \text{Nracs}\\ &= \frac{\pi}{4}Ers\sqrt{(\alpha\overline{U}_{n_r} - \overline{U}_{n_s})^2 + \beta\overline{U}_{n_r}\overline{U}_{n_s}}\,N_{r0}N_{s0}\\ &\quad\times\int_0^\infty\int_0^\infty (Dr+Ds)^2\exp(-\lambda_r Dr)\exp(-\lambda_s Ds)dDrdDs\\ &= \frac{\pi}{2}Ers\sqrt{\alpha(\overline{U}_{n_r} - \overline{U}_{n_s})^2 + \beta\overline{U}_{n_r}\overline{U}_{n_s}}\,N_{r0}N_{s0}\left(\frac{1}{\lambda_r^3\lambda_s} + \frac{1}{\lambda_r^2\lambda_s^2} + \frac{1}{\lambda_r\lambda_s^3}\right)\end{aligned} \tag{11-60}$$

where $\alpha = 1.7$ $\beta = 0.3$ and the collection efficiency of snow for rain (or that of rain for snow), Ers, is assumed to be unity. Eq. (11-60) is used for the case shown in C-3 where b_r is not equal to 0.5 but 0.8.

The portion of the accreted rain by snow consumed for production of graupel in mass is

$$\text{Pg.sacr} = (1 - \alpha_{rs})\text{Psacr}, \tag{11-61}$$

where $(1 - \alpha_{rs})$ is the ratio at which the collisions between raindrops and snow particles result in graupel production. The equation chosen to express α_{RS} (Murakami, 1990: (M-25)) is

$$\alpha_{rs} = \frac{\rho_s^2 \left[\frac{4}{\lambda_s}\right]^6}{\rho_s^2 \left[\frac{4}{\lambda_s}\right]^6 + \rho_w^2 \left[\frac{4}{\lambda_r}\right]^6} = \frac{m_s^2}{m_s^2 + m_r^2}. \tag{11-62}$$

The portion of the accreted snow by rain consumed for production of graupel in mass is

$$\text{Pg.racs} = (1 - \alpha_{rs})\text{Pracs}. \tag{11-63}$$

The portion of the accreted rain by snow consumed for production of snow is

$$\text{Ps.sacr} = \alpha_{rs}\text{Psacr}. \tag{11-64}$$

The number of graupel particles generated by collision of snow and rain is

$$\text{Ng.racs} = (1 - \alpha_{rs})\text{Nracs} = \text{Ng.sacr}. \tag{11-65}$$

A similar approximation is used in deriving the rates involving collision between graupel and snow and between graupel and rain. Collision between graupel and snow is almost suppressed in the simulation shown in C-3 by setting $Esg = 0.001$.

d) Graupel generation via collision between ice and rain

The number of graupel generated via collision between ice and rain is given as

$$\begin{aligned} \text{Niacr} = \text{Nraci} &= \frac{\pi}{4}\int_0^\infty Dr^2 Ur Ni N_{r0} \exp(-\lambda_r Dr) dDr \\ &= \frac{\pi}{4}\frac{\Gamma(3 + b_r)}{\lambda r^{3+b_r}} Ni N_{r0} \left(\frac{\rho_0}{\rho}\right)^{1/2} \\ &= \text{Praci}(Ni/Qi). \end{aligned} \tag{11-66}$$

The mass of cloud ice accreted by rain, Praci, is given by (L-25).

e) Graupel generation via immersion freezing of rain

The number of graupel generated via immersion freezing of rain is given, based on Bigg (1953) as

$$\mathrm{Ngfzr} = B''\frac{\pi}{6}\int D^3 N_{0r}\exp(-\lambda_r D)dD = B''\pi N_{0r}\lambda_r^{-4}, \tag{11-67}$$

where $B'' = B'(\exp(A(T_0 - T)) - 1)$, $B' = 100$ ($\mathrm{m^{-3}s^{-1}}$) and $A' = 0.66$ ($\mathrm{K^{-1}}$). The increase in mass, Pgfzr, is given by (L-45).

B-11-5. Production terms for cloud water

a) Conversion from water vapor into cloud water (Pccnd)

"Instantaneous adjustment procedure" is applied to the newly time-integrated Qc, θ and Qv in which advection, diffusion and cloud microphysical terms are taken into account except for the term (Pccnd) discussed here. During condensation or evapration, pressure is assumed to be invariant. Let $Qc + \Delta Qc$, $Qv + \Delta Qv$ and $\theta + \Delta\theta$ be the adjusted values for Qc, Qv and θ. Let $Qvsw(\theta,\ P)$ be the saturation mixing ratio of water vapor with respect to water.

1) If $Qvsw\ (\theta,\ P) > Qv$ and $Qc = 0$, then no adjustment is made.
2) Otherwise, adjustment is made as below. The following equation is solved up to the second-order approximation in $\Delta\theta$:

$$\begin{aligned} Qv + \Delta Qv &= Qvsw(\theta + \Delta\theta) \\ &\simeq Qvsw(\theta) + (\partial Qvsw/\partial\theta)(\theta)\Delta\theta + 0.5(\partial^2 Qvsw/\partial^2\theta)(\theta)\Delta\theta^2, \end{aligned} \tag{11-68}$$

$$C_p\Pi\Delta\theta = -L_v\Delta Qv, \tag{11-69}$$

$$\Delta Qv = -\Delta Qc. \tag{11-70}$$

The equation to be solved for $\Delta\theta$ is

$$Qv - Qvsw(\theta) = (C_p\Pi/L_v + (\partial Qvsw/\partial\theta)(\theta))\Delta\theta + 0.5(\partial^2 Qvsw/\partial\theta^2)(\theta)\Delta\theta^2. \tag{11-71}$$

The first guess of $\Delta\theta$ is given as

$$\Delta\theta_1 = \frac{Qv - Qvsw(\theta)}{C_p\Pi/L_v + (\partial Qvsw/\partial\theta)(\theta)}. \tag{11-72}$$

The second guess of $\Delta\theta$ is given by use of $\Delta\theta_1$ as

$$\Delta\theta_2 = \frac{Qv - Qvsw(\theta)}{C_p\Pi/L_v + (\partial Qvsw/\partial\theta)(\theta) + 0.5(\partial^2 Qvsw/\partial\theta^2)(\theta)\Delta\theta_1} \tag{11-73}$$

$$\mathrm{Pccnd} = (C_p\Pi/L_v)\ \Delta\theta_2/2\Delta t. \tag{11-74}$$

Usually, this second guess is accurate enough.

A similar procedure is applied for the deposition of water vapor to form cloud ice at $T_c < -40°\mathrm{C}$ (Pidsn), using $Qvsi$ and L_s instead of $Qvsw$ and L_v.

B-11-6. Production term for rain

a) Conversion from cloud water into rain

The collision and coalescence of cloud droplets to form raindrops has been parameterized in different ways. "Kessler's parameterization" (Cotton and Anthes, 1989, §4-3-1) is

$$\mathrm{Pccnr} = a(Qc - Q_{co})H(Qc - Q_{co}) \tag{11-75}$$

where H is the Heaviside function (Q_{co} is the threshold value for conversion). Ikawa (1988) used this parameterization with $a = 10^{-3}\mathrm{s}^{-1}$, $Q_{co} = 10^{-3}$.

Cotton (see Cotton and Anthes, 1989) modified this by making a and Q_{co} dependent on Qc and the prescribed number concentration of cloud water, Nc:

$$Q_{co} = \frac{4\pi\rho_w Nc\, r_{cm}^3}{3\rho} = 4\times 10^{-12}Nc \qquad (\text{for } r_{cm} = 10^{-5}\mathrm{m}), \tag{11-76}$$

$$a = \pi EccU_{dc}Nc\,r_c^2 = 1.3\times 10^3 Qc^{4/3}Nc^{-1/3}\left(\frac{\rho_0}{\rho}\right). \tag{11-77}$$

Lin *et al.* (1983), Nickerson *et al.* (1986) and Matsuo and Mizuno (1988) proposed the parameterization based upon Berry (1968) or Berry and Reinhardt (1973):

$$\mathrm{Pccnr} = aQc^2, \tag{11-78}$$

where a is function of Qc, Nc and dispersion of the size distribution. Lin *et al.* used a modified form of the relation suggested by Berry (1968). It may be written as

$$\mathrm{Pccnr} = \rho(Qc - Q_{co})^2[1.2\times 10^{-4} + \{1.569\times 10^{-12}N_1/[D_0(Qc - Q_{co})]\}]^{-1}, \tag{L-50}$$

where N_1 is the number concentration of cloud droplets and D_0 the dispersion (0.15) of cloud droplets distribution. When the amount of cloud water exceeds Q_{co}, raindrops are formed. The introduction of the threshold in (L-50) is an empirical modification to Berry's original form made to better simulate observations of first echoes. Lin *et al.* reported that, for cold-based clouds typical of the northern High Plains region, they normally turned off Pccnr consistent with observations which indicate that the collision-coalescence process is rarely active.

For the simulation of the convective snow cloud to be shown in C-3, "Kessler's parameterizaiton" is used for simplicity and uncertainty.

B-11-7. Some numerical artifices

In leap-frog time integration, the values not at the central time step (it) but at the old time step ($it-1$) is used for evaluating cloud microphysical production terms to maintain numerical stability.

Sometimes, some sink terms of cloud microphysical processes become so large that the mixing ratio at the next time step ($it+1$) becomes negative. A basic remedy for preventing this is to adopt smaller Δt at the expense of computational time. However, instead of doing so, sink terms are always adjusted in order to fulfill the following constraint:

$$\mathrm{Pqqqq} < \frac{Qx}{2\Delta t}. \tag{11-79}$$

Sometimes, mass (Qx) becomes negative due to finite discretization errors in advection term in spite of the above-mentioned adjustment on Pqqqq. Negative mixing ratios are forced to be zero. If the values at the neighboring grid points are greater than zero, a certain value is subtracted from them, in order to maintain the conservation property of Qx as much as possible.

Sometimes, imbalance between mass (Qx) and number (Nx) occurs mainly due to numerical errors, especially for small Qx ($< 10^{-15}$kg/kg), and gives rise to erroneous results and numerical troubles (overflow etc.). To prevent this, Nx is adjusted for the given Qx to fulfill the following constraints:

for cloud ice

$$\frac{0.5\times\rho Qi}{m_{i\,\max}} < Ni < 100\,\frac{\rho Qi}{m_{i0}} \qquad ;\ m_{i\,\max} = 0.8 m_{s0} \tag{11-80}$$

for snow and graupel

$$\left(\frac{N_{x0}}{1000}\right)^{3/4}\left(\frac{\rho Qx}{\rho_x \pi}\right)^{1/4} < Nx < (1000N_{x0})^{3/4}\left(\frac{\rho Qx}{\rho_x \pi}\right)^{1/4}, \qquad (11\text{-}81)$$

$$10^{-7}\times\left(\frac{\rho Qx}{m_{x0}}\right) < Nx < 100\times\left(\frac{\rho Qx}{m_{x0}}\right). \qquad (11\text{-}82)$$

The prescribed N_{x0} and m_{x0} are shown in Table B-11-1.

Appendix B-11-1. List of symbols

In this list, L-nn, CT-nn and M-nn indicate that these terms are given by the formula nn in Lin *et al.* (1983), Cotton *et al.* (1986) and Murakami (1990).

Notation	Description		
Value	Unit		
a_c	constant in empirical formula for U_{dc}	3×10^{-7}	$\mathrm{m}^{1-b_c}\mathrm{s}^{-1}$
a_g	constant in empirical formula for U_{dg}	124	$\mathrm{m}^{1-b_g}\mathrm{s}^{-1}$
a_i	constant in empirical formula for U_{di}	700	$\mathrm{m}^{1-b_i}\mathrm{s}^{-1}$
a_r	constant in empirical formula for U_{dr}	842	$\mathrm{m}^{1-b_r}\mathrm{s}^{-1}$
a_s	constant in empirical formula for U_{ds}	17	$\mathrm{m}^{1-b_s}\mathrm{s}^{-1}$
A'	constant in Bigg's equation	0.66	K^{-1}
b_c	constant in empirical formula for U_{dc}	2.0	
b_g	constant in empirical formula for U_{dg}	0.64	
b_i	constant in empirical formula for U_{di}	1.0	
b_r	constant in empirical formula for U_{dr}	0.8	
b_s	constant in empirical formula for U_{ds}	0.5	
B	constant in Huffmann and Vali's equation	4.5	
B'	constant in Bigg's equation	100	$\mathrm{m}^{-3}\mathrm{s}^{-1}$
C_p	specific heat of air at constant pressure	1005	$\mathrm{Jkg}^{-1}\mathrm{K}^{-1}$
Dg	diameter of graupel		m
Dr	diameter of rain		m
Ds	diameter of snow		m
$\overline{D}c$	mean diameter of cloud water		m
$\overline{D}i$	mean diameter of cloud ice		m
Dv	diffusivity of water vapor in the air		$\mathrm{m}^2\mathrm{s}^{-1}$

Ecg	collection efficiency of graupel for cloud water $Stk^2/(Stk+0.5)^2$ (Murakami, 1990; Lew *et al.*, 1986)		
Ecr	collection efficiency of rain for cloud water $Stk^2/(Stk+0.5)^2$		
Ecs	collection efficiency of snow for cloud water $Stk^2/(Stk+0.5)^2$		
Eig	collection efficiency of graupel for cloud ice	0.1	
Eii	collection efficiency among cloud ice particles	0.1	
Eis	collection efficiency of snow for cloud ice	1.0	
Erg	collection efficiency of graupel for rain	1.0	
Ers	collection efficiency of snow for rain	1.0	
Esg	collection efficiency of graupel for snow	0.001	
Ess	collection efficiency among snow particles	0.1	
g	gravitational acceletation	9.8	$\mathrm{ms^{-2}}$
L_f	latent heat of fusion	3.34×10^5	$\mathrm{Jkg^{-1}}$
L_s	latent heat of sublimation	2.83×10^6	$\mathrm{Jkg^{-1}}$
L_v	latent heat of evaporation	2.5×10^6	$\mathrm{Jkg^{-1}}$
m_{i0}	mass of the smallest cloud ice	1×10^{-12}	kg
m_{g0}	mass of the smallest graupel particle	1.6×10^{-10}	kg
m_r	mean mass of rain		kg
m_s	mean mass of snow		kg
m_{s0}	mass of the smallest snow particle	4.4×10^{-11}	kg
Nc	number concentration of cloud water	1.0×10^8	$\mathrm{m^{-3}}$
N_{g0}	parameter of graupel size distribution	1.1×10^6	$\mathrm{m^{-4}}$
Ni	number concentration of cloud ice		$\mathrm{m^{-3}}$
N_{i0}	parameter of Fletcher's equation: (M-26)	1.0×10^{-2}	$\mathrm{m^{-3}}$
N_{r0}	parameter of rain size distribution	8.0×10^6	$\mathrm{m^{-4}}$
Ns	number concentration of snow		$\mathrm{m^{-3}}$
N_{s0}	parameter of snow size distribution	1.8×10^6	$\mathrm{m^{-4}}$
Niacr	number of collisions between rain and cloud ice in unit time: (11-66)		$\mathrm{m^{-3}s^{-1}}$
Niag	decrease in number concentration of cloud ice by		$\mathrm{m^{-3}s^{-1}}$

	aggregation (M-39)	
Nicng	number generation rate of graupel due to accretion of cloud water by cloud ice: (11-37)	$m^{-3}s^{-1}$
Nicns	number generation rate of snow due to depositional and riming growth of cloud ice and aggregation of cloud ice: (11-31)	$m^{-3}s^{-1}$
Nidsn	number generation rate for deposition/sorption nucleation of cloud ice at the expense of water vapor (M-29) (11-17)	$m^{-3}s^{-1}$
Nifzc	number generation rate of cloud ice due to homogeneous and heterogeneous freezing (M-30) of cloud water: (11-19)	$m^{-3}s^{-1}$
Nimlt	number generation rate for melting of cloud ice to form cloud water	$m^{-3}s^{-1}$
Nispl	number generation rate for ice splinter multiplication of cloud ice: (11-23)	$m^{-3}s^{-1}$
Ngaci	number of collisions in unit time between cloud ice and graupel	$m^{-3}s^{-1}$
Ngacr	number of collisions in unit time between rain and graupel; similar to Nsacr	$m^{-3}s^{-1}$
Ngacs	number of collisions in unit time between snow and graupel; similar to Nsacr	$m^{-3}s^{-1}$
Ngfzr	number of rain drops which freeze to form graupel: (11-67)	$m^{-3}s^{-1}$
Ng.raci	generation rate of graupel by collision between cloud ice and rain	$m^{-3}s^{-1}$
Ngprc	rate of change in number concentration due to the precipitation of graupel: (11-12)	$m^{-3}s^{-1}$
Ng.racs =Ng.sacr	generation rate of graupel by collision between snow and rain: (11-65)	$m^{-3}s^{-1}$
Nraci	number of collisions in unit time between rain and cloud ice: (11-66)	$m^{-3}s^{-1}$
Nracs	number of collisions in unit time between rain	$m^{-3}s^{-1}$

	and snow: (11-60)	
Nsacr	number of collisions in unit time between snow and rain: (11-60)	$m^{-3}s^{-1}$
Nsaci	number of collisions in unit time between cloud ice and snow: similar to Niacr	$m^{-3}s^{-1}$
Nsag	decrease in number concentration of snow by aggregation (M-44)	$m^{-3}s^{-1}$
Nscng	number genration rate of graupel due to the riming growth of snow to form graupel: (11-51)	$m^{-3}s^{-1}$
Nsprc	rate of change in number concentration due to the precipitation of snow: (11-12)	$m^{-3}s^{-1}$
Pccnd	condensation of water vapor in unit time to form cloud water which is calculated by "instantaneous adjustment procedure": (11-74)	s^{-1}
Pccnr	generation term of rain via collision and coalescence of cloud droplets: (11-75 $\sim$ 76)	s^{-1}
Piacw	accreted cloud water by cloud ice in unit time which is the sum of Pi.iacw and Pg.iacw: (11-25)	s^{-1}
Pi.iacw	portion of accreted cloud water by cloud ice in unit time to be consumed for riming growth of cloud ice itself: (11-26)	s^{-1}
Piacr	production rate for accretion of rain by cloud ice (L-26)	s^{-1}
Picng	generation rate of graupel in mass due to accretion of cloud water by cloud ice: (11-36)	s^{-1}
Picns	generation rate of snow in mass due to depositional and riming growth of cloud ice and aggregation of cloud ice: (11-30)	s^{-1}
Pidep	production rate for depositional growth of cloud ice: (11-24)	s^{-1}
Pidsn	generation rate for deposition/sorption nucleation of cloud ice at the expense of water vapour	s^{-1}

	(M-29)	
Pifzc	production rate for homogeneous and heterogeneous freezing (M-30) of cloud water to form cloud ice: (11-20)	s^{-1}
Pimlt	production rate for melting of cloud ice to form cloud water	
Pispl	production rate for ice splinter multiplication of cloud ice at riming process (Hallet-Mossop, 1974) (11-21)	s^{-1}
Pgaci	production rate for accretion of cloud ice by graupel (L-41)	s^{-1}
Pgacr	production rate for accretion of rain by graupel (L-42)	s^{-1}
Pgacs	production rate for accretion of snow by graupel (L-29)	s^{-1}
Pgacw	production rate for accretion of snow by graupel (L-40)	s^{-1}
Pgdep	rate for depositional growth of graupel, similar to (11-33)	s^{-1}
Pgfzr	probabilistic freezing of rain to form graupel (L-45)	s^{-1}
Pg.iacw	portion of the accreted cloud water by cloud ice which is converted into graupel	s^{-1}
Pgmlt	production rate for graupel melting to form rain, $T > T_0$ (L-47)	s^{-1}
Pg.racs	portion of the accreted snow by rain which is converted into graupel: (11-63)	s^{-1}
Pg.sacw	portion of the accreted cloud water by snow which is converted into graupel: (11-47)	s^{-1}
Pg.sacr	portion of the accreted rain by snow which is converted into graupel: (11-61)	s^{-1}
Pgwet	wet growth of graupel; may involve Pgacs and Pgaci and must include Pgacw or Pgacr, or both.	s^{-1}

Pgdry	dry growth of graupel; involves Pgacs, Pgaci, Pgacw and Pgacr (L-49)	s^{-1}
Pgprc	rate of change in mixing ratio due to the precipitation of graupel: (11-14)	s^{-1}
Praci	production rate for accretion of cloud ice by rain (L-25)	s^{-1}
Pracw	production rate for accretion of cloud water by rain (L-27)	s^{-1}
Prevp	production rate for rain evaporation (L-52)	s^{-1}
Praci	generatin rate of graupel by collision between cloud ice and rain (L-25)	s^{-1}
Pracs	production rate for accretion of cloud water by snow: (11-58)	s^{-1}
Prprc	rate of change in mixing ratio due to the precipitation of rain: (11-14)	s^{-1}
Psacw	accreted cloud water by snow which is the sum of Ps.sacw and Pg.sacw. (L-24)	s^{-1}
Ps.sacw	part of accreted cloud water by snow which is consumed for riming growth of snow itself: Ps.sacw=Psacw−Pg.sacw	s^{-1}
Ps.sacr	portion of the accreted rain by snow which is consumed for the growth of snow: (11-64)	s^{-1}
Psacr	accreted rain by snow: (11-57)	s^{-1}
Psaci	production rate for accretion of cloud ice by snow (L-22)	s^{-1}
Pscng	generation of graupel in mass due to the riming of snow: (11-54)	s^{-1}
Psdep	production rate for depositional growth of snow: (11-33 ∼ 34)	s^{-1}
Psmlt	production rate for snow melting to form rain (L-32)	s^{-1}
Psprc	rate of change in mixing ratio due to the precipitation of snow: (11-14)	s^{-1}

$Qvsw$	saturation mixing ratio for water vapor with respect to water		
$Qvsi$	saturation mixing ratio for water vapor with respect to ice		
$\overline{r}_I$	mean radius of cloud ice		m
r_{s0}	radius of the smallest snow	0.75×10^{-4}m	
R_w	gas constant for water vapor	461.5	$\mathrm{Jkg^{-1}K^{-1}}$
S_i	saturation ratio over ice, $Qv/Qvsi$		
S_w	saturation ratio over water, $Qv/Qvsw$		
Stk	Stokes number for mass-weighted mean size of cloud water and precipitable hydrometeor, x (Eq. (11-26)). $\overline{D}c^2\overline{U}x\rho_w/(9\eta\overline{D}x)$		
T	temperature		K
T_0	temperature at the freezing point	273.16	K
T_c	temperature in Celsius $T - T_0$		°C
T_s	supercooled temperature $(T_0 - T)$		°C
U_{dc}	terminal velocity of cloud water of radius Dc		$\mathrm{ms^{-1}}$
U_{dg}	terminal velocity of graupel of radius Dg		$\mathrm{ms^{-1}}$
U_{di}	terminal velocity of cloud ice of radius Di		$\mathrm{ms^{-1}}$
U_{dr}	terminal velocity of rain of radius Dr		$\mathrm{ms^{-1}}$
$\overline{U}_{ng}$	number weighted mean terminal velocity for graupel		$\mathrm{ms^{-1}}$
$\overline{U}_{nr}$	number weighted mean terminal velocity for rain		$\mathrm{ms^{-1}}$
$\overline{U}_{ns}$	number weighted mean terminal velocity for snow		$\mathrm{ms^{-1}}$
$\overline{U}_c$	mean terminal velocity of cloud water		$\mathrm{ms^{-1}}$
$\overline{U}_g$	mass-weighted mean terminal velocity of rain		$\mathrm{ms^{-1}}$
$\overline{U}_s$	mass-weighted mean terminal velocity of snow		$\mathrm{ms^{-1}}$
X	dispersion of the fall velocity spectrum of cloud ice: (11-62)	0.25	
α_{rs}	the ratio at which collision between rain and snow generates not graupel but snow		$\mathrm{ms^{-1}}$
α_{scng}	tuning parameter associated with the dispatcher function which determines the portion of the ac-	4	

	creted cloud water by snow to be consumed for graupel generation: (11-43)		
β_2	parameter in Fletcher's equation (M-28)	0.6	K^{-1}
κ_a	thermal conductivity of air	2.4×10^{-2}	$Jm^{-1}s^{-1}K^{-1}$
π	non-dimensional pressure		
λ_g	slope parameter in graupel size distribution		m^{-1}
λ_r	slope parameter in rain size distribution		m^{-1}
λ_s	slope parameter in snow size distribution		m^{-1}
ψ	diffusivity of water vapor		
ν	dynamic viscosity of air		
η	viscosity of air $\eta = \rho\nu$.		
ρ	air density of the basic state		kgm^{-3}
ρ_0	air density of the basic state at $z = 0$ m		kgm^{-3}
ρ_g	density of graupel	2.0×10^2	kgm^{-3}
ρ_i	density of cloud ice	5.0×10^2	kgm^{-3}
ρ_s	density of snow	8.4×10^1	kgm^{-3}
ρ_w	density of water	1.0×10^3	kgm^{-3}
Δt	time step of leap-frog time integration	4.0	s^{-1}

Appendix B-11-2. Figures of production terms for elementary cloud micro-physical processes

Production terms (Pqqqq) are plotted under several conditions in Fig. B-11-4 ~ B-11-10. The parameters are the same as in Table B-11-1 except for $r_0 = 50\mu$m. For a given Qi, Qs and Qg, Ni, Ns and Ng are computed from Eq. (M-28) and Eq. (11-11) using the prescribed N_{s0} and N_{g0} (see Table B-11-1), respectively. The ordinate denotes $\log_{10}$(Pqqqq), where the unit of Pqqqq is s^{-1}. Sensitivity of Pscng and Pg.sacw (see Eqs. (11-54), (11-46)) to the parameter $\alpha 2\Delta t$ used in Eq. (11-43) is shown in Figs. B-11-6 and B-11-8. In the following, the parameter $\alpha 2\Delta t$ used in Eq. (11-43) is set to 40, unless specifically mentioned.

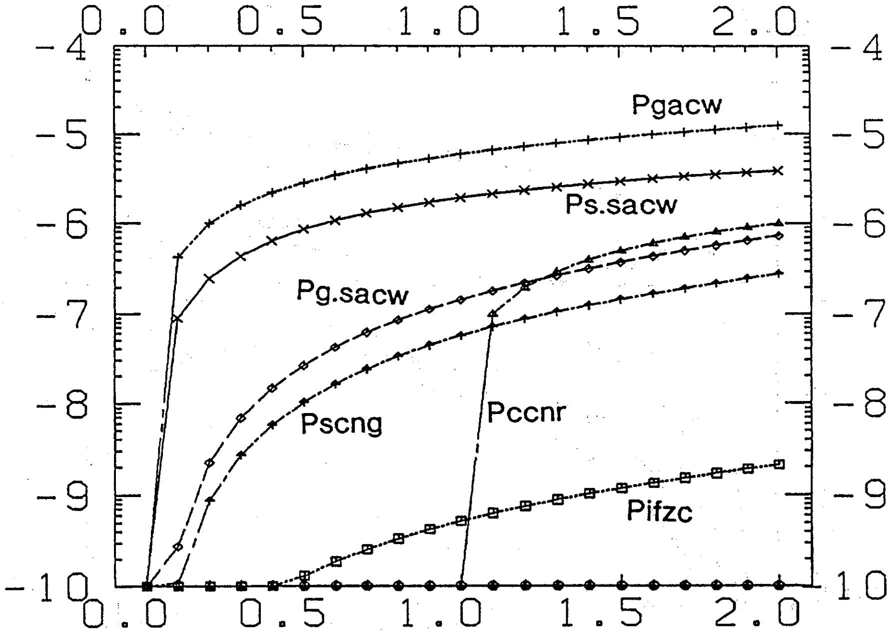

Fig. B-11-4 Cloud microphysical processes involving cloud water as a function of Qc varying from 0 to 2 g/kg, under the condition of $T_c = -20°\mathrm{C}$, $P = 700$ hPa, $Qv = Qvsw$, $Qr = 0$, $Qi = 0$, $Qs = 0.5 \times 10^{-3}$ kg/kg and $Qg = 0.5 \times 10^{-3}$ kg/kg.

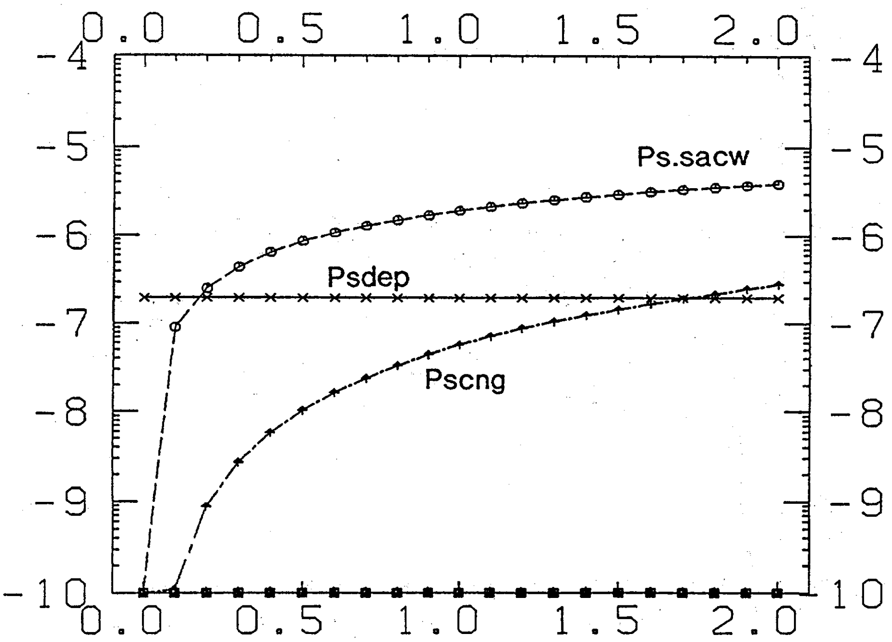

Fig. B-11-5 Cloud microphysical processes involving snow as a function of Qc varying from 0 to 2 g/kg, under the condition of $T_c = -20°\mathrm{C}$, $P = 700$ hPa, $Qv = Qvsw$, $Qr = 0$, $Qi = 0$, $Qs = 0.5 \times 10^{-3}$ kg/kg and $Qg = 0.5 \times 10^{-3}$ kg/kg.

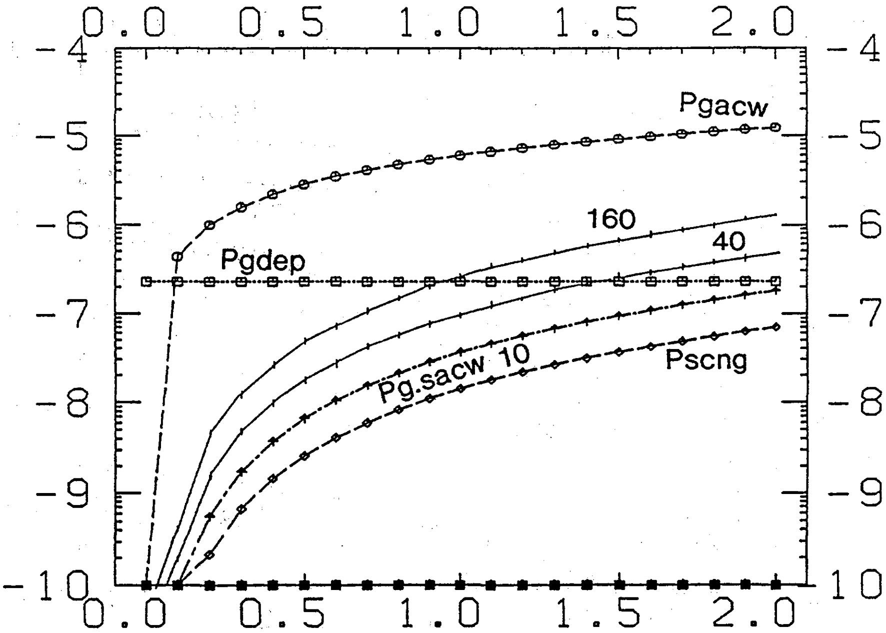

Fig. B-11-6 Cloud microphysical processes involving graupel as a function of Qc varying from 0 to 2 g/kg, under the condition of $T_c = -20°$C, $P = 700$ hPa, $Qv = Qvsw$, $Qr = 0$, $Qi = 10^{-11}Ni/\rho$ ($Ni = 10^3$ m^{-3}), $Qs = 0.5 \times 10^{-3}$ kg/kg, $Qg = 0.5 \times 10^{-3}$ kg/kg and $\alpha 2\Delta t = 10$ (see Eq. (11-43)). Pg.sacw's for $\alpha 2\Delta t = 40$ and 160 are added for comparison.

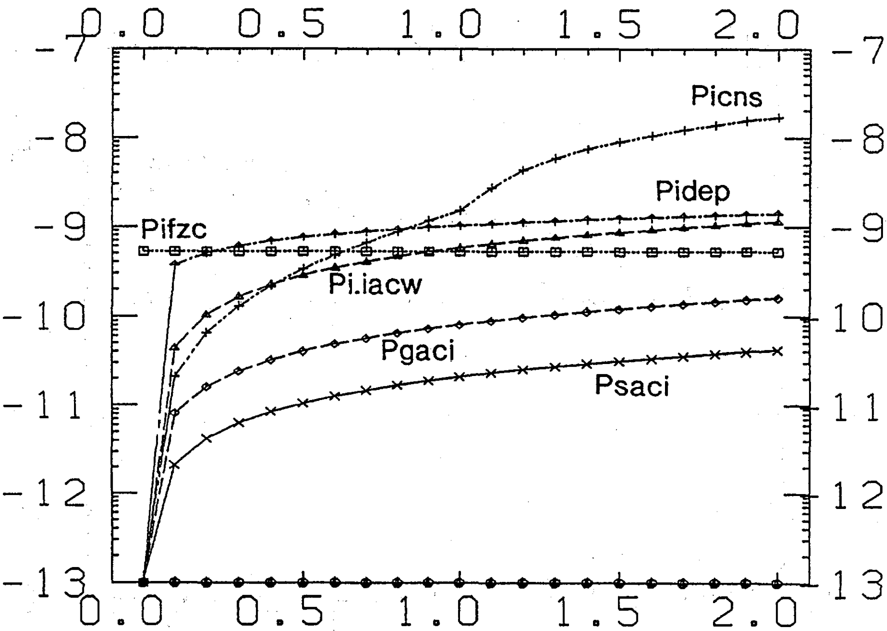

Fig. B-11-7 Cloud microphysical processes involving cloud ice as a function of ρQi varying from 0 to $Ni \times m_{s0}$, under the condition of $T_c = -20°$C, $P = 700$ hPa, $Qv = Qvsw$, $Qc = 1.0 \times 10^{-3}$ kg/kg, $Qr = 0$, $Qs = 0.5 \times 10^{-3}$ kg/kg and $Qg = 0.5 \times 10^{-3}$ kg/kg. The abscissa denotes $\rho Qi = Ni \times m_{s0} \times (j/20)$, where j varies from 0 to 20, $m_{s0} = 0.44 \times 10^{-10}$ kg and $Ni = 10^3 m^{-3}$.

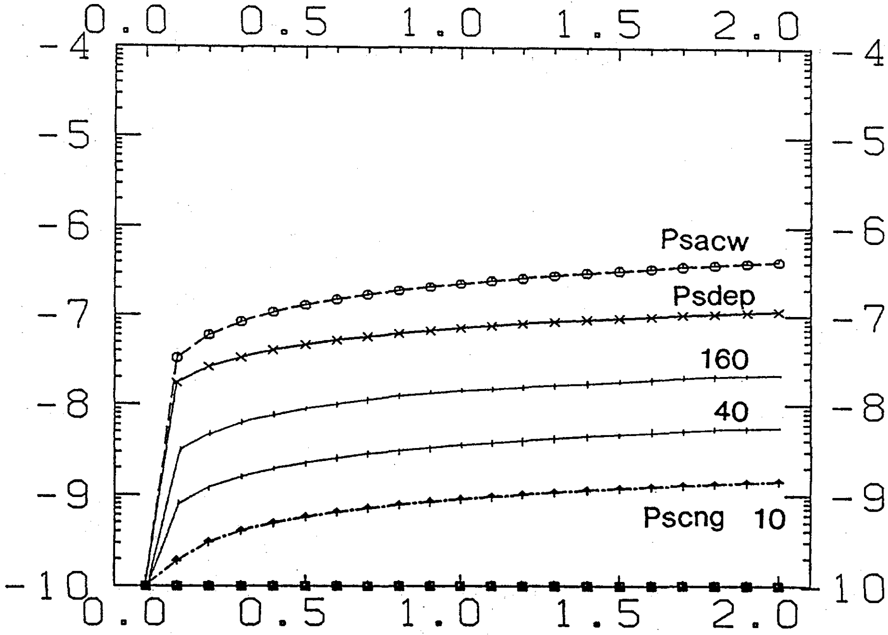

Fig. B-11-8 Cloud microphysical processes involving snow as a function of Qs varying from 0 to 2 g/kg, under the condition of $T_c = -20°$C, $P = 700$ hPa, $Qv = Qvsw$, $Qc = 0.5 \times 10^{-3}$ kg/kg, $Qr = 0$, $Qi = 0$, $Qg = 0.5 \times 10^{-3}$ kg/kg and $\alpha 2\Delta t = 10$ (see Eq. (11-43)). Pscng's for $\alpha 2\Delta t = 40$ and 160 are added for comparison.

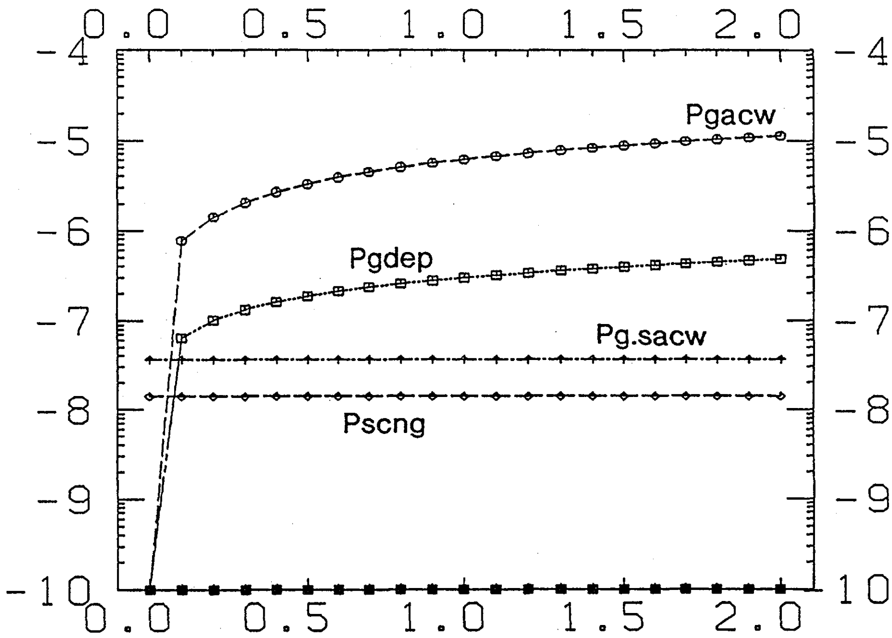

Fig. B-11-9 Cloud microphysical processes involving graupel as a function of Qs varying from 0 to 2 g/kg, under the conditon of $T_c = -10°$C, $P = 850$ hPa, $Qv = Qvsw$, $Qc = 0.5 \times 10^{-3}$ kg/kg, $Qr = 0$, $Qi = 0$ and $Qg = 0.5 \times 10^{-3}$ kg/kg.

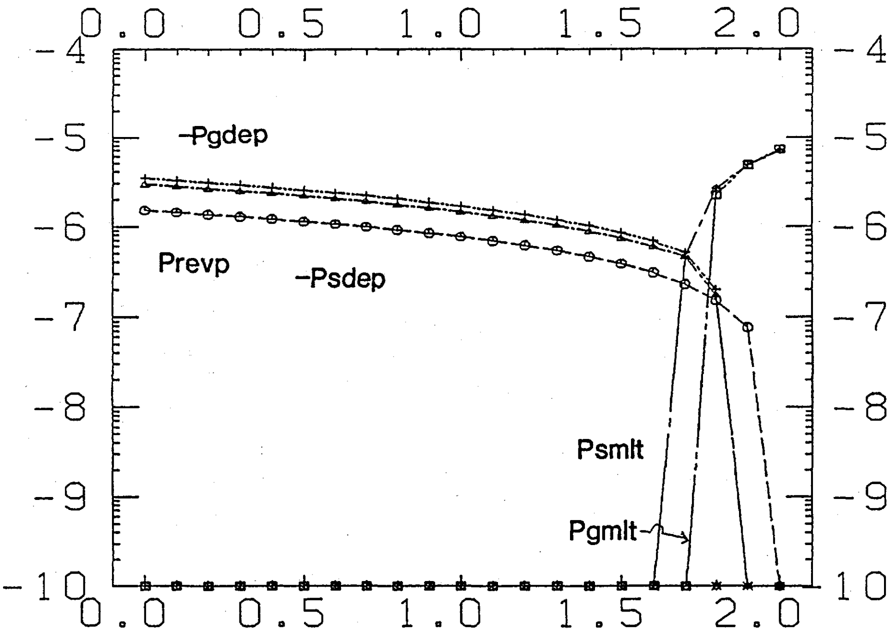

Fig. B-11-10 Cloud microphysical processes relevant to forming a cold dome as a function of relative humidity varying from 0 to 100%, under the condition of $T_c = 1°$C, $P = 970$ hPa, $Qc = 0$, $Qr = 0.5 \times 10^{-3}$ kg/kg, $Qi = 0$, $Qs = 0.5 \times 10^{-3}$ kg/kg and $Qg = 0.5 \times 10^{-3}$ kg/kg.

B-12. Computational diffusion

Artificial computational diffusion terms are added to the diffusional term by subgrid scale turbulence (Eqs. (10-16) and (10-17)) in order to suppress computational noises and to overcome some problems near the upper and lateral boundaries. In leap-frog time integration from the time step '$it-1$' to '$it+1$', these terms are evaluated using the values at the time step '$it-1$' instead of 'it' in order to maintain numerical stability.

i) Nonlinear damping Dn (Nakamura, 1978)

$$Dn(f) = \frac{DX^3}{8m_n \Delta t|\Delta f|}\frac{\partial}{\partial x}\left(\left|\frac{\partial f}{\partial x}\right|\frac{\partial f}{\partial x}\right) + \frac{DZ^3}{8m_n \Delta t|\Delta f|}\frac{\partial}{\partial z}\left(\left|\frac{\partial (f-f.\mathrm{ext})}{\partial z}\right|\frac{\partial (f-f.\mathrm{ext})}{\partial z}\right), \tag{12-1}$$

where f.ext denotes the horizontally averaged value of initial f.

ii) Fourth-order linear damping for suppressing mainly 2-grid noises is given as

$$D_{4\ell}(f) = \frac{-DX^4 \mathrm{EKH}(k)\,\mathrm{FKMXF}(k)}{16 m_{4\ell}\Delta t}\frac{\partial^4 f}{\partial x^4}. \tag{12-2}$$

iii) Rayleigh damping near the upper boundary to prevent the false reflection of internal gravity waves from the upper rigid wall.

$$D_{ru}(f) = -\frac{1}{2m_{ru}\Delta t}\left(1+\cos\left(\frac{\pi(LZ-z)}{LZ-z_d}\right)\right)(f-f.\mathrm{ext}) \tag{12-3}$$

for $z > z_d$.

Here, LZ is the height of the model domain.

iv) Rayleigh damping near the lateral boundary is imposed in order to prevent the false reflection of internal gravity waves from the lateral boundary, enforce the environmental external conditions and suppress noises.

$$D_{r\ell}(f) = -\frac{1}{2m_{r\ell}\Delta t}\left(1+\cos\left(\frac{\pi(LX-x)}{x_d}\right)\right)(f - f.\mathrm{ext}) \tag{12-4}$$

for $x > LX - x_d$.

$$D_{r\ell}(f) = -\frac{1}{2m_{r\ell}\Delta t}\left(1+\cos\left(\frac{\pi x}{x_d}\right)\right)(f - f.\mathrm{ext})$$

for $x < x_d$.

Here, LX is the width of the model domain.

v) Damping in the time integration schemes

v-1) Asselin's time filter

$$f(it) = f^*(it) + 0.5\nu(f^*(it+1) - 2f^*(it) + f(it-1)) \tag{12-5}$$

v-2) α parameter used in E-HI-VI scheme (Eq. (3-4))

v-3) β and γ parameters used in E-HE-VI scheme (Eqs. (4-4) and (4-5))

B-13. Initial set-up procedures

B-13-1. Preparation of eigen-vectors and eigen-values

After variable grids are generated (see D-4), matrix A, Y_A, B and Y_B which are used in the finite discretization expression of the pressure equation (see section B-6) are generated, and the generalized eigenvalue problems

$$AP = Y_A P \Lambda(A) \quad \text{and} \quad BQ = Y_B \Lambda(B) \qquad \text{(see Eq. (6-17))}$$

are solved by Jacobi method. Eigen-vectors, P and Q, are arranged in the decreasing order of their eigen-values. They are stored in magnetic tape.

<u>P.G.</u>

sub.CVEVSI ----- INIVG1 ----- GMAT ----- VRGDIS
----- JACOBI
----- arrange eigen-vectors
----- normalize eigen-vectors
----- store eigen-vectors and values in magnetic tape.

B-13-2. Initial environmental fields

Currently, vertical profiles of u, v, Θ and Qv without any horizontal variation can be specified in the input parameter list (arrays.KZIN and VALIN). The specified values for u and v are not for $\bar{\rho}G^{1/2}u$ but for u; those for Θ are biased ($\Theta_{\text{init}} = \Theta_{\text{input}} + \Theta_{\text{bias}}$); those for Qv are specified in relative humidity.

Inputted u is converted to $\bar{\rho}G^{1/2}u$ and is stored in array U and is predicted. $\theta = \Theta_{\text{init}} - \Theta_{\text{bias}}$ is stored in array PT and is predicted. From inputted relative humidity, the mixing ratio of water vapour is calculated and stored in array QV and is predicted.

<u>P.G.</u>

See D-6 and sub.INIFLD, INIVAL, GENPTD, QVSATU.

B-13-3. Reference atmosphere

From the given initial vertical profile $\Theta_{\text{init}}(z)$, $\Theta_{\text{ref}}(z)$ is determined in the following form:

$$\left.\begin{aligned} \Theta_{\mathrm{ref}}(z) &= az + \Theta_{\mathrm{ref}}(z_0) && \text{for } z_0 < z < z_1, \\ \Theta_{\mathrm{ref}}(z) &= c(z - z_2)^2 + b(z - z_2) + \Theta_{\mathrm{ref}}(z_2) && \text{for } z_1 < z < z_2, \\ \Theta_{\mathrm{ref}}(z) &= b(z - z_2) + \Theta_{\mathrm{ref}}(z_2) && \text{for } z_2 < z < z_t, \end{aligned}\right\} \tag{13-1}$$

where

$$\left.\begin{aligned} a &= -\frac{\Theta_{\mathrm{ref}}(z_1) - \Theta_{\mathrm{ref}}(z_0)}{z_1 - z_0}, \\ b &= \frac{\Theta_{\mathrm{ref}}(z_t) - \Theta_{\mathrm{ref}}(z_2)}{z_t - z_2}, \\ c &= \frac{\Theta_{\mathrm{ref}}(z_1) - \Theta_{\mathrm{ref}}(z_2) - b(z_1 - z_2)}{(z_1 - z_2)^2}. \end{aligned}\right\} \tag{13-2}$$

Here, z_0 is 0m and z_t is the height of the model domain.
Θ_{ref} is required to be as close as possible to Θ_{init}, and as smooth as possible.

Once Θ_{ref} is determined, nondimensional pressure of the reference atmosphere, Π_{ref}, is determined from hydrostatic balance as follows:

$$\frac{\partial \Pi_{\mathrm{ref}}}{\partial z} = -\frac{g}{C_p}\,\Theta_{\mathrm{ref}}(z), \tag{13-3}$$

with the lower boundary condition of $\Pi_{\mathrm{ref},k=1} = 1$. P_{ref} and T_{ref} are obtained from Π_{ref} and Θ_{ref}; $\overline{\rho} = \rho_{\mathrm{ref}}$ is obtained from the state equation of gas.

P.G.

See sub.ORGINO; sub.CREFST; $\Theta_{\mathrm{ref}}(x, \xi)$ is set in array VPTREF.

B-13-4. Reduction methods of initial shocks in the presence of mountains

a) Mountain growing method

Mountain shape function is expressed as

$$Z_s(x, y) = h(t) Z_{s0}(x, y), \tag{13-4}$$

where the maximum value of Z_{s0} is one. $h(t)$ is linearly raised up to Z_{top} for the first 600 time steps at every 6 time steps. In accordance with the time change of Z_s, metric tensors such as $G^{1/2}$, G^{13} and G^{23} and $\overline{\rho}G^{1/2}$ are changed. In accordance with the time change of $\overline{\rho}G^{1/2}$, time derivatives of $U = \overline{\rho}G^{1/2}u$ and $V = \overline{\rho}G^{1/2}v$ and $W = \overline{\rho}G^{1/2}w$ are changed as follows:

$$\begin{aligned}\frac{\partial(\overline{\rho}G^{1/2}u)}{\partial t} &= \frac{\partial(\overline{\rho}G^{1/2})}{\partial t}u + \overline{\rho}G^{1/2}\frac{\partial u}{\partial t} \\ &= \frac{\partial(\overline{\rho}G^{1/2})}{\partial t}u + (-\mathrm{ADVU} - \mathrm{PFX})\end{aligned} \tag{13-5a}$$

Eq. (1-34) is changed into

$$\begin{aligned}\overline{\rho}G^{1/2}\frac{d\xi}{dt} = W^* &= \overline{\rho}G^{1/2}\left[\frac{1}{G^{1/2}}w + \frac{H}{H-\xi}\left(\frac{\xi}{H} - 1\right)\left(\frac{\partial Z_s}{\partial x}\frac{dx}{dt} + \frac{\partial Z_s}{\partial t}\right)\right] \\ &= \overline{\rho}G^{1/2}\left[\frac{1}{G^{1/2}}w + G^{13}u + \frac{1}{G^{1/2}}(H-\xi)\frac{\partial G^{1/2}}{\partial t}\right].\end{aligned} \tag{13-5b}$$

At the upper and lower boundaries, W^* is zero. The upper and lower boundary conditions for the pressure equations such as Eqs. (2-8), (3-58) and (4-10) are changed in accord to the change of Eq. (1-34) into Eq. (13-5b).

P.G.

See D-6 and sub.ADJUVW and ORGIN0 in mem.SFXTPG1. Z_{top} is specified in the input parameter list VALIN(35,4).

b) Wind growing method

U is linearly increased from 0 to U_{init} (initial environmental field of U) by Rayleigh friction for the first 600 time steps. U_{ext} is changed at every 6 time steps for the first 420 time step as follows:

$$U_{\mathrm{ext}} = \frac{it}{420}U_{\mathrm{init}} \tag{13-6}$$

Rayleigh friction is imposed at every time step over the entire domain for the first 600 time steps as

$$\frac{\partial(\overline{\rho}G^{1/2}u)}{\partial t} = -\left(\mathrm{ADVU} - \frac{U_{\mathrm{ext}} - U^{it-1}}{2\Delta t}\right) - \mathrm{PFX} \tag{13-7}$$

P.G.

See sub.WDGRW2 in mem.SFXTPG1.

B-13-5. Initialization of pressure in elastic models

To prevent the excitation of sound waves from the initial fields,

$$\mathrm{DIVT}(U^{it},\ V^{it},\ W^{it}) = 0, \qquad it = 0$$

is necessary. But this alone is not sufficient to ensure the non-divergence of the wind field at the next time step, $\mathrm{DIVT}(U^{it+1},\ V^{it+1},\ W^{it+1}) = 0$. The condition that pressure satisfy the pressure equation of AE is necessary. This ensures $\mathrm{DIVT}(U^{it+1},\ W^{it+1}) = 0$ as discussed by Ikawa (1988). In E-HI-VI and E-HE-VI, the pressure obtained from the pressure equation of AE is given as the initial pressure.